Streaking on Aluminium alloy extrusions

Joshua Walker

Thesis submitted for Master of Engineering

AUT University
School of Engineering
2012

Acknowledgements

This work was carried out at the Auckland University of Technology in the department of mechanical engineering in collaboration with Fletcher Aluminium a subsidiary of Fletcher Building. I would like to thank the following people who helped with this research in the form of technical expertise and guidance.

The first acknowledgment is to my supervisor Professor Zhan Chen who provided guidance and immense expertise on mechanical and material science throughout the project. His professional attitude meant that support and advice was always available and made the academic and research processes much easier.

A second acknowledgement is to both Bill Hayward, chief metallurgist and Sen Chen, business support manager at Fletcher Aluminium for their assistance and expertise in conducting the research at Fletcher Aluminium. Bill Hayward provided advice and technical expertise from years of extrusion experience which ensured I was able to keep the research process on track.

The last acknowledgement is to the ministry of science and Innovation which provided the funding for this project and thus enabled me to undertake this research.

Abstract

Extrusion is a process in which a billet of most commonly aluminium is pushed through a die aperture of a desired cross sectional shape to produce lengths of extrudate. The type of streaking being investigated is due to differing thermomechanical conditions created due to changing cross sectional thicknesses of an extrusion profile. These differing thermomechanical conditions then may cause possible issues of differing distributions of intermetallics or grain orientations. At the start of this research many possible reasons for streaking were presented in literature but no single mechanism identified as being the primary cause. Therefore it needed to be identified what the mechanism for causing streaking on the product being investigated was due to. In addition the evolution of streaking after different etch durations needed to be examined as this type of finding has not been reported in literature. The streaking observed therefore might not be the same for all levels of material removal.

To conduct this research on streaking, samples were submitted to differing chemical etch durations which produced different levels of material removal. The chemical etch differs in and out of the streak region and the different durations thus allow possible different types of streaking to be observed at different levels of material removal. In addition to chemical etching an electro-etching experiment was conducted so that primarily the grain boundaries were etched out to examine if these features play an insignificant, minor or major role in the streaking phenomenon.

In summary there are two features that are etched on the surface of an extrudate, these are grain boundary grooves and etch pits. It was established through a thorough investigation that etch pits are the primary factor for streaking to occur with the grain boundary grooves being an insignificant factor for the extrusion product examined. For the top surface layers a glossy streak appeared and as more material was removed two dull parallel bands and then a single dull band streak appeared. The dull streaking was due to more pitting in the streak region and the glossy streaking due to less pitting and less densely distributed die lines. Overall the streaking observed most commonly in the manufacturing environment is the dull gloss streaks which occur after a longer etch duration and larger volume of surface material removal. Therefore the streaking phenomenon is mainly a subsurface issue but only to a small depth. Therefore if abrasive blasting in conjunction with a short etch duration is used the issue of streaking created by etching can be resolved.

Table of Contents

List of Figures

List of Tables

Statement of Originality

I hereby declare that this submission is my own work and that, to the best of my knowledge and belief it contains no material previously published or written by another person (except where explicitly defined in the acknowledgements), nor material which to a substantial extent has been accepted for the qualification of any other degree or diploma of a university or other institution of higher learning.

Name:_____

Date:_____/_____/_____

Signed:_____

1. Introduction& Literature Review

1.1. Extrusion

Extrusion is a process used to convert cast billets of solid metal into continuous lengths of generally uniform cross section by forcing it through a die of the required cross sectional shape of the product. The manufacturing process conducted to extrude products at Fletcher Aluminium (Falum) is represented in Figure 1-1 below.

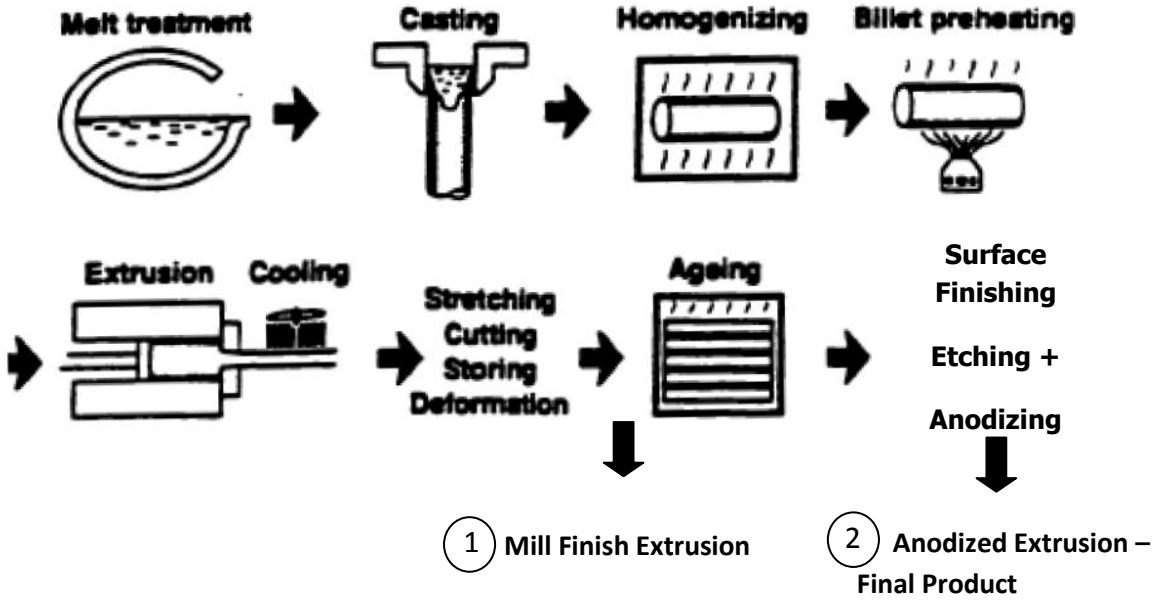

Figure 1-1Schematic representation of extrusion process[1]

Fletcher Aluminium (Falum) is an aluminium extrusion facility based in Mt Wellington, Auckland. Fittingly their name identifies their extrusion material which is also the most popular extrusion material used worldwide. Aluminium extrusions are popular because of the ease of extruding aluminium, they are highly versatile, have relatively modest prototyping costs, possess good strength and corrosion resistance, and yield a high benefit-costs ratio [2]. At Falum 90% of their production is conducted extruding AA6060. The AA6060 alloy used has the approximate chemical composition shown in Table 1-1.

Table 1-1 AA6060 Specification

AA No	Si	Fe	Cu	Mn	Mg	Cr	Zn	Ti
6060	0.3-0.6	0.1-0.3	0.1	0.1	0.35-0.6	0.05	0.15	0.1

1.1.1. Pre-extrusion

The billet is a cylindrical length of cast metal which is pushed through a die shape to extrude lengths of generally uniform cross section. These cylindrical billets are cast as logs and then sheared into billets. A billet loaded in the extrusion press is shown in Figure 1-2.

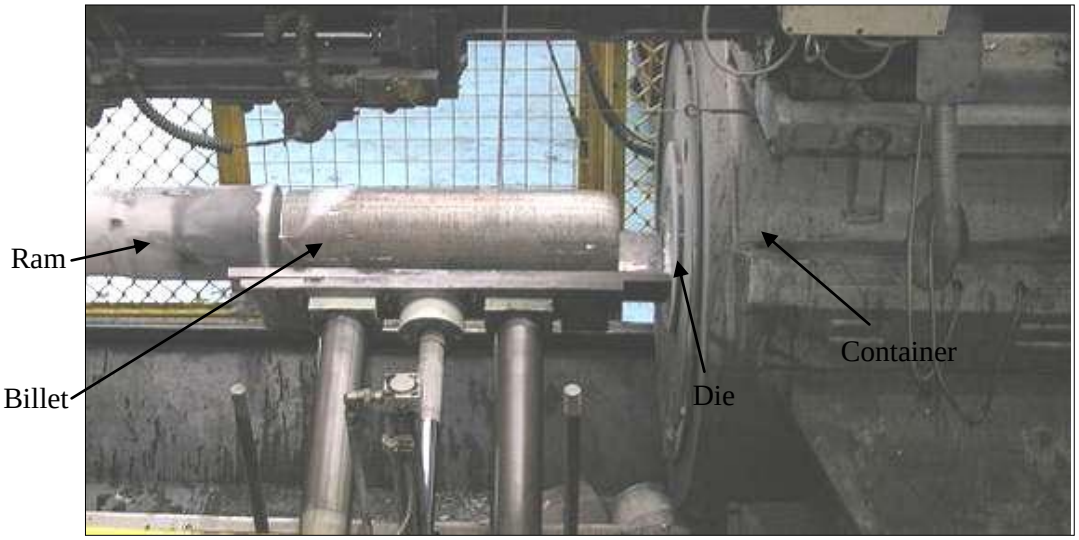

Figure1-2 Billet loaded into the extrusion press [3]

These logs are supplied to Falum by outside contractors and hence the task of billet casting and homogenising is not carried out at Falum. To cast these logs the process is direct chill casting. In this process metal is poured into an uncapped mould. Cooling occurs through the mould wall and by direct water chill applied at the exit of the mould. This cooling allows most of the cylindrical section to be solidified as it exits the mould. This is a continuous or semi continuous casting process and as such the solid section is pulled forward by hydraulics and another section becomes solidified forming a continuous cast log of Aluminium. Because of the different cooling rates occurring in the core and the outer regions of the logs the casting rate must be optimized and also scalping may occur to remove the outer layer of the casting. These techniques minimize structure variation of the cast log.

After casting the logs are then homogenised to ensure the microstructure of the casting is homogeneous throughout. The microstructure of the cast condition is quite heterogeneous and has a cored dendritic structure with solute content increasing from centre to edge with a interdendritic distribution of second phase particles [4]. This homogenising process improves workability or extrudability of the billets and minimizes the chance of variations in the surface structure of the extruded product. To conduct homogenization the billets are placed in a furnace for 3-4 hours at approximately 550°C - 600°C and then cooled in a cooling

chamber. The homogenising causes soluble constituents to be dissolved and dispersed uniformly throughout the cast log. The main function of homogenization is to transform needle like β-AlFeSi into more globular likeα-AlFeSi particles to improve workability or rather extrudability[3]. This effect is illustrated in Figure 1-3 where the as cast structure shows needle like β-AlFeSi particles as shown in Figure 1-3(a). After homogenization these particles are transformed into more globular like α-AlFeSi particles as shown in Figure 1-3(b). The other function of homogenization is to dissolve magnesium Silicide (Mg_2Si).

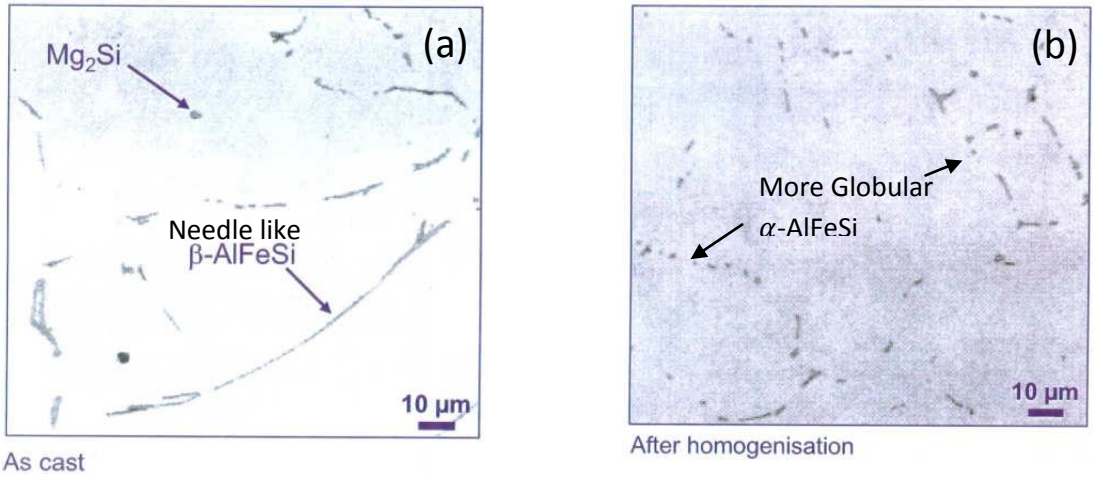

Figure1-3The microstructure of the cast logs (a) As Cast (b) After Homogenization[1]

The Aluminium cast logs arrive at Falum in seven metre lengths and diameters of 202mm. The next phase is the preheating of the billet or rather the log just before extrusion. A log is loaded into the preheating furnace for 40 minutes and stepped up to a temperature of 430°C – 470°C depending on the profile being extruded.

This preheating process is carried out to make the logs more plastic and reduce strength so they can be extruded with ease through the die. The preheating also helps to further dissolve any remaining Mg_2Si particles and convert any remaining needle like β-AlFeSi particles to more globular α-AlFeSi particles.

1.1.2. Extruding

After pre heating the log is sheared into lengths of between 570-600mm to form a billet. The billet is then loaded into the extrusion press as shown in Figure 1-2. There are two different types of extrusion techniques used, direct extrusion and indirect extrusion. Referring to Figure 1-4 it can be seen that for direct extrusion the ram is pushed towards the billet which is

then pushed through the die. For indirect extrusion however the die is fixed to the ram and the die is then pushed through the billet material.

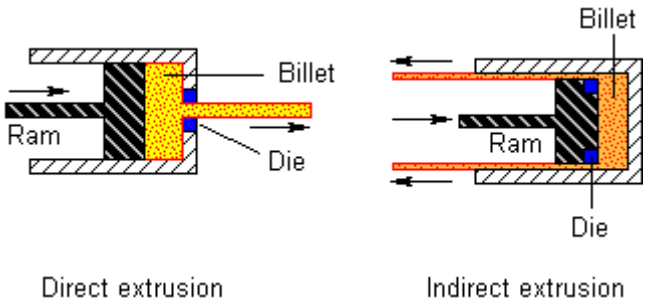

Figure 1-4Schematic of Direct and Indirect Extrusion[5]

By far the more common of these two techniques is direct extrusion. This is because of the difficulties of ram construction for the indirect process and the greater circumscribing circle diameter available for the extrudate in the direct mode[4]. The method used at Falum and as shown in Figure 1-2 is direct extrusion. To extrude the ram pushes the billet through the die at a speed set according to the extrusion profile. Figure 1-5 shows a typical extrusion profile extruding from the die exit to be air cooled.

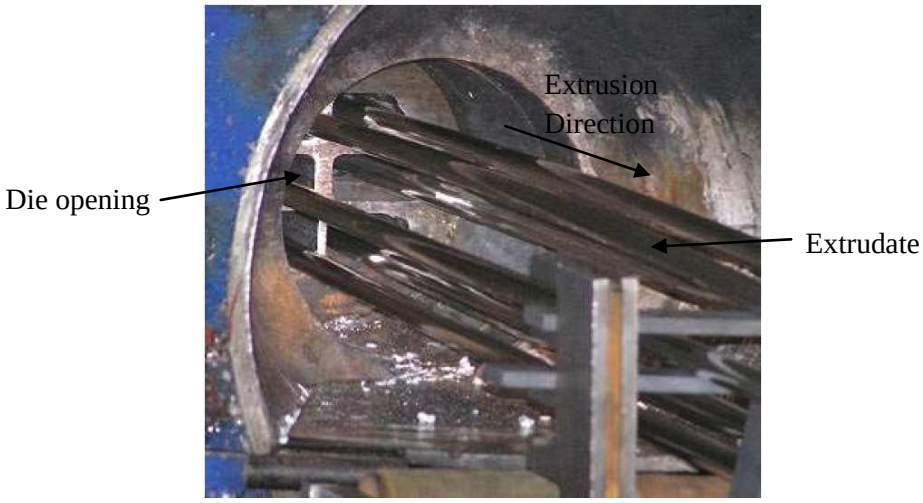

Figure 1-5Metal flowing (extrudate) at the exit door [3]

The air cooling should be enough to prevent precipitation of Mg_2Si particles although this may depend on the temperature profile which may vary in different areas of the extrusion. For example in areas of larger cross sectional thicknesses and subsequent larger deformation the temperature may rise due to greater strain and friction. If this is the case it could be possible that Mg_2Si particles may precipitate.

1.1.3. Post-extrusion

After extruding the cold metal is clamped at either end of the length of extrudate and a tensional force applied. This is done to straighten the lengths and bring the dimensions into specification. Stretching elongates the metal by approximately +1% of its original length. After stretching the lengths are moved to a saw machine where the crushed ends from stretching are removed and the extrusion length is cut into lengths required by the customer. After stretching and cutting the extrusion sections are then placed in an oven to conduct a process known as artificial ageing. This process is conducted to increase the strength of the extrusion product. At Falum the extrusions are heated at 185-215°C for 2 to 5 hours, the variance in temperature and duration depending on the strength requirement for the particular extrusion product. Depending on the ageing process parameters the ultimate strength could vary between 180 – 210 MPa for AA6060 alloy [3].The ageing process will cause Mg_2Si particles which were dissolved in the billet homogenising and preheating steps to precipitate. This is known as precipitation hardening. Once Mg_2Si particles grow to a certain size the tensile strength decreases. Therefore to ensure optimal tensile strength Mg_2Si particles must be an optimal size through optimization of the temperature and duration of the ageing process.

1.1.4. Surface Finishing

To provide a uniform surface appearance which is matte and appealing to the customer and is also protected from environmental elements (e.g. rain, dust), surface finishing is conducted on the extrusion. Currently Falum has two surface finishing techniques employed to produce extrusions with a matte surface appearance which will appeal to the customer. These techniques are etching and abrasive blasting. The abrasive blasting technique has only recently been introduced at Falum as a result of this study and research on current trends in larger overseas extrusion facilities. The abrasive blast and etched product are both offered to the customer as an option however the abrasive blast product is offered at a premium price. After matting the surface using these techniques the surface is then anodized to provide a protective coating.

For conducting etching the extrusions are first etched in a proprietary etching solution supplied by chemical manufacturer Henkel. This etching solution main ingredient is NaOH (Sodium Hydroxide) with additional chemicals added designed to optimally matte the surface and mitigate the appearance of defects and also supress fumes and soften the water added to

the solution. The extrusions are placed in the etching solution which is at a temperature of55°C for duration of 15 minutes. For a 15 minute etching duration a metal removal layer of depth of approximately 30 microns will occur, this corresponds to 82.7 g/m^{2}of metal removal. At Falum caustic etch tanks are maintained to provide a metal removal of between 75-85 g/m^{2}within a 15 minute etch time frame. Etching solutions attack the aluminium structure causing a pitted cell structure. Properties of the extrusion which may change the etching attack are grain orientations or intermetallics which would cause a different surface roughness and hence increase the matte factor of the surface finish.

Recently Abrasive blasting was introduced as a surface finishing technique at Falum. The abrasive blasting machine is a conveyor type system in which extruded lengths are loaded onto a conveyor and run through the blast chamber and exit as a blasted product. The abrasive blasted extrusions are then cleaned by etching for two minutes. The conveyor type abrasive blasting system used at Falum is shown in Figure 1-6 below.

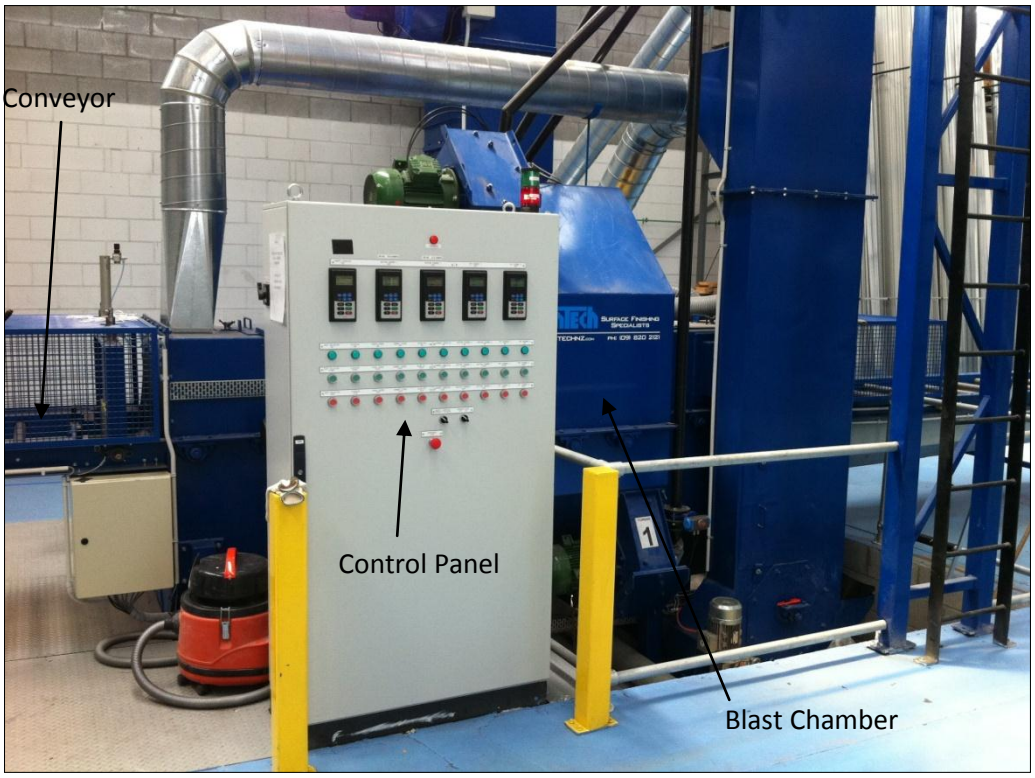

Figure 1-6 Abrasive blasting machine at Fletcher Aluminium

The following are the three main reasons for introducing abrasive blasting.

1. The first reason is the reduction of toxic etch waste due to the etch duration being reduced from 15min to 2min. This means this extrusion product is more

environmentally friendly and will appeal to the increasing number of more environmentally conscious customers.

2. The number of etch related defects can be significantly reduced or eliminated due to the reduced etch duration.
3. The abrasive blast product has a highly matte defect free surface which will appeal to the aesthetically conscious customer for use in high quality buildings.

Abrasive blasting produces a matte surface with the gloss or matteness of the surface being a function of the surface roughness. Surface roughness using abrasive blasting is controlled by the following blast parameters, density, profile of velocity, size and hardness of the abrasive particles[6]. The parameters of density, size and hardness of the abrasive particles can be changed by using different abrasive particle mediums of which many are commercially available. The profile of velocity of the abrasive particles can be changed by altering turbine settings which blast the abrasive particles onto the surface of the work piece. Once these parameters are set the level of material removal will then depend on the blast time.

To provide a protective coating the extrusion whether abrasive blast or etched is then anodized. Anodising is a controlled electro-chemical process that uniformly creates a thick oxide film as part of the aluminium itself. Generally, the greater the thickness of oxide the greater the ability to withstand harsh corrosive conditions[7]. Products are anodised in H2SO4 at18°C±5 and rinsed. The anodic oxide layer is generally between 5 and 20 µm. The thicker the oxide layer the greater the protection from environmental conditions. A study by [8] found that reflectance is slightly decreased by the oxide film. Because the oxide film is relatively transparent any defects would be visible if present before anodizing. In addition the defect visibility would be slightly reduced because of the lower reflectance of light.

1.2. Streaking

This study is based around a common defect of aluminium extrusions. This defect is known as streaking or flow lines (referred to as streaking in this study) and consists of light or dark bands stretching along the length of the extrusion. The type of streaking examined in this study is location specific streaking not streaking types which are explained in section 1.4. Location specific streaking is located around areas of changing cross sectional thickness and is the most widespread form of streaking. Figure 1-7 below shows location specific streaking on an AA6060 anodized aluminium extrusion. The streak has occurred in the region of the screw ports.

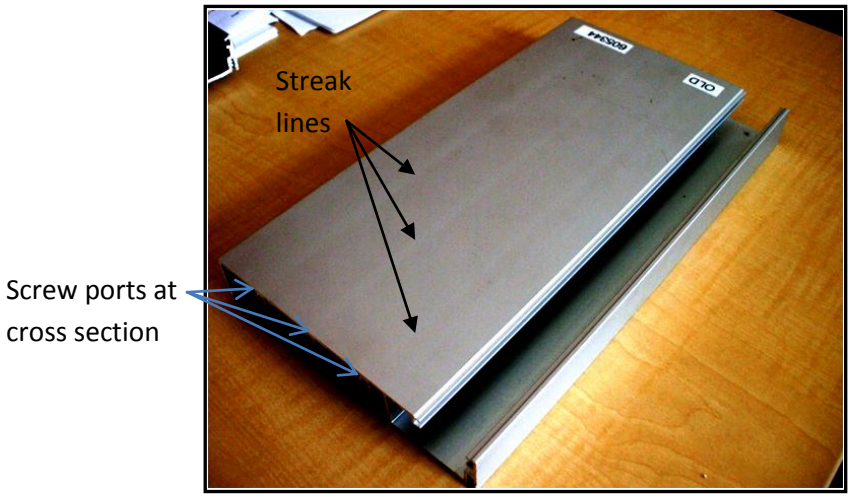

Figure 1-7 Streaking on an anodised AA6060 extrusion from Fletcher Aluminium

The light or dark shade which can be referred to as glossiness may vary depending on the case of streaking causing either low or high gloss bands. Further examples of location specific streaking are shown in Figure 1-8 (a) and (b). From these examples of location specific streaking it can be seen that the streaking originates around areas of greater cross sectional thickness and hence greater deformation.

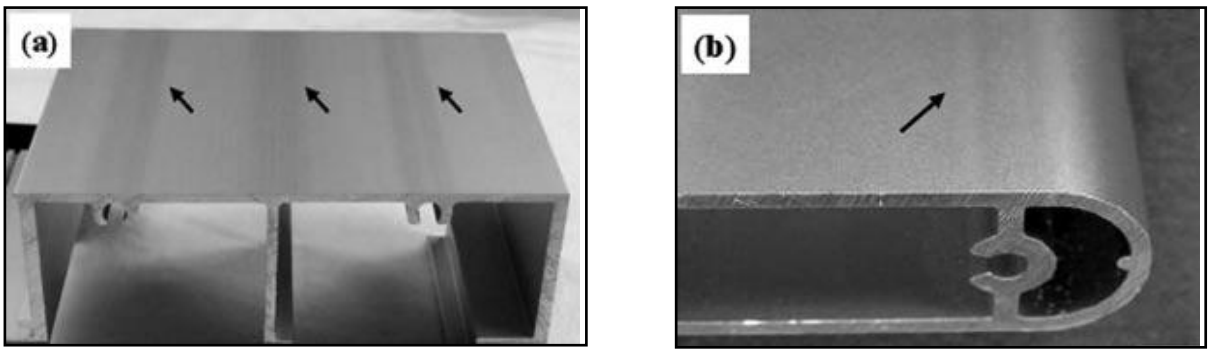

Figure 1-8 Streak Defects on anodized aluminium extrusions (Arrows identify location of streak band)[9]

1.3. Roughness – The Optical Origins of Streaking

The most widely held opinion and also the most probable reason for varying surface gloss is due to topographical differences in and out of the streak region. Streak defects can be detected by the naked eye due to the difference in surface gloss of the streak compared to the surrounding extrudate [9]. The factors that affect surface gloss are the refractive index of the material, the angle of incident light, and the surface topography [1]. Since the refractive index of a material and the angle of incident light are constant throughout the surface of the material the intensity and diffuse reflectance of light causing altered surface gloss is dependent on the surface topography of the final surface. Materials with smooth surfaces

appear glossy while very rough surfaces reflect no specular light and appear matte [9]. When surface roughness varies down to the micrometre the specular reflectance of light is affected [9].

Zhu et al [9] found that until the surface roughness reaches 0.2µm glossiness decreases sharply and then after 0.2µm the glossiness decreases at a reduced rate as shown in Figure 1-9. As can be seen from Figure 1-9 only small differences in roughness in and out of the streak region could cause considerable differences in surface gloss. Since there are not any other identified mechanisms for differences in surface gloss it can be concluded that it is most likely that the root cause of streaking must cause a topography difference in and out of the streak regions.

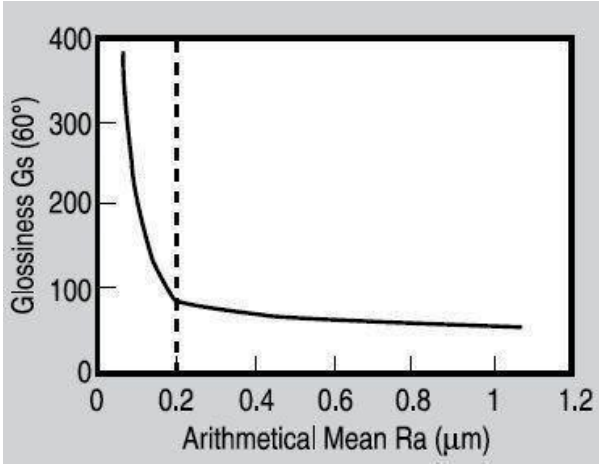

Figure 1-9 Relationship between arithmetic mean roughness, Ra and glossiness, Gs[9]

1.4. Defining a Streak

Previous literature has labelled many surface variations on extrusion products as streaking. In this study however streaking is more clearly and narrowly defined as for many of these cases the mechanism which causes the streaking is simply due to methods or techniques employed during extrusion manufacturing. Ultimately these methods may cause a compositional difference in different areas of the extrusion. If this compositional difference causes a differing etching response then the topography may differ causing different surface gloss in different regions of the extrusion. The type of streaking being investigated in this study is NOT due to extrusion manufacturing processes or techniques but rather differing thermo mechanical conditions created during extruding due to changing cross sectional thicknesses of extrusion designs. The following paragraphs explain the theory behind

streaking due to methods or techniques employed during extrusion manufacturing which can be eliminated through good extrusion manufacturing knowledge and practices.

The first issue related to poor extrusion manufacturing processes or rather the techniques employed is billet quality. The factors which can affect billet quality are inhomogeneous chemical composition or microstructure of the billet and billet contamination. The first factor which may cause material related streaking is an inhomogeneous chemical composition or microstructure of the billet, which when surface segregation occurs may produce regions of differing colour on the extrusion surface. Surface segregation occurs during the casting of the billet. The billet is then pushed through the die in the extrusion manufacturing process creating a length of extrusion. To define surface segregation it is a composition difference between the bulk material and its surface and is common in alloys [10]. The mechanisms for surface segregation during the billet casting process are exudation (enriched metal is forced through partly solidified metal), inverse segregation (wall effect, after-feeding of solidification shrinkage) and meniscus segregation (overflow due to solidification towards hot-top) [11]. This surface segregation which results in an altered surface microstructure of the billet can then cause a varying surface microstructure of the extrusion.

Another factor which may have the same result as surface segregation and cause a varying surface microstructure of the extrusion is a surface chill zone of the billet. Surface chill is also formed during billet casting due to rapid cooling using mechanisms such as water spray. This casting process is known as direct chill casting and is the primary casting process for aluminium alloys [12]. This surface chilling forms a different microstructure on the surface when compared with the billet core. Remedies such as surface scalping are used to remove surface chill. Overall good billet casting processes can eliminate surface segregation and surface chill. These types of surface variations on extrusion products are classified as billet streaks. Other causes of billet streaks are due to billet quality and the inflow of contaminations (e.g. billet skin), lubricant oil, oxidized metal, inclusions and foreign materials which cause a different etching response from the aluminium matrix and imperfections to form [9]. An example of a streak due to billet skin is shown in Figure 1-10. The billet skin contains enrichment of Mg_2Si and AlFeSi intermetallic particles. When etching occurs there is a dissolution of the Mg_2Si precipitates and detachment of AlFeSi particles forming etching pits [9].

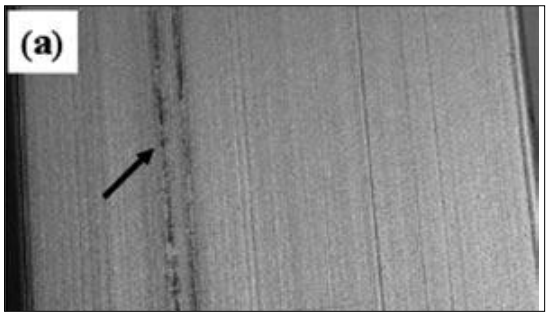

Figure1-10 - Streak due to billet skin

The above outlined streaking is due mainly to poor billet manufacturing processes which can be prevented and is known as billet streaks. In addition billet streaks can be caused by techniques employed during the extruding process. These billet streaks occur when welding two billets in a continuous extrusion process and when changing from one alloy to another. The first factor relating to welding of billets is due to the problem of entrapment of billet skin [9]. This occurs when two billets are welded in a continuous extrusion process and the end of the previous billet contains billet skin. For a solid section, the dirty welding interface is extended as a conical interface, and then the transverse weld line is developed as a sub-surface line in the cross section [9]. For a hollow extrusion, a separate transverse weld is carried through each port of the die, forming a longitudinal weld line.

The second factor due to the extrusion process which can cause inhomogeneous distribution of surface imperfections is the mixing of alloys. This can be caused due to the fact that some hollow dies have a big pre-chamber and when changing from on alloy to another, the weld area may have a mixture of two different alloys [9]. Figure 1-11 shows streaking due to this mechanism.

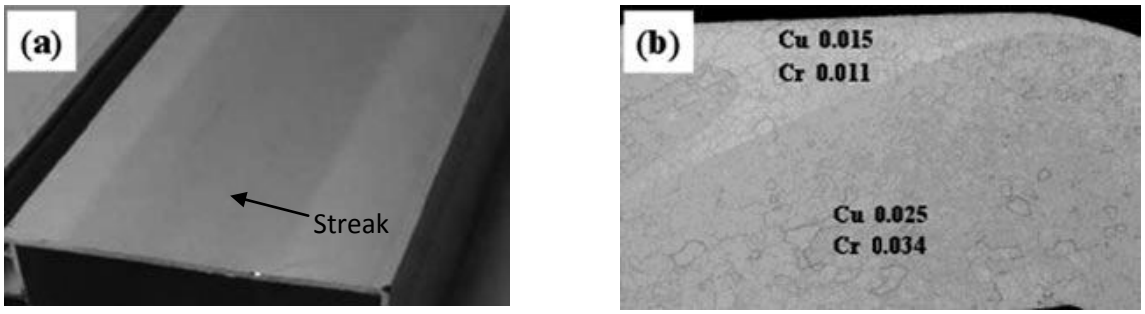

Figure1-11 (a) Streak on the aluminium extrusion (b) Differing colours show the compositional differences in the streak region at the cross section of the extrusion shown in (a)[9].

The last streaking mechanism due to the extrusion process is due to the ram approaching the extrusion too close during the end of the stroke. The surface of the original billet can flow

into the core of the extrusion and stretch to the surface of the extrudate, ultimately resulting in streaking [9]. Obviously all these types of streaking can be eliminated by using good extrusion manufacturing techniques. This study will NOT investigate these types of streaking but rather streaks related to varying thermomechanical conditions due to changing cross sectional thicknesses of an extrusion design as previously mentioned. This type of streaking will be referred to as thermomechanical streaking.

1.5. Possible Causes of Thermomechanical Streaking

As previously mentioned streaking is characterized by narrow bands with a different surface gloss from the surrounding material [13]. In addition the different surface gloss is most likely due to a varying topography in and out of the streak region. The two main features which may cause a varying topographical component in and out of the streak region from literature are grain boundary grooves and surface pits. If either of these microstructural features differs in and out of the streak zone an altered reflectance of light and differing surface gloss may result. Figures 1-12 and 1-13 illustrate examples of surface pitting and grain size/grain boundary grooves on surface topography in and out of a hypothetical streak region.

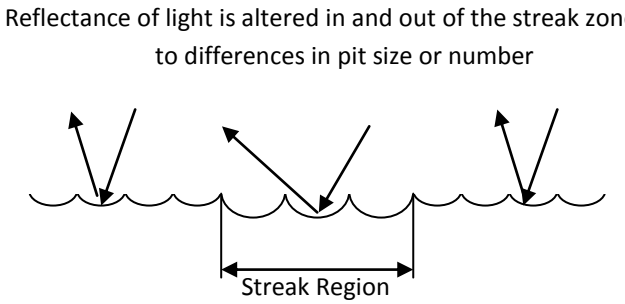

Figure 1-12 Schematic of possible differences in surface pitting occurring in and out of the streak

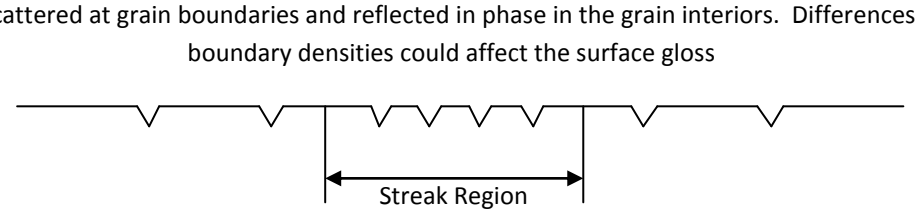

Figure 1-13 Schematic of more densely distributed grain boundary grooves in the streak region

In addition these two factors can be affected by thermomechanical conditions which may differ in and out of the streak region. For example grain size can vary on the surface of the extrusion due to inhomogeneous distribution of temperature during the extrusion process.

Also intermetallics may distribute differently in and out of the streak regions also due to inhomogeneous distribution of strain rate or temperature. These intermetallics will in turn affect the etching response in the form of varying distributions of etching pits or the degree of grain boundary groove severity. Finally grain orientations may differ in the streak region due to differing strain rates in regions during extrusion. Grains in a preferred orientation in the streak region will cause the surface to be etched differently. It is important to note streaking often only becomes apparent after etching and anodizing which makes identifying the root cause or causes difficult.

1.5.1. Grain Boundary Densities

Grain boundary grooves are formed during etching where preferential attack of grain boundaries occurs while the surrounding aluminium matrix remains relatively intact. Etching is a highly common process in extrusion manufacturing to promote a matte surface and overall attractive extrusion product. Figure 1-14 below shows images of before and after etching. As can be seen from Figure 1-14 (a) before etching, the surface is an un-uniform gloss and die line features are prominent across the surface. Figure 1-14 (b) after etching shows the surface is a uniform surface gloss and die line features have been removed. This matte and die line free surface finish is appealing to the customer and hence shows why etching is necessary especially for extrusions which are to be used as decorative finishes.

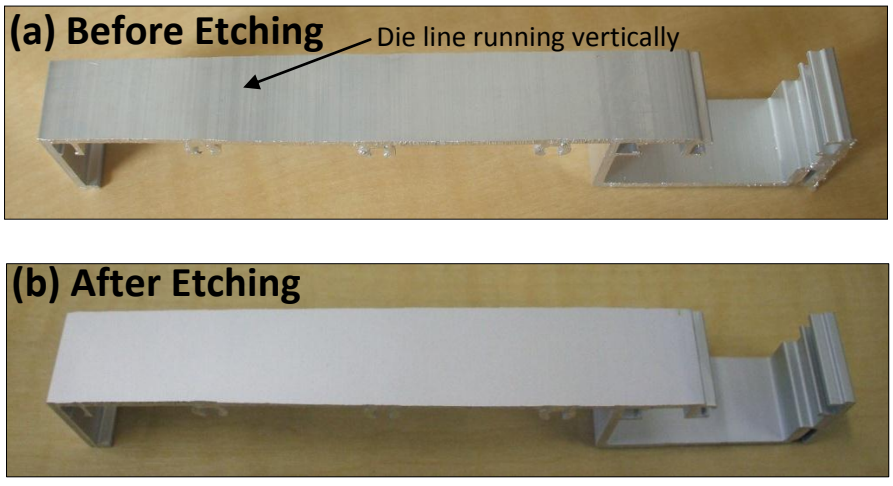

Figure 1-14 Surface Finish before and after etching

Most commonly etchants used are sodium hydroxide based which preferentially attacks grain boundaries and intermetallics and also has a matting effect on the aluminium matrix as can be seen from an etched surface shown in Figure 1-15. If grain size differs in and out of the streak region the distributions of grain boundary grooves will also differ possibly causing an

altered reflectance of light and subsequent differing surface gloss in and out of the streak region.

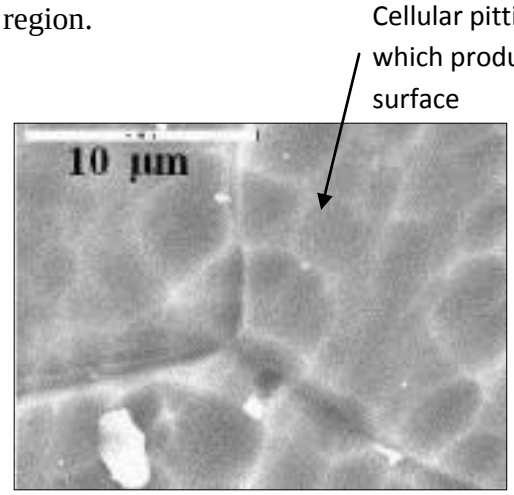

Figure 1-15 Sodium Hydroxide etching AA6060[14]

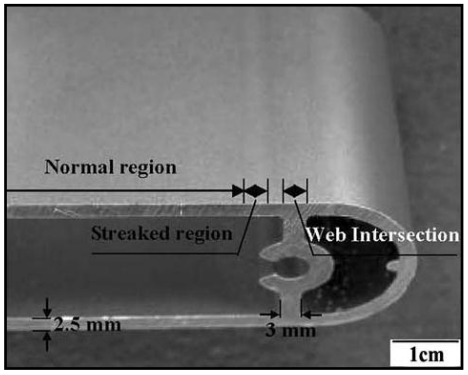

Figure 1-16 Extrusion relating to images shown in figure 1-17 [13]

The theory behind this altered surface gloss is that at grain boundaries instead of reflecting light in phase as in the grain interior the light is scattered which may alter the surface gloss. Knowing that the fraction of grain boundary grooves is linked to the grain size an investigation was made of possible grain size differences in and out of the streak regions from findings made by other researchers. Grain size on the surface of aluminium extrusions usually changes from location to location due to large plastic deformation and inhomogeneous distribution of temperature [13]. It was found by Zhu et al [13] that grain size decreased in the following order in different areas of the extrusion shown in Figure 1-16.

(a) Normal extruded region
(b) Streaked Region
(c) Web intersection region

Figure 1-17shows light optical microscopy (LOM) images of the grain microstructure of this extrusion in the (a) Normal region, (b) Streaked region and (c) Web intersection region clearly showing grain size reduction in descending order. It can be seen from extrusion shown in Figure 1-16 that where the largest difference occurred in grain size between the normal and web intersection areas there was no visible difference in surface gloss.

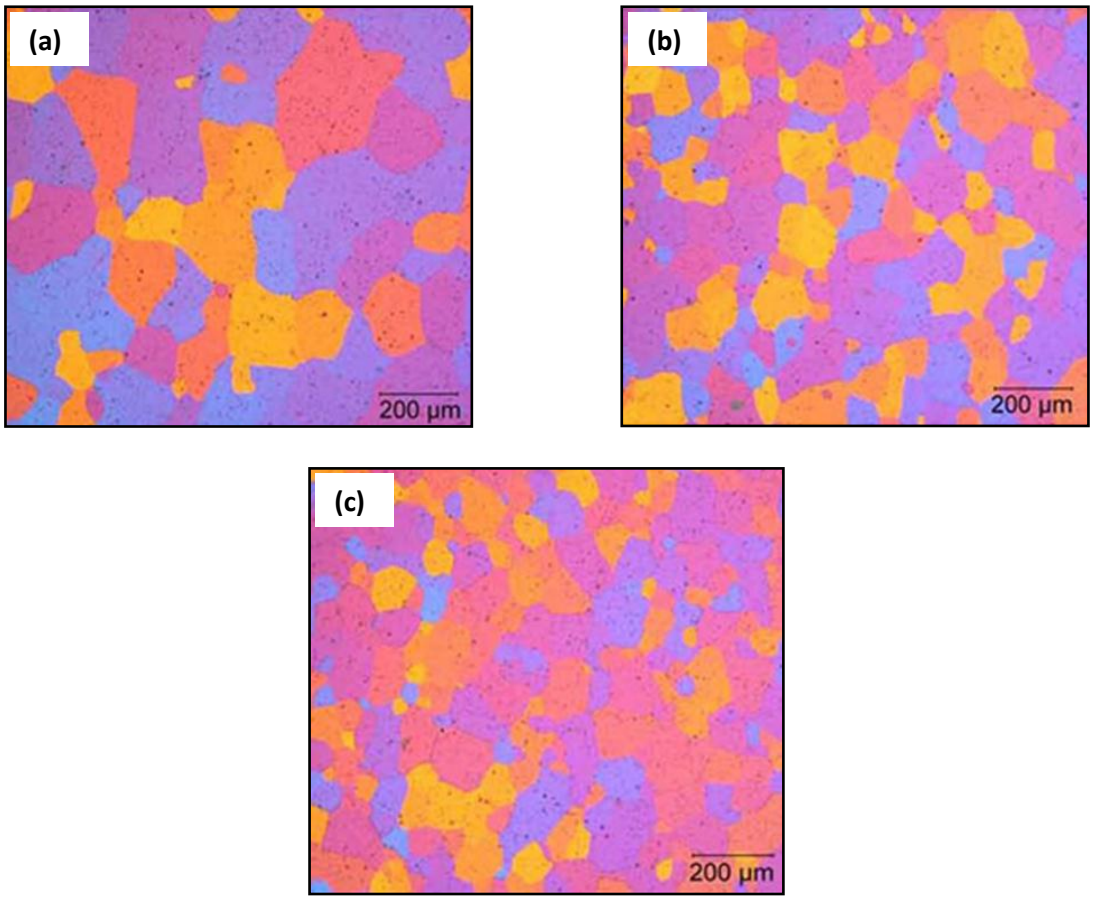

Figure 1-17 LOM Microstructure (a) Normal Region; (b) Streaked Region (c) Web Intersection area [13]

From this it can be concluded based on the assumption that the extrusion in Figure 1-16 has been etched to reveal grain boundary grooves, and also that the LOM images were taken on the surface and not the cross section, that for the degree of differing distributions of grain boundary grooves in the different regions this was not the cause of streaking. In another study of streaking [15] it was also claimed that grain size differed in and out of the streaked regions. It was claimed that the grain size on the surface increases when moving out of the streak zone from the images shown in Figure 1-18. It must be noted that this is not clearly shown by the images and hence may not be correct. It seems that the method of reviewing grain size at the cross section is not as satisfactory as top down grain size inspection of the surface.

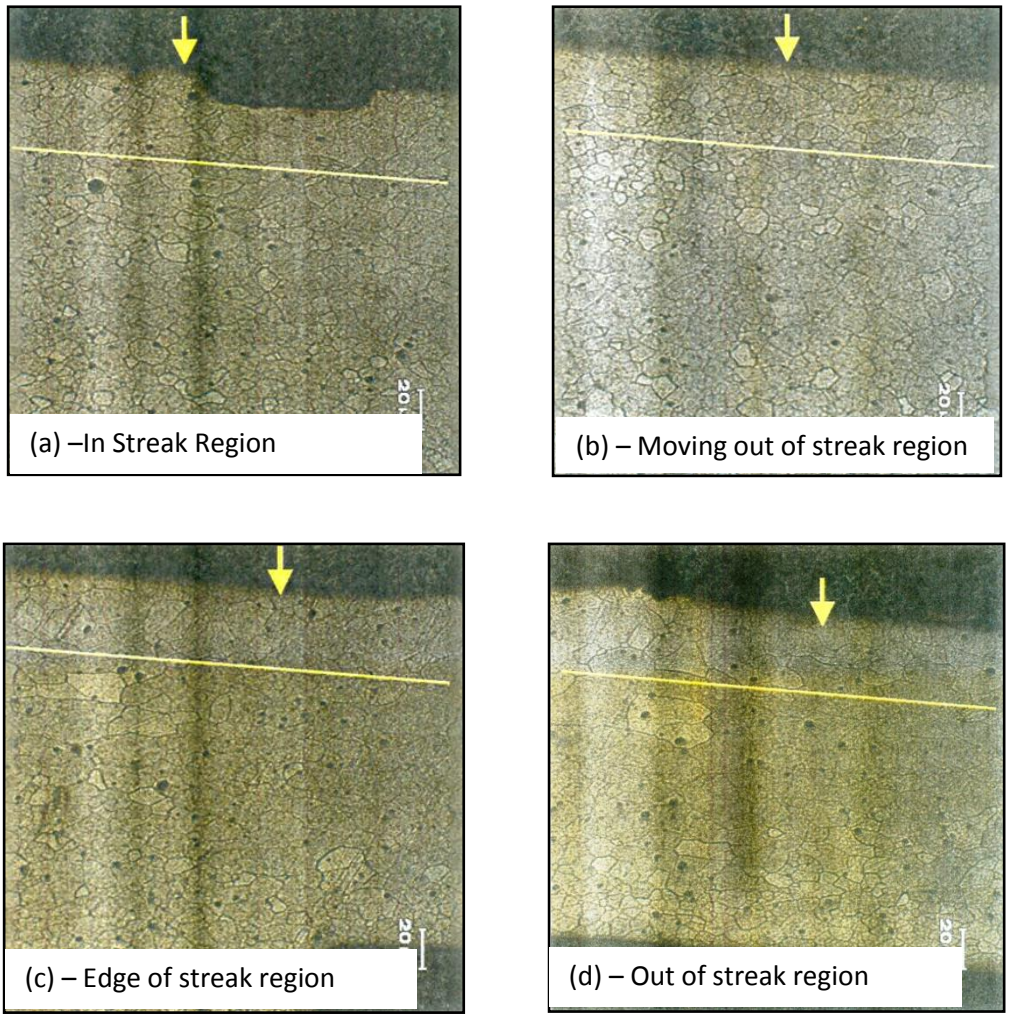

Figure 1-18 Grain Size on the surface of the extrusion: (a) Inside streak region, (b) moving away from streak region, (c) At the edge the streak region, (d) Out of streak region. [15]

Overall it cannot be proved that grain size and subsequent differing distributions in grain boundary grooves after etching does or does not cause streaking. However to better clarify and prove this more information on surface finishing of the extrusion and methods used to acquire these images is needed.

1.5.2. Grain Boundary Groove Severity

Another possible cause of streaking related to the grain is grain boundary groove severity. If the severity of grain boundary grooves differs in and out of the streak regions an altered reflectance of light and streaking may result. This altered reflectance of light can be caused by light being less scattered by low severity grain boundary grooves compared to high severity (deep and large width) grain boundary grooves and ultimately a different surface

roughness. The following gives a description of the possible mechanisms which occur to alter grain boundary severities from literature.

The main possibility which may provide a mechanism to alter the severity in grain boundary grooves is the distributions of intermetallics and their subsequent etching response. Grain boundary grooves are formed due to a preferred grain boundary attack (i.e. the grain boundaries dissolve more quickly than the grain matrix during etching) [9]. There are factors which can decrease the difference in dissolution rates between the grain matrix and the grain boundaries.

The most serious of these factors is the presence of intermetallic particles. In 6xxx series alloys, the major intermetallic phases are primary Fe-rich intermetallic particles and Mg-Si primary particles and/or precipitates [16]. In 6xxx aluminium alloys, coherent $\beta'' - Mg_2Si$needles, partly coherent $\beta' - Mg_2Si$ rods, or incoherent $\beta - Mg_2Si$ equilibrium phase particles precipitate in the grain interior depending on thermo-mechanical extrusion conditions and on subsequent cooling and aging conditions[1]. Figure 1-19 shows optical micrograph (OM) images (a),(c),(e) and scanning electron microscopy images (b), (d), and (f)in which (a) and (b) are part of the normal extruded region, (c) and (d) are from the web intersection region and (e) and (f) are from the streak region. The coarse particles are identified as Fe-rich intermetallic particles and the small white particles are identified as Mg-Si particles. It can be seen from the images there was no significant difference in the amount of Fe-rich particles. There was however a pronounced difference in the quantity of Mg-Si particles in the streak region images (e) and (f). Zhu *et al* [16] verified this in another extrusion in which more Mg-Si particles were observed in the streak region than the normal extruded region and web intersection regions.

Hence if intermetallic particles such as Mg-Si particles are present in great enough numbers that they were able to decrease the difference in dissolution rates between the grain boundaries and grain matrix, then they could decrease the width and depth of the grain boundary grooves and perhaps even prevent their formation [16]. This altered severity in grain boundary grooves in and out of the streak regions may alter the reflectance of light and cause streaking. Overall any differences in temperature could vary the distributions of intermetallics and affect grain boundary severities. It must be said however that evidence of differences in grain boundary severity causing streaking has not been presented in literature.

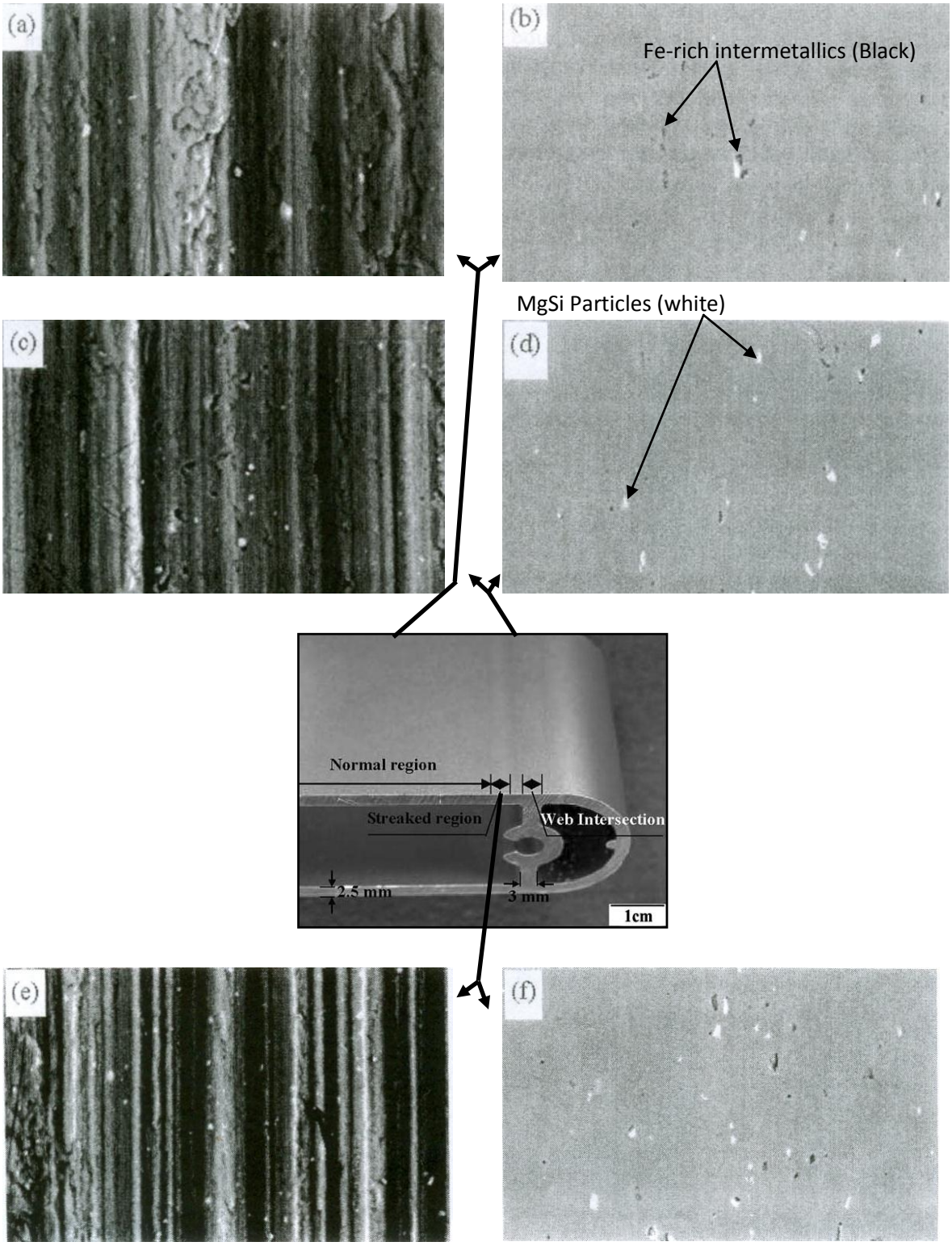

Figure 1-19 The distribution of intermetallic particles in different locations of the extrusion (a) and (b) normal region, (c) and (d) web intersection region and (e) and (f) streak region[16]

Zhu et al [13] also tried to find a correlation between grain size and the severity of grain boundary grooves. From Figure 1-20 it can be seen that the severity of grain boundary grooves in the streak region (b) was lower than in the normal region (a) or web intersection

region (c). However from comparing images (a) –Normal region and (c) - web intersection region the regions in which grain size differed the most it can be seen that the grain boundary groove severity is not affected by grain size. Therefore from this finding it is most likely grain size does not play a role in grain boundary groove severity which when differing in and out of the streak region may cause streaking. Overall no definite correlation for intermetallics or grain size causing differing grain boundary groove severities could be found in literature.

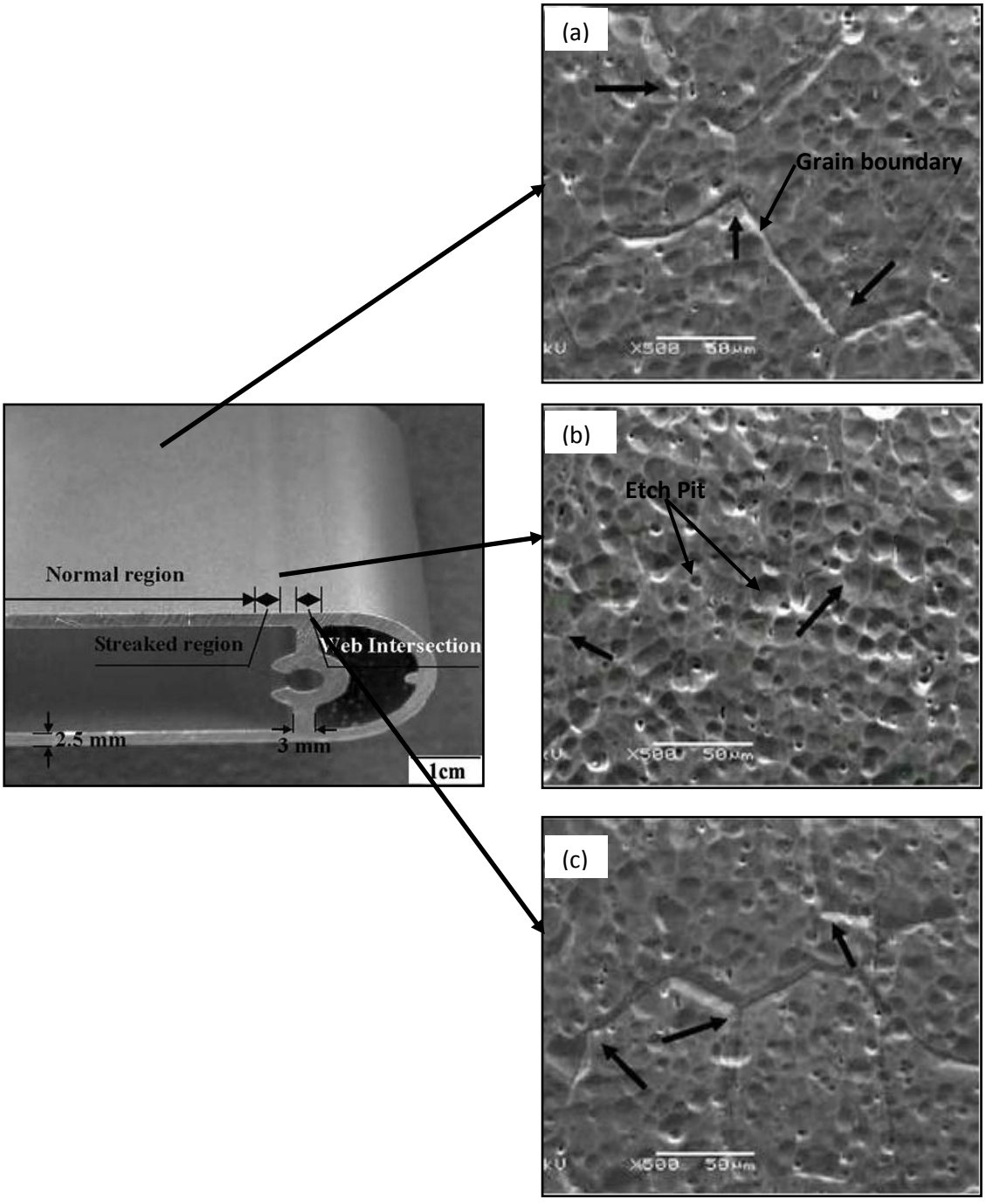

Figure 1-20 Grain boundaries (a) - normal region (b) – Streaked region (c) – web Intersection region

1.5.3. Etching Pits

Etching pits are created on the extrusion surface during etching due to different reaction rates between intermetallic particles or inclusions and the aluminium matrix [16]. Primarily intermetallics can be distributed differently in different regions of an extrusion due to inhomogeneous deformation or temperature distribution. Etching pits are a highly possible cause for streaking because of their effect on surface topography. If etching pit distributions differ in and out of the streak region their effect on the surface roughness could change the surface gloss causing streaks. An example from literature of possible streaking caused by etching pits is shown in Figure 1-20. It can be clearly identified that the streak region image Figure 1-20 (b) has increased pitting compared to the images from outside the streak region.

Pits may alter the reflectance of light causing differing surface gloss in and out of the streak region and streaking to occur. The mechanisms which can cause etching pits are as follows. In 6xxx series alloys, the major intermetallic phases are primary Fe-rich phases e.g. $Al_3Fe, \alpha - AlFeSi$ and $\beta - AlFeSi$ and precipitation phases based on magnesium silicide ($\beta - Mg_2Si$ equilibrium phase, $\beta'' - Mg_2Si$ intermediate phase, $\beta' - Mg_2Si$ intermediate phase) [1]. During etching the Fe-rich intermetallic particles have a higher electrochemical potential compared to the aluminium matrix, thus acting as cathodic reaction sites for hydrogen evolution and stimulating anodic dissolution of the surrounding aluminium to form aluminate [9]. The larger primary Fe-rich intermetallic particles forms deeper etch pits which survive further dissolution of the surface. As dissolution continues, intermetallics can be lost from the surface by undercutting and the pits continue to grow larger [9]. As such the size of the etching pits is always larger than the size of the intermetalllics and the detachment of the Fe-rich intermetallic particles from the Al matrix results in the formation of large etching pits with size up to 10µm diameter on the etched surface [16].

In contrast $\beta - Mg_2Si$ particles can act as anodes during alkaline etching, resulting in the particles dissolving in preference to the aluminium matrix [1]. Because of this unlike the dissolution caused by Fe-rich intermetallics the etch pits related to$\beta - Mg_2Si$ are directly related to the original size of the particles. In addition Mg_2Si precipitates can make a significant contribution to achieving a matte finish due to a high density of small pits created by the particles superimposed on the larger pits caused by primary iron-rich particles [9]. The heat treatment history of the alloy and extrusion conditions determine the morphology of coarse $\beta - Mg_2Si$ precipitates and are thus expected to have an effect on the distribution of

small etching pits. Figure 1-21 shows the morphology of etching pits when a different Fe compositional percentage is used. It shows a marked increase in etch pit depth for the sample with greater Fe percentage in the composition.

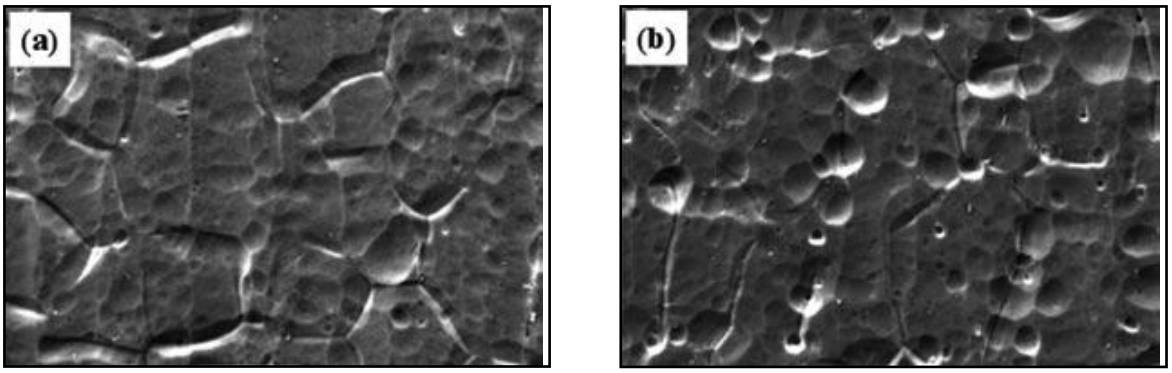

Figure 1-21 Morphology of etching pits in anodized sample with (a) 0.14 wt.% Fe and (b)0.29 wt.% Fe

In essence streaking may be caused by inhomogeneous distributions of intermetallics due to inhomogeneous deformation or temperature distribution, which etch out during etching creating pits which may vary in and out of the streak region. Apart from the evidence shown in Figure 1-20 no one has pinpointed etching pits as the main mechanism which causes thermomechanical (location specific) streaking. The large differences in surface topography it may cause in and out of the streak region make it a very possible mechanism for causing streaking. The literature on this however is very poor even though there is suggestive evidence this may be a likely cause for streaking.

1.6. Electro-polishing and Electro-etching

For the investigation of streaking, electro-polishing and electro-etching techniques were used. The following gives an overview of the mechanics behind each process from literature which is in fact essentially the same except a different voltage or current density setting is used. For electro-etching a lower voltage is used where etching will occur and for electro-polishing a higher voltage is used where the main mechanism is polishing but no so high that pitting will occur. A typical although exaggerated graph of an electro-polishing/electro-etching setup is shown in Figure 1-25. Referring to Figure 1-25 the following outlines the mechanisms that take place in each zone. Firstly in zone I the primary mechanism is dissolution of metal and in this region etching occurs. In zone II the current and voltage are such that a passivation layer forms. In zone III the passivation layer becomes stable and the metal is eroded by diffusion through the passivation layer. When the dissolution of metal occurs in zone III the peaks of the surface are eroded preferentially thus smoothing and polishing the surface. In

zone IV the passivation layer breaks down as oxygen evolution occurs at the surface. In this zone a pitting will occur.

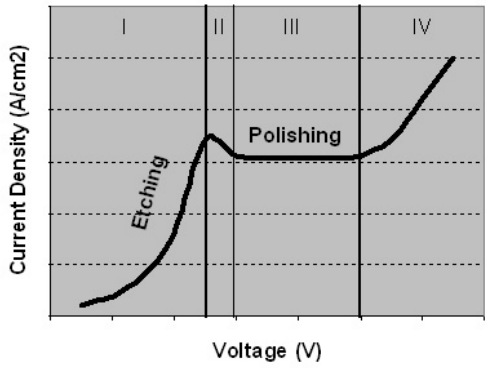

Figure 1-22 Typical current density Vs. Voltage graph obtained from an electro-polishing setup[12]

1.7. Aim

The objective of this research is to pinpoint the mechanism of streaking which causes a topography difference. If there are different topographic features it must be identified which feature is the primary cause for an altered reflectance of light in and out of the streak region and thus streaking to occur. To get a better understanding of the evolution of streaking different levels of material will be removed from the extrusion surface and then the streaking formations observed. No other research has identified if different streak formations can be observed or if the streak gloss or dullness differs after different levels of material removal. Therefore a model of streaking will be obtained for the particular extrusion product being investigated. This will allow for better knowledge of mitigating or preventing streaking.

2. Methodology

This chapter explains the experimental methods used to carry out the investigation of streaking. To investigate streaking, product type 605344 manufactured at Fletcher Aluminium was studied from mill finish to anodized samples. This product exhibited thermomechanical (location specific) streaking and as such the streaking occurred in regions of changing cross sectional thickness. To investigate streaking on this product mill finish samples were sectioned in an identical manner and subjected to the following sample treatments.

- Electro-polishing & Electro-etching
- Chemical etching
- Mechanical polishing

Electro-polishing and electro-etching is described in section 1.6 and involves creating a current density in a chemical solution to attack the surface of the AA6060 extrudate and smooth and etch the surface respectively. Chemical etching on the other hand is conducted without a power source and attacks and etches away the surface microstructure of the AA6060 extrudate. Finally mechanical polishing is achieved using rotary grinders with different grit pads to grind away and smooth the surface. After conducting these treatments the samples were then viewed using optical and scanning electron microscopy on the surface of the samples in and out of the streak regions. To analyse the images acquired relating to surface features such as grain size, grain boundary densities and surface pitting, image J analysis and the Heyn intercept procedure were used. Finally to further prove that these surface features may vary in and out of the streak region, roughness testing was conducted.

2.1. Sample Conditions

The following table outlines the sample treatments and the subsequent various material investigation techniques undertaken in terms of etching and then examination. Twenty one samples were created all with varying treatments and then examined using a variety of methods as shown in Table 2-1. For the etch solution column, etch solution - 1 refers to etching in Graff and Sargent's etchant and etching solution - 2 refers to etching in a proprietary etchant supplied by Henkel which main ingredient consists of sodium hydroxide.

Table 2-1 - Sample conditions and analysis

Sample	Mill Finish	Electro -Polish	Duration (min)	Mechanical Polish	Duration (sec)	Electro -etch	Duration (min)	Chemical etch	Etch solution	Duration (min)	Examination &Analysis	Sample figures
S1	×										-Optical Microscopy setup 1 -Roughness testing	Fig 3-1,3-2, 3-6
S2	×	×	2									Fig 3-3,3-4
S3	×					×	6min				-Optical Microscopy setup 1 -Image J analysis -Heyn Analysis	Fig 3-8,3-9, 3-10
S4	×	×	1					×	1	18	-Optical microscopy setup 1 -Image J analysis	Fig 3-21(a)
S5	×	×	1					×	1	26		Fig 3-21(b)
S6	×	×	1					×	1	36		Fig 3-21(c)
S7	×	×	1					×	1	48		Fig 3-21(d), Figure 3-23, Figure 3-24

Sample	Mill Finish	Electro-Polish	Duration (min)	Mechanical Polish	Duration (sec)	Electro-etch	Duration (min)	Wet Etch	Etch solution	Duration (min)	Examination & Analysis	Sample Figures
S8	×	×	1					×	1	62		Fig 3-21(e), Fig 3-27, Fig 3-28
S9	×	×	2					×	1	48	-Optical microscopy setup 1 -Image J analysis	Fig 3-21 (f)
S10	×	×	2					×	1	62		Fig 3-21(g), Fig 3-35, Fig 3-36
S11	×							×	2	2.5	-Optical microscopy setup 2 -Scanning electron microscopy -Image J analysis	Fig 3-39(a), Fig 3-40, Fig 3-41
S12	×							×	2	5		Fig 3-39(b), Fig 3-44, 3-74, 3-75, 3-76
S13	×							×	2	7.5		Fig 3-39(c), Fig 3-46, Fig 3-47, 3-48
S14	×							×	2	10		Fig 3-39(d), Fig 3-62
S15	×							×	2	12.5		Fig 3-39(e), 3-64,3-65, 3-77, 3-78,3-79
S16	×							×	2	15		Fig 3-39(f) Fig 3-67, Fig 3-68
S17	×							×	2	17.5		Fig 3-39(g) 3-70, 3-71,3-80,3-81,3-82

Sample	Mill Finish	Electro-Polish	Duration (min)	Mechanical Polish	Duration (sec)	Electro-etch	Duration (min)	Wet Etch	Etch solution	Duration (min)	Examination & Analysis	Sample Figures
S18	×							×	2	20		Fig 3-39(h)
S19	×	×	1	×	10			×	1		-Optical microscopy setup 1 -Scanning electron microscopy -Image J analysis	Fig 3-49, Fig 3-50
S20	×	×	1.5	×	10			×	1			Fig 3-52, Fig 3-53
S21	×	×	2	×	10			×	1			Fig 3-55 Fig 3-56

2.2. Material

The product being investigated is known as product type 605344 as shown in Figure 2-1 at the cross section. This extrusion profile is a high volume product and was found to exhibit prominent streaking at each of the three points indicated by vertical arrows.

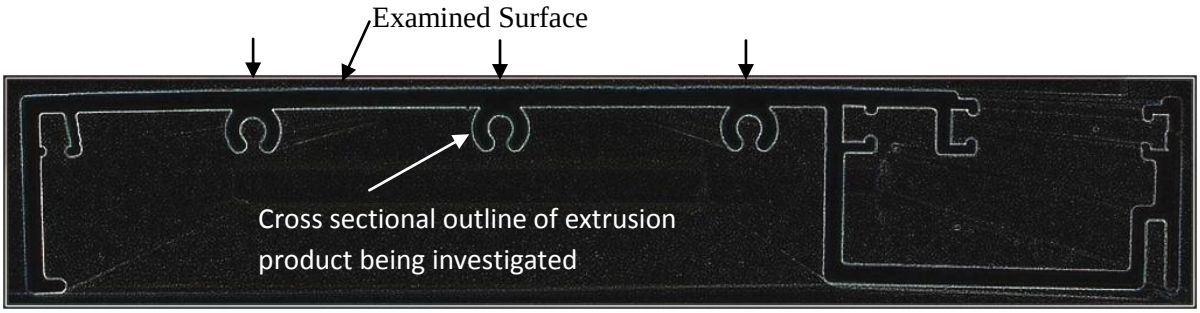

Figure 2-1 Outline of the extrusion Product being investigated

This product is extruded from a billet of AA6060 material. See Table 1 (page 1) for the AA6060 specification. To extrude this product the billet was first preheated to approximately 400°C. The billet was then loaded into the extrusion press and then pushed through the die at 27m/min.

After extruding the product was stretched to straighten the extruded lengths and bring the dimensions into specification. This is achieved by clamping at either end of the extrusion and applying a tensional force. The stretching elongates the metal by approximately 1% of its original length and plastic deformation takes place. After stretching the lengths were sawed to remove the crushed ends from stretching and cut into lengths. This product is known as mill finish and no other processes were carried out such as surface finishing.

2.3. Sample Sectioning

For all analysis except for the initial analysis of the as-extruded product the section of the extrusion from which samples were cut from on product type 605344 was the same. Figure 2-2 below highlights in red at the cross section the section which was cut from the extrusion. As can be seen the focus of the study will be on streak 1 which is identical to streak 2 and 3.

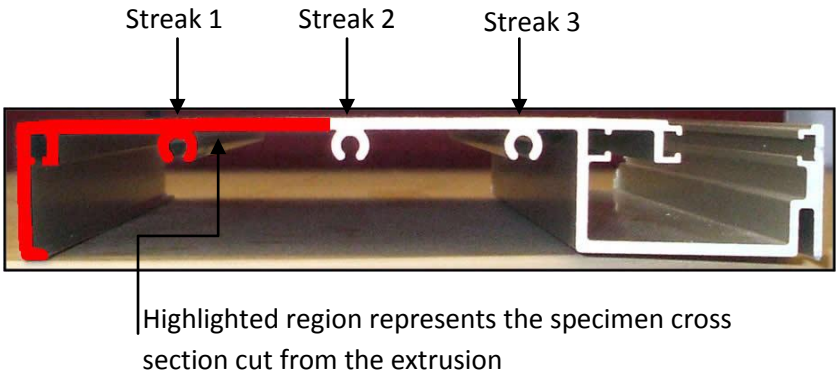

Figure 2-2 Specimen Cross section highlighted by red

To gain further perspective of the specimen sectioning, Figure 2-3 below shows a top down view of the sample from a short section of the extrusion. The box encloses the approximate total area of extrusion which comprises one sample.

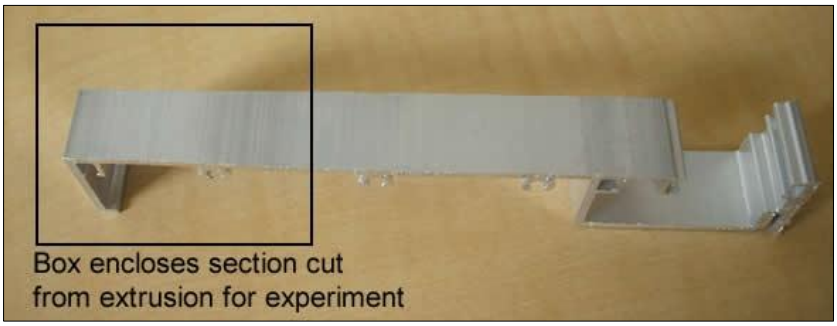

Figure 2-3 Total specimen section area

2.4. Sample Treatments

To investigate different aspects which may cause streaking various sample treatments were used. From Table 2-1 it can be seen that the following sample treatments were employed on the various samples:

- Electro-polishing
- Electro-etching
- Wet etching
- Mechanical Polishing

2.4.1. Electro-polishing and Electro-etching

For the grain size investigation samples were electro-etched to reveal grain boundaries and not significantly etch out any other features of the surface. In addition, to smooth the surface of the mill finish extrusion and allow better quantification of differences in and out of the

streak region electro-polishing was employed. To conduct electro-etching/polishing a setup as shown schematically in Figure 2-4 was used.

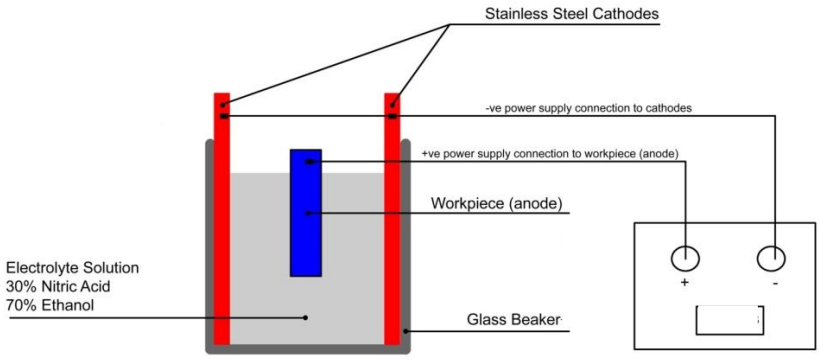

Figure 2-4Schematic of Electro-polishing Setup

Table 2-2 outlines the solution, voltage and current density (A/cm^2) used for both electro-polishing and electro-etching. To control the voltage and current a volt and amp meter was used connected to the circuit.

Table 2-2 - Electro-polishing and electro-etching solution, voltage and current density parameters

Treatment	**Solution**	**Voltage(V)**	**Current Density ($Amps/cm^2$)**
Electro-etching	- 30 % HNO3 (Nitric Acid) - 70% C_2H_6O (Ethanol)	4.5	≈ 0.22
Electro-polishing	- 30 % HNO3 (Nitric Acid) - 70% C_2H_6O (Ethanol)	7.5	≈ 0.39

To obtain the voltage settings at which etching and polishing occurs the voltage was incrementally increased and the current recorded using digital meters. The graph obtained is shown in Figure 2-5. From this graph it is ascertained that polishing will occur between approximately 7.5 and 8.5 volts and etching between approximately 1.75 and 7.5 volts. For the electro-etching a voltage of 4.5 volts was used. As can be seen when comparing a typical electro-polishing graph as shown in Figure 1-25and the electro-polishing graph obtained

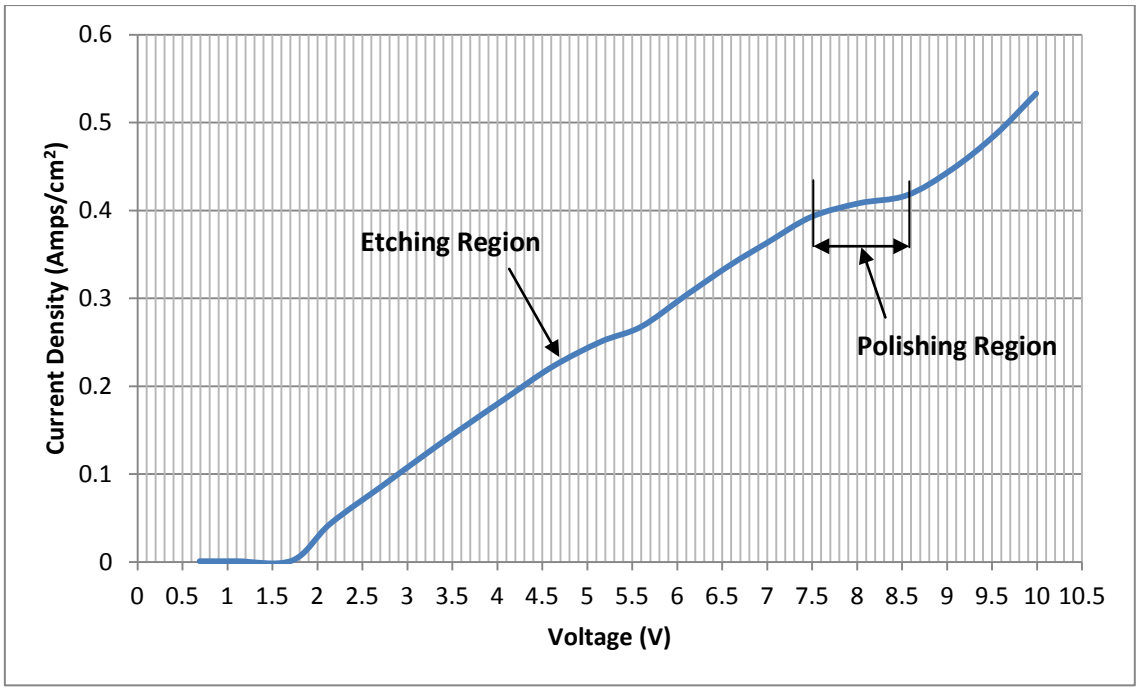

Figure 2-5Current Density Vs. Voltage Relation for 30% Nitric Acid, 70% ethanol electrolyte solution at room temperature

experimentally in Figure 2-5there is no indication of a passivation layer creation (zone II). This may be due to the electrolyte used in which the primary mechanism is etching and slight polishing is occurring at 8 volts. Another possible factor could be that the voltage increments were not small enough to pick up the passivation layer creation and subsequent increase in voltage and current.

2.4.2. Chemical Etching

To investigate the effect of etching on the surface in and out of the streak zone chemical etching was conducted on a series of specimens. In the extrusion manufacturing process chemical etching is conducted to promote a matte surface which is appealing to the customer. Table 2-3 is a table of solutions used for investigating chemical etching. Table 2-1 in section 2.2 outlines durations of etching for the etched samples.

Table 2-3 – Table of solutions for chemical etching

Etchant	Solution
Graff and Sargent's	- 84% H_2O (Water) - 15.5% HNO_3 (Nitric Acid) - 0.5 % HF (Hydrofluoric Acid) - 3g CrO_3 (Chromic Acid
Henkel P3 etch solution	- Main ingredient sodium hydroxide (other ingredients sorbitol and fume suppressant with other unknown additives)

2.4.3. Mechanical Polishing

Mechanical polishing was conducted using a rotary grinder as shown in figure 2-6 with a 2500 grit paper. The samples were held with an equal application of pressure pressing against the gritted pads to ensure an even surface polish on the specimens.

2-6 Rotary grinder

2.5. Methods of Examination & Analysis

The following outlines the methods of examination used for each of the samples. The methods employed for examination and analysis for each sample are outlined in the second to last column in table 2-1.

2.5.1. Optical Microscopy

Microscopic images taken using Optical Microscopy setup 1 were acquired using an Nikon Epiphot fitted with a Q imaging micropublisher camera as shown in figure 2-7 interfaced with Q capture pro software version 5.0.1.26

Figure 2-7 Nikon Epiphot Optical Microscope

Microscopic images taken using optical microscopy setup 2 were acquired using an Olympus BX51M fitted with an Infinity 1 camera as shown in figure 2-8 interfaced with Infinity Capture version 5.0.4.

Figure 2-8 Olympus BX51M Optical Microscope

2.5.3. Scanning Electron Microscopy

A Hitachi SU-70 scanning electron microscope (SEM) as shown in figure 2-9was used to obtain high resolution microscopic SEM images and conduct compositional analysis.

Figure 2-9 Hitachi SU-70 Scanning Electron Microscope

2.6. Grain Size Measurement Using Heyn Method

To analyse the grain size from the micrographs taken, the following Heyn Intercept Procedure was used. The Heyn Intercept procedure is a method to determine average grain properties such as size and area. The following outlines the method used to carry out this procedure.

Six images or six fields of view were taken in and out of the streak zone of grain boundary etched specimens which were etched using the electro-etching procedure outlined in section 2.5.1. Fourteen test lines with 60 micron spacing were drawn vertically from top to bottom on the six images as shown in Figure 2-10. Each time the lines cut through a grain is counted as one interception. Where the line partially cuts through a grain at either end of a test line is counted as half an interception. The total length (L) of the 14 lines was measured to be 3.85mm. The total number of intercepts for a 3.85 mm test line for one field of view isN_i.

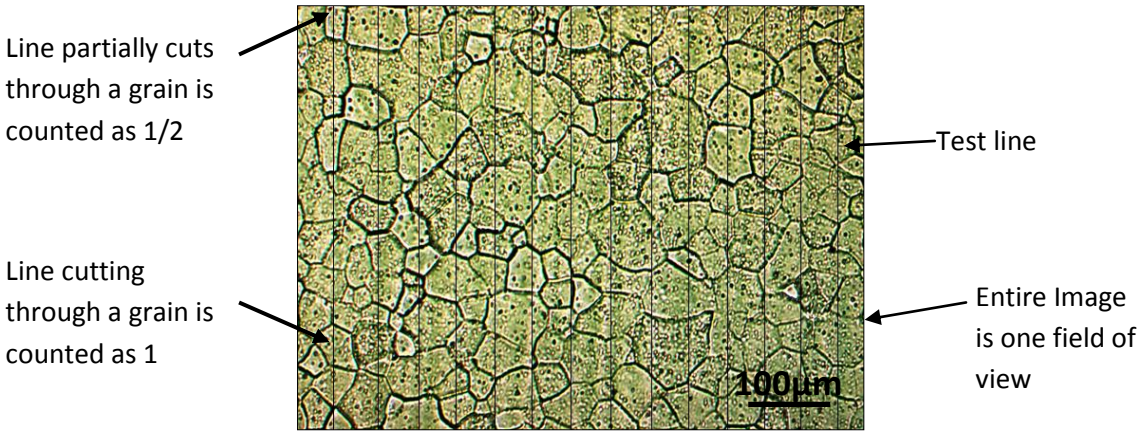

Figure 2-10 Grain Intersection Method

From the intercept data values for each field of view (N_i) the grain size number can be found which allows the average grain properties of size, area and distribution to be found. The first step to calculate the grain number is to calculate the number of intercepts per unit of test line (N_L).

$$N_L = \frac{N_i}{L}$$

The next step is to calculate the average of N_L for all fields of view. With the average number of intercepts per unit length of test line ($\bar{N}_L$) the grain size number formula can then be applied [11].

$$G = (6.643856\ log_{10}\bar{N}_L) - 3.288$$

Using the table A1 in appendix A the average grain area, diameter and distribution per 1mm unit area can then be interpolated from the data.

To check the relative accuracy of the grain size analysis using the Heyn Intercept method the following calculations were made. To ensure that the grain size analysis is relatively accurate the aim is to have the relative accuracy within 10%.

The first step is to calculate the lineal intercept length for each individual field and then the mean lineal intercept length for all fields

$$lineal\ Interecpt\ length = X_i = l = \frac{1}{N_L}$$

$$mean\ lineal\ intercept\ length = \bar{X} = \bar{l} = \frac{1}{\bar{N}_L}$$

Using the individual and the average lineal intercept lengths the standard deviation is then calculated.

$$standard\ deviation = s = \left[\frac{\sum(X_{i-}\bar{X})^2}{n-1}\right]^{1/2}$$

Using the standard deviation and table A2 in appendix A to find t, the 95% confidence interval can then be calculated.

$$95\%CI = \frac{t \cdot s}{\sqrt{n}}$$

Finally the percentage of relative accuracy is calculated by dividing the 95%CI value by the mean and expressing the result as a percentage.

$$\%RA = \frac{95\%\ CI}{\bar{X}} \cdot 100$$

The final relative accuracy must be well within 10% and/or more view fields must be added and the test line length for each field of view must be increased.

2.7. Image J Analysis of Grain Size Difference

As a secondary technique to further identify and prove if grain size difference is present in and out of the streak region grain size images where further quantified using image J software. Image J is a software program which enables features on an image to be quantified such as particles or grains. For image J analysis of grain size difference in and out of the streak region the specimens were electro-etched to etch out grain boundaries according to the method outlined in section 2.5.1. These were the same images used to conduct analysis using the Heyn intercept procedure. Microscopic grain size images were acquired from six fields of view in and out of the streak region using the microscope setup 1 shown in section 2.6.1. Using the microscopic images the grain boundaries were then traced and a map of the grain outlines produced. An example of a grain outlined image is shown in Figure 2-11 from one field of view.

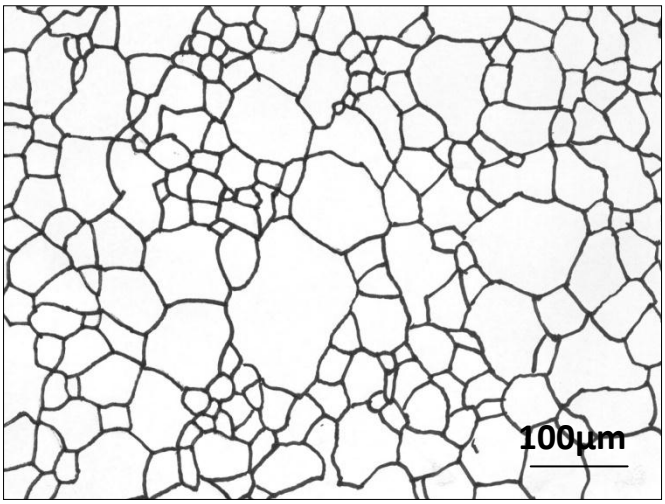

Figure 2-11 Map of grain outlines from one field of view

Each image was then loaded into image J and a threshold of 133-255 applied. The minimum grain size was set at 6µm^2 to ensure any very small particle like features were not counted as a grain area. The grains were then analysed and an overall average grain size calculated for each field of view. An overall average grain size was then calculated across all fields of view.

2.8. Identifying Grain Boundary Groove Density Using Image J

To calculate the fraction of grain boundary grooves in and out of the streak region the same Image J processing procedure was carried out as outlined in section 2.7. The difference for this image J analysis was that the data acquired related to the total area fraction of the grain interiors for each field of view. The remaining fraction then relates to the total area fraction of the grain boundary grooves for each field of view.

2.9. Identifying Pit Distributions Using Image J

To quantify differences in distributions of surface pitting in and out of the streak region image J was used to count the number of the pit like features for fields of view in and out of the streak region. To gain an accurate sense of etching pit distribution from the images some changes were made to the default settings. The first problem with Image J is the fact that analysing the particles of an image will mean the analysis of any object with an outline as can be seen when comparing Figures 2-12 and 2-13. From Figures 2-12 and 2-13 it can be seen that when using the default settings of image J particularly prominent grain boundary grooves

have been counted as particles. To rectify this problem the circularity was changed from 0-1 to 0.5- 1.00. This ensures pits which are in most cases fairly circular are being counted and no other features of the surface microstructure such as grain boundary grooves.

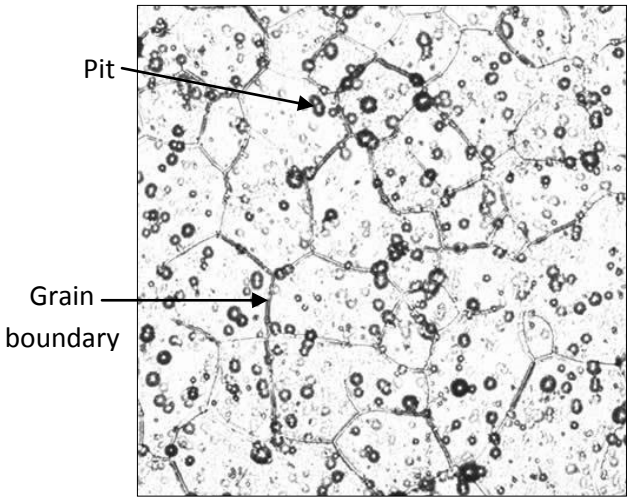

Figure 2-12 Surface microstructure before Image J Analysis

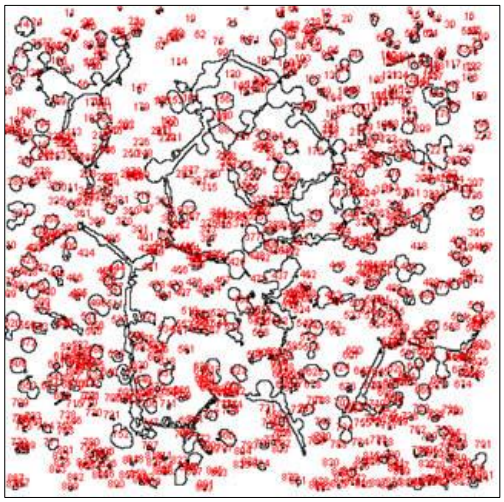

Figure 2-13 Outlines of particles after Image J Analysis using Image J default settings

In addition to changing the circularity setting the size of the particles being counted were limited from the default setting of 0 - ∞ to 6.3μm^2 - ∞. This minimum size was set by analysing the images for the average smallest sized etching pit. Setting this minimum size ensures particles which have not been etched out are not counted. Figure 2-14 shows the final processed outlines of etching pit distributions using Image J with the modified settings. Although this image analysis is not highly accurate it will give an indication of etching pit differences in and out of the streak regions. All image J analysis of etching pit density/distribution was carried out using these settings.

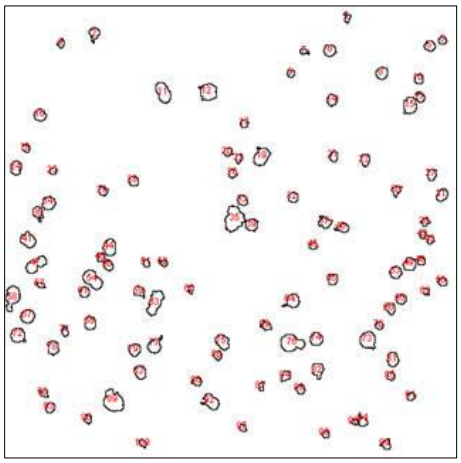

2-14 Outlines of etching pits after Image J analysis using modified settings

2.10. Roughness Testing

Roughness testing was carried out using a Taylor and Hobson Intra Talysurf 50 roughness tester as shown in figure 2-15 interfaced with Taylor and Hobson Ultra Version 5.14.12.74 software.

Figure 2-15 Taylor & Hobson Intra Talysurf 50 Roughness tester

For the roughness testing conducted a 0.25mm stylus traverse speed and 0.08mm cut off length was used. The traverse length of the stylus was 1mm to ensure the roughness values were inside the streak region when measured normal to the streak. The stylus tip is 2µm which means topographical features smaller than this cannot be measured. This is because to collect this roughness data a stylus is run across the surface and the deflections caused by changes in surface topography measured. The Ra value is then the mean value of the deflection graph. Therefore if topographical surface features are smaller than the stylus tip the roughness measurement will not be precise and some error would be involved. The schematic in Figure 2-16 illustrates this stylus tip caused error.

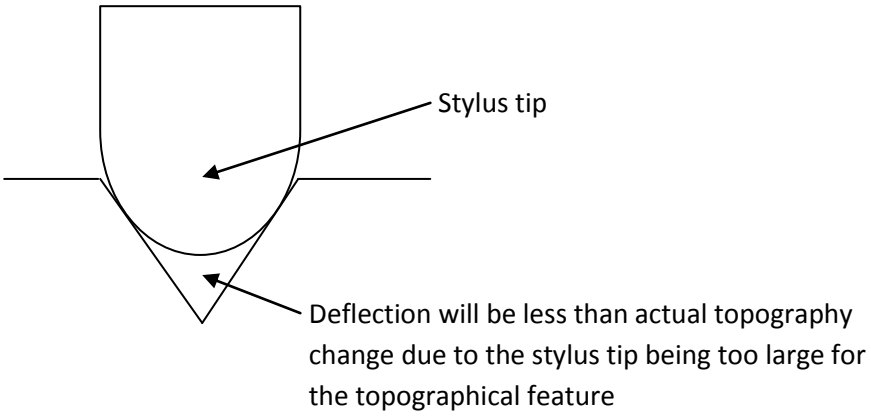

2-16Schematic of stylus tip induced roughness measurement error

3. Results and Discussion

This chapter presents the results of experimentation and analysis as described in the previous chapter carried out on streaking of AA6060 extrusions manufactured by Fletcher Aluminium. The following topics of investigation are presented

1. The effect of die lines on streaking
2. The effect of grain size on streaking
3. The effect of pitting on streaking
4. The relationship between roughness and etching response
5. The effect of surface treatments on streaking

3.1. The Effect of Die Lines on Streaking

The mill finish extrusion is the product immediately after extrusion. On this extrusion streaking is present in the form of slightly more glossy streaks as can be seen in Figure 3-1.

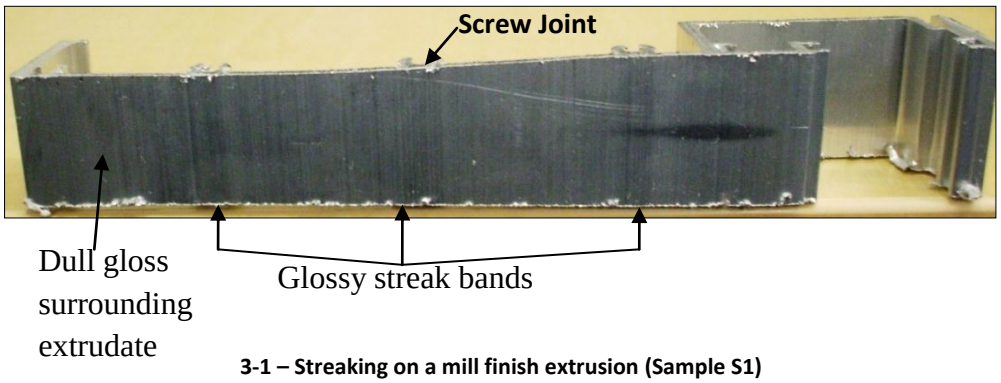

3-1 – Streaking on a mill finish extrusion (Sample S1)

To examine possible differences which may exist in and out of the streak region the mill finish extrusion, product type 605344, was examined on the surface in and out of the streak regions. The surface of the mill finish product is shown in Figure 3-2. Regions 2, 4 and 6 are where glossy streaks are present and regions 1, 3 and 5 are where streaking does not occur and the surface is a dull gloss. This sample is sample S1 (see table 2-1).

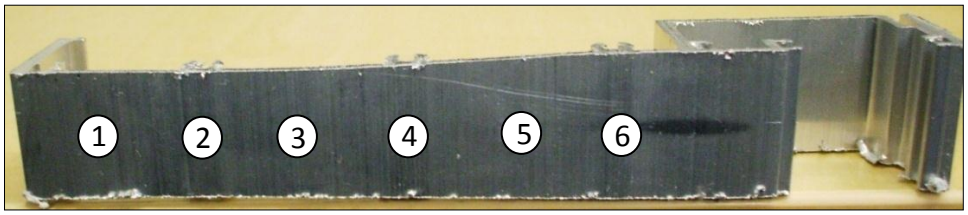

Figure 3-2–A Section of extrusion product 605344 manufactured by Fletcher Aluminium, Regions 1, 3 and 5 are located outside the streak zones and regions 2, 4 and 6 are regions where streaking was found to occur after additional surface finishing processes were carried out. (Sample S1)

Optical microscopy images were acquired in each region to observe any differences in and out of the streak region. These images are shown in Figure 3-3. It can be seen from these images that the surface topography of the as-extruded mill finish product is quite rough and die line features are apparent on the surface (die lines running vertically in the images).No clear observational differences can be made from the images in and out of the streak region shown in Figure 3-3. Possibly some of the surface roughness (black areas) may be attributed to surface adhesion between the die/extrusion interfaces.

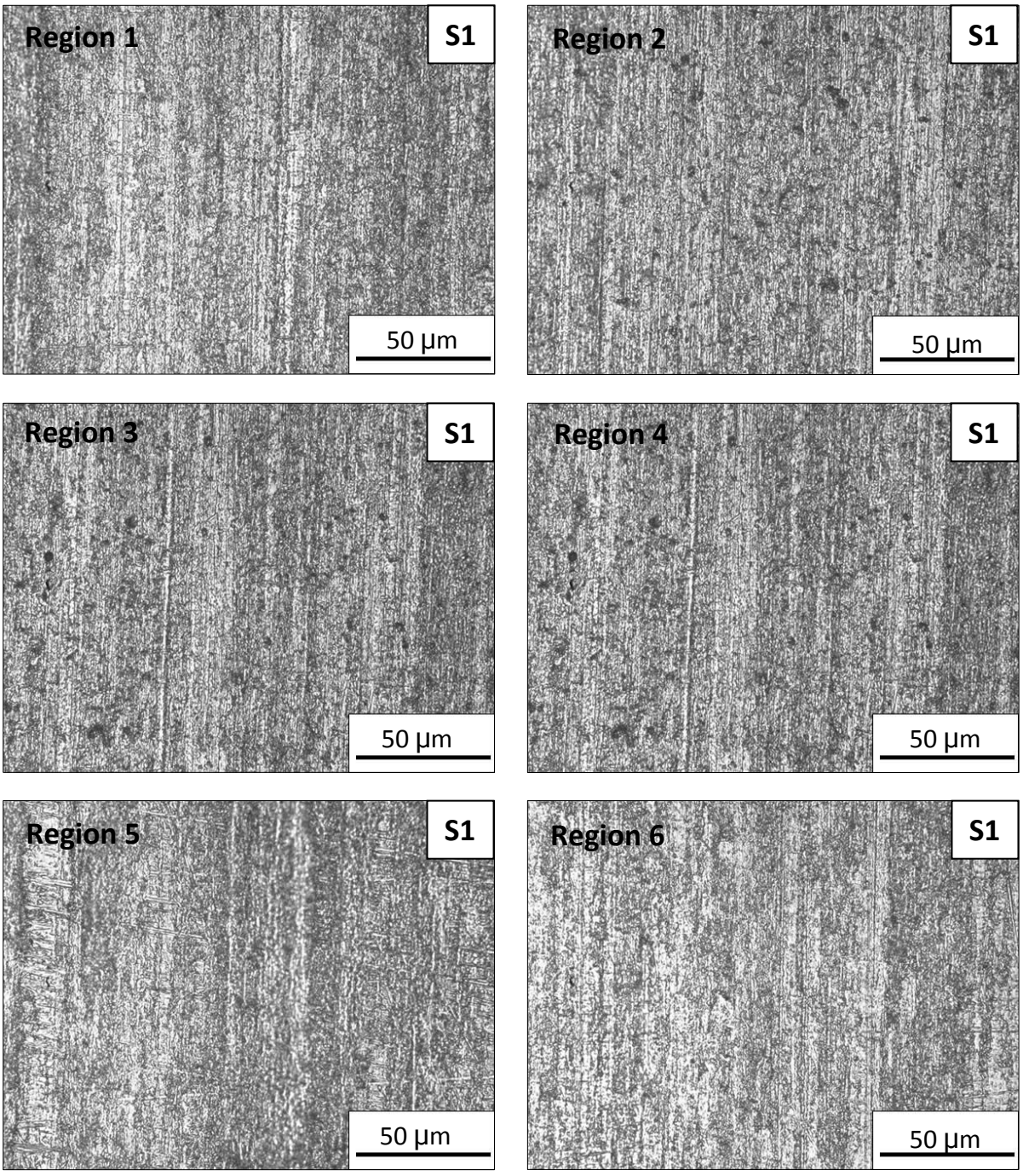

Figure 3-3Microscopic Images of the surface of as-extruded mill finish product (product type: 605344) in regions 1-6 as specified in figure 3-2 (Regions 1, 3 and 5 – outside streak region, regions 2, 4 and 6 – Inside streak region) Sample S2

Because of this rough surface topography the possible differences in surface topography in and out of the streak regions could not be observed. To investigate why the optical micrograph images shown in Figure 3-3 have the dark surface which means die lines are not visible, scanning electron microscopy (SEM) images were taken of the mill finish extrusion before electro-polishing in and out of the streak region. It can be seen from Figure 3-4 that there has been some adhesion or wear between the die-extrusion interfaces. This would cause the dark texture seen on the surface when viewing images obtained using optical microscopy (Figure 3-3). Furthermore adhesion/wear seems to be significantly greater for images 1 and 3 from inside the streak region. This indicates the die/extrusion interface conditions must differ in and out of the streak region.

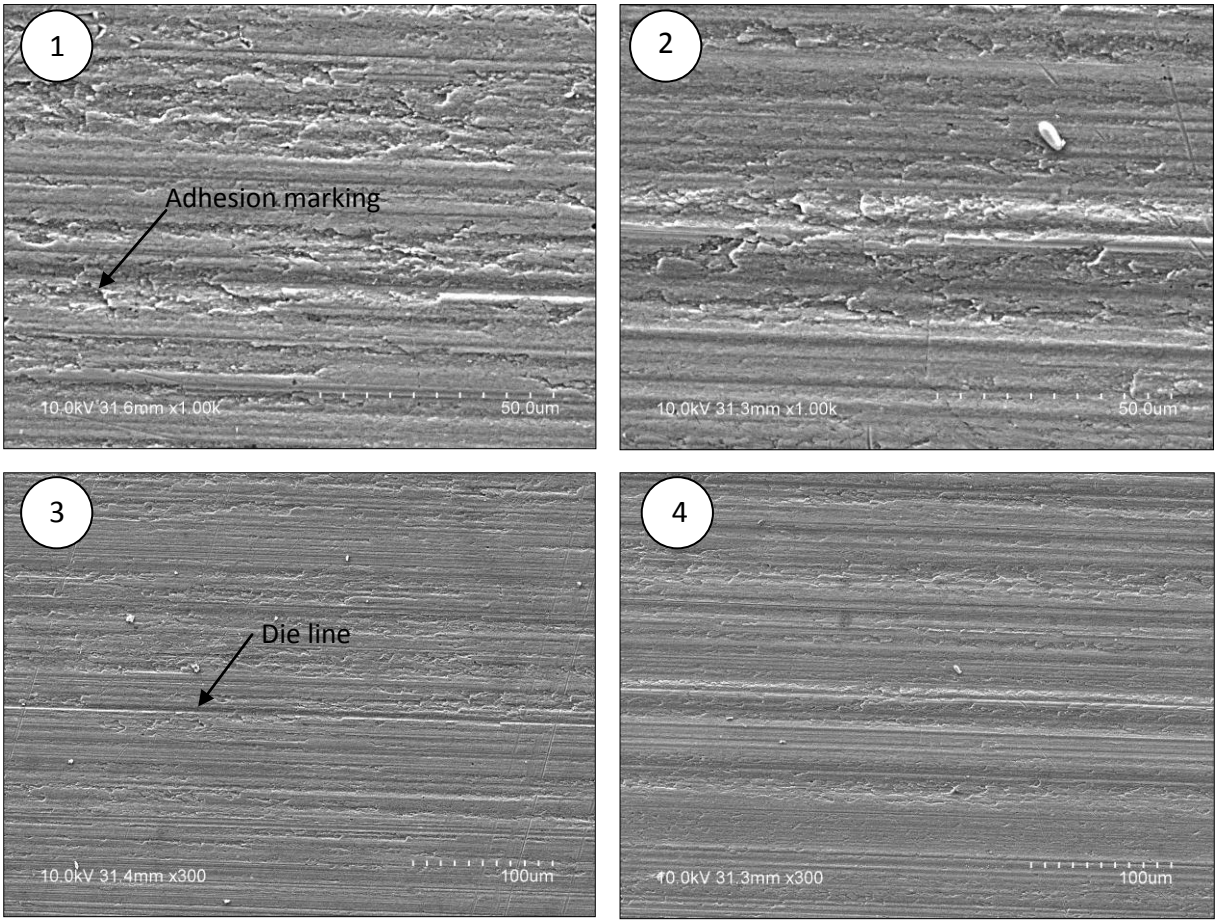

3-4 SEM images of the surface of the mil finish extrusion where images 1 and 3 are from inside the streak region and images 2 and 4 from outside the streak region

To enable observation of the surface topography in and out of the streak region the surface was electro-polished for a short duration to remove a small layer of material without completely removing topographical features such as die lines. Figure 3-5 shows the optical microscopy images taken in the six regions outlined in Figure 3-2 from the surface of sample

S2 (see table 2-1). It can be seen that there is less die lines and also the die lines are less prominent for the streak region images 4 and 6 and to a lesser degree image 2 compared to images 1, 3 and 5 from outside the streak regions.

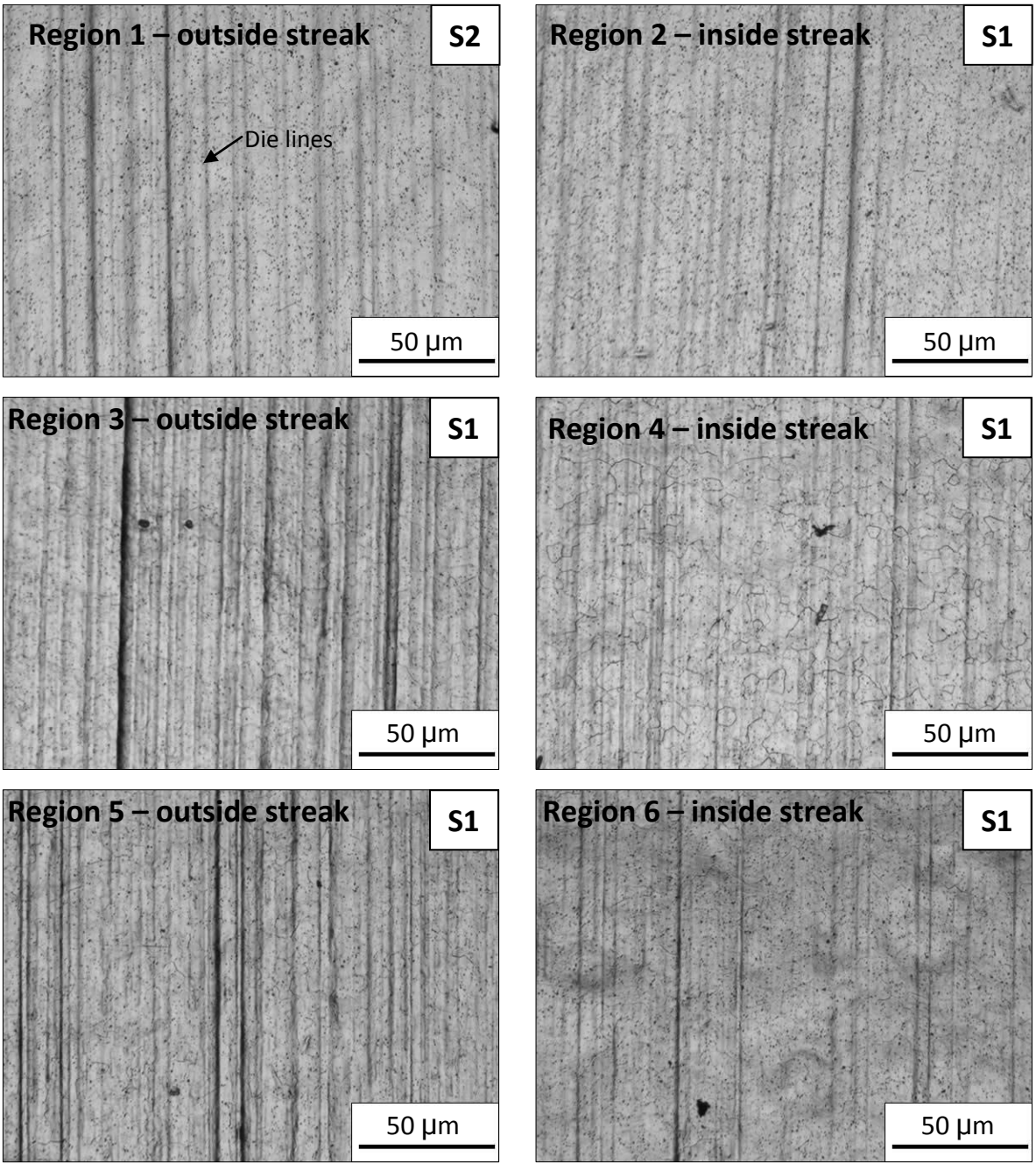

Figure 3-5 Microscopic Images of the surface of the mill finish product (product type: 605344) which has been electro-polished(Regions 1, 3 and 5 – outside streak region, regions 2, 4 and 6 – Inside streak region) Sample S2

Knowing that roughness may differ in and out of the streak regions caused by more prominent and densely distributed die lines, roughness tests were taken in the six regions outlined in Figure 3-2. This is too further confirm, beyond visual observation of microscopy images, that die lines are more densely distributed outside the streak regions. Roughness

measurements were taken at five random locations in each region on sample S1 which is the mill finish extrusion which was not electro-polished. Also the roughness was measured normal to the die line features. From the five roughness tests taken in each region the overall average roughness in each region was calculated as shown in Figure 3-6 below (See appendix C for all roughness data collected). It can be seen that the average roughness in each streak region is lower than the adjacent non-streaked regions.

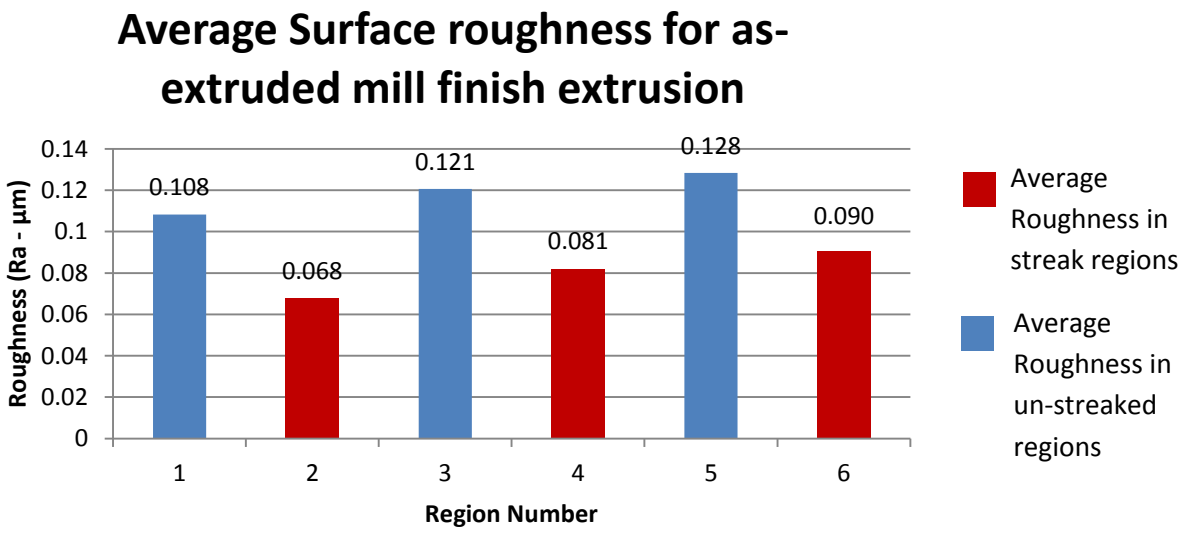

Figure 3-6Average Surface Roughness in each of the 6 regions outlined in Figure 3-2 for the as-extruded mill finish extrusion (Sample S1)

Therefore roughness measurements further prove that the surface is smoother in the streak zone which agrees with macroscopic and optical microscopy observation. Furthermore when looking at Figure 1-9 relating to Ra surface roughness Vs. Glossiness at light reflected at an angle of 60°, it can be seen that for the average roughness values in the streak region and the average roughness in the un-streaked regions a large difference in glossiness would occur. Therefore the surface assessment made indicates that the mechanism causing streaking on the mill finish as-extruded product is due to a smoother surface in the streak regions. This smoother surface is due to less densely distributed die lines and this lower roughness consequently increases the glossiness creating streak bands which are a higher surface gloss than the surrounding extrudate.

In summary it is noted that the initial glossy streaking on the mill finish product before surface treatment is due to less densely distributed die lines and less adhesion wear in the streak region.

3.2. The Effect of Grain Size on Streaking

The anodized product shows a different type of streaking from the mill finish product in which the streak region is a slightly duller surface gloss than the surrounding extrudate. This can be seen when comparing Figure 3-7 of streaking on an anodized extrusion and Figure 3-1 of streaking on a mill finish extrusion.

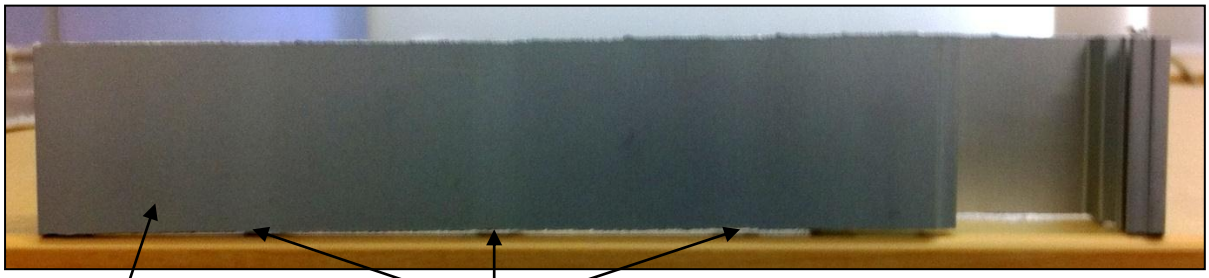

3-7 Streaking on an anodized extrusion

In literature it was identified that a rougher surface causes a duller surface gloss. Because the oxides of the anodizing layer block the view of the surface using microscopy the anodizing finished product cannot be simply investigated for differences in surface topography in and out of the streak region. Instead a systematic investigation will be made of the mill finish product which has not been anodized. By subjecting this product to different treatments for different durations the mechanisms which cause surface topography differences and streaking can be examined. The first possible reason for differences in surface roughness may be due to grain boundary groove distributions/densities differing in and out of the streak region caused by possible grain size difference. To simulate in a laboratory the etching of grain boundaries due to an uneven etch attack a sample was electro-etched to reveal grain boundary grooves. Sample S3 (see table 2-1 for sample treatment) shown in Figure 3-8 was etched to reveal grain boundary grooves and grain size. Therefore depending on the density of grain boundary grooves in and out of the streak region the surface gloss may be altered causing streaking. If streaking is not apparent then this is not the controlling mechanism for streaking for this product. Figure 3-8 shows the electro-etched specimen at different viewing angles. It can be seen that streaking is not present on the surface.

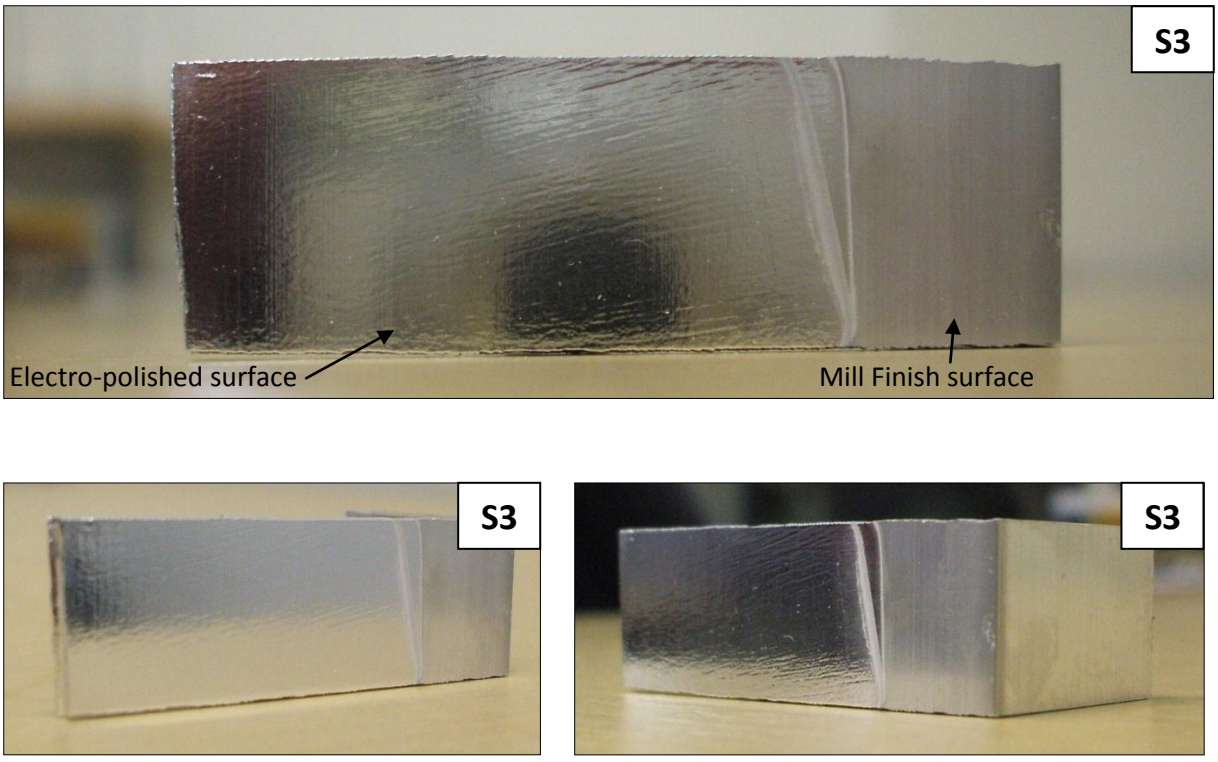

Figure 3-8 Electro-etched surface of sample S3 at different viewing angles

Since streaking is not visible the next step of the investigation is to examine whether grain size differences are present in and out of the streak region. If grain size differences are present does this difference cause large differences in the area fraction of grain boundaries in and out of the streak zone? Conclusions on the role that grain boundaries play in the streaking phenomenon can then be made.

To see if grain size differs in and out of the streak region optical microscopy images were acquired from six view fields outside the streak region and six view fields inside the streak region as shown in Figures 3-9 and 3-10 respectively on the surface of sample S3.Visually it is not clear if grain size differences are present, therefore an analysis will be carried out using the Heyn grain size method and Image J software image analysis.

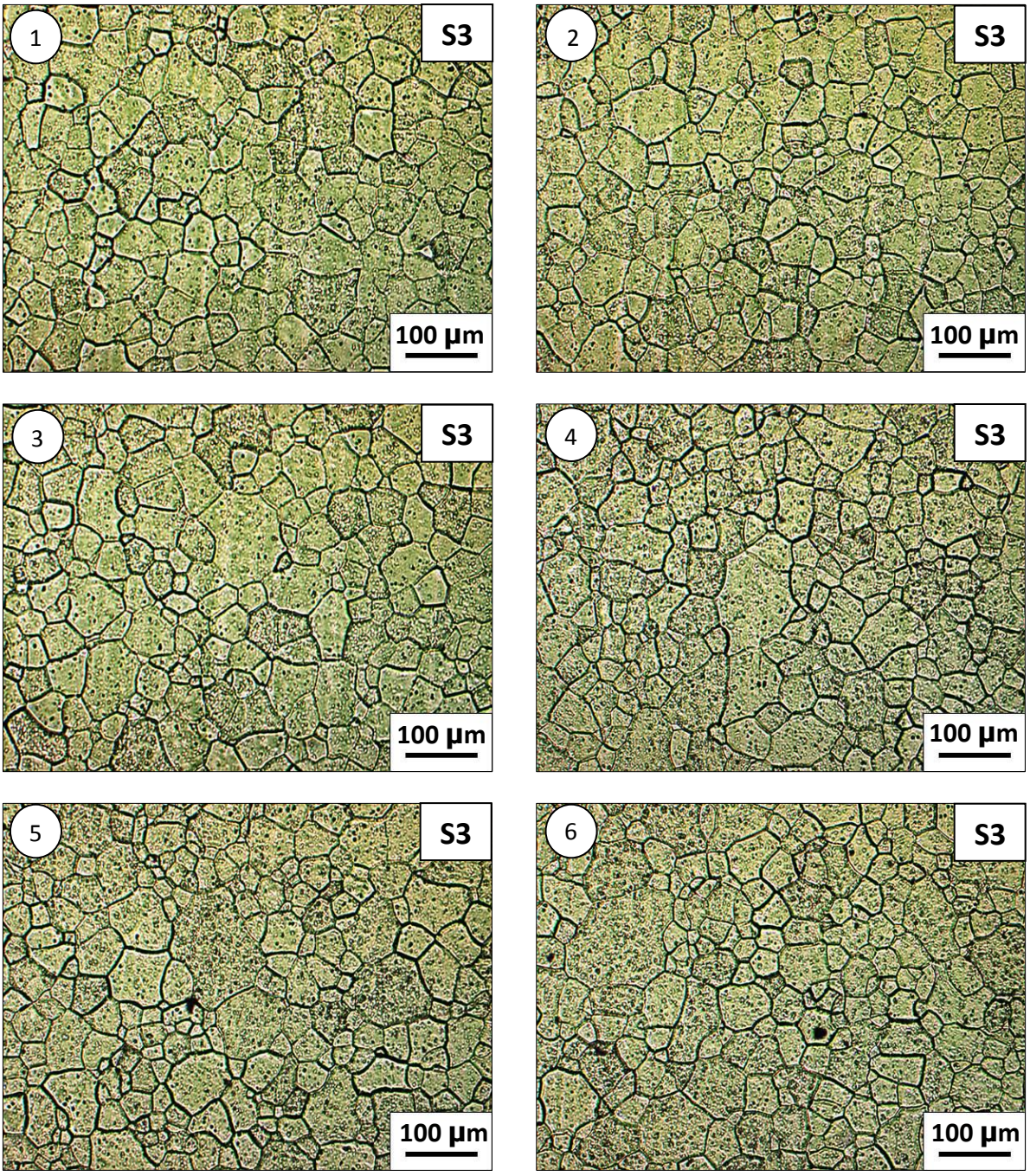

Figure 3-9 Microscopic Images from six view fields outside the streak region (sample S3)

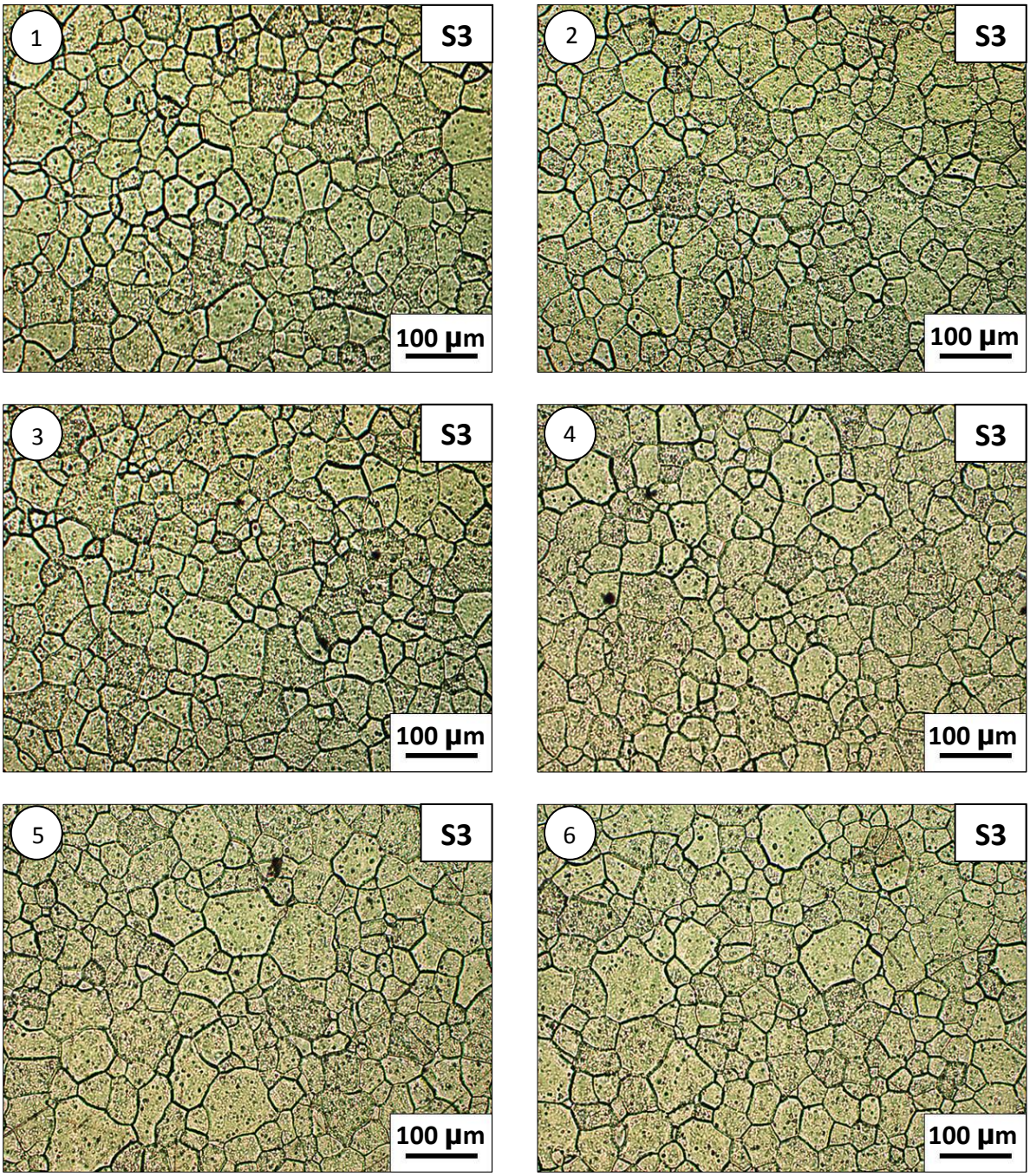

Figure 3-10 Microscopic Images from six view fields inside the streak region (Sample S3)

3.2.1. Grain Size Measurement Using the Heyn Intercept Procedure

Using the Heyn grain size method as described in section 2.7 the following data for the average grain size in and out of the streak zone was accumulated as shown in Table 3-1. Details of calculations made for this method is given in Appendix A. It can be seen from Table 3-1 that the grain size on average does differ in and out of the streak region.

Table 3-1– Grain Size Data including upper and lower limits of relative accuracy (results calculated from grain size numbers shown in appendix A1, table A1)

	$\bar{A}$ **Average Grain Area**	
For the six fields outside the streak region	641μm^2	**Upper Error Limit**
		878.2μm^2
		Lower Error Limit
		465.5μm^2
For the six fields inside the streak region	493μm^2	**Upper Error Limit**
		613μm^2
		Lower Error Limit
		403μm^2

Based on the average grain area found in and out of the streak zone as shown in Table 3-1 the percentage difference in grain size in and out of the streak region based on the average grain area is:

$$\%\ Difference\ in\ grain\ size\ in\ and\ out\ of\ the\ streak\ region = \left(1 - \frac{493}{641}\right) * 100$$

$$= 23\%$$

However the relative error upper and lower limits calculated according to the relative accuracies overlap as can be seen by the error bars shown in Figure 3-11. Therefore there is still some uncertainty on whether grain size difference in and out of the streak region is present. For this reason a second analysis will be conducted using image J to further identify whether grain size differences in and out of the streak zone are present more conclusively.

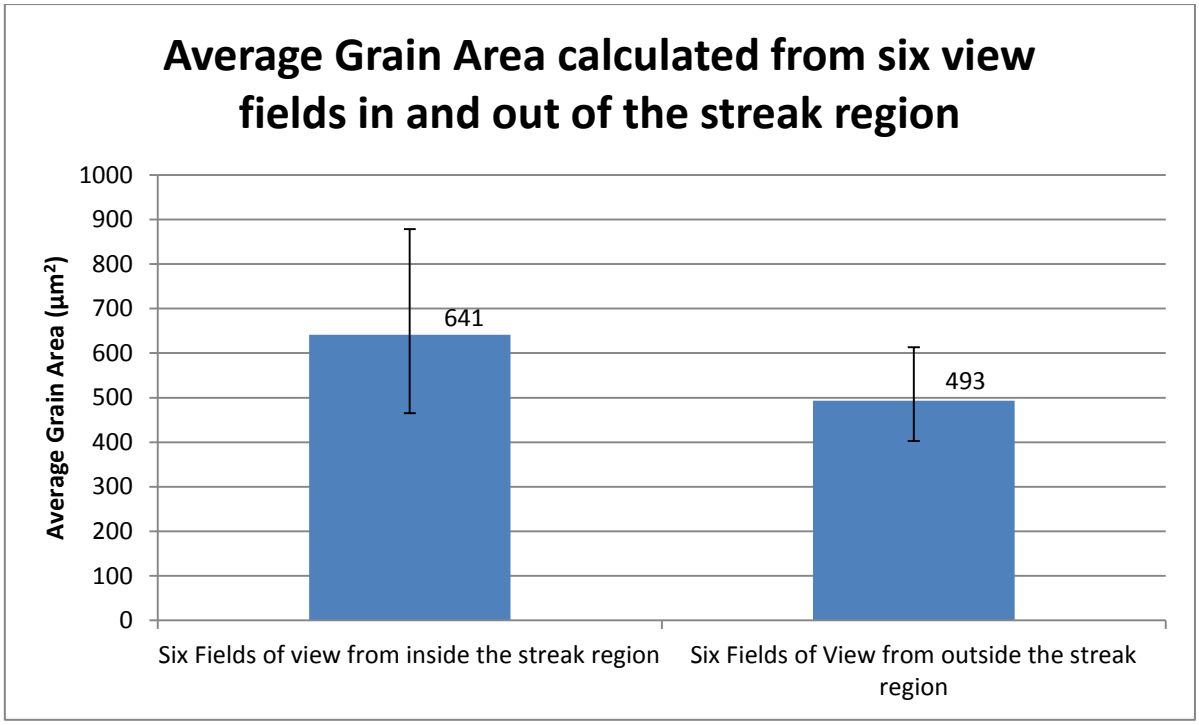

Figure 3-11Average Grain area in and out of the streak region with error bars (Average grain area calculated using the Heyn procedure)

For further clarity of grain size difference found using the Heyn intercept procedure Table 3-2 below outlines the average grain diameters.

Table 3-2 - Average grain diameter for the six fields of view in and out of the streak region

	$\bar{D}$ **Average Grain Diameter**	
For the six fields outside the streak region	204µm	**Upper Error Limit**
		279.5µm
		Lower Error Limit
		148.2µm
For the six fields inside the streak region	157µm	**Upper Error Limit**
		195µm
		Lower Error Limit
		128.3µm

3.2.2. Grain Size Measurement Using Image J

The six fields of view from in and out of the streak zone as shown in Figures 3-9 and 3-10 were analysed using image J for the average grain size for each field of view. This was carried out in conjunction with the Heyn intercept procedure to further prove without a doubt

that differences in grain size in and out of the streak region are present. The images shown in Figures 3-12 and 3-13 show the processed outlines produced by image J from the grain size images shown in Figures 3-9 and 3-10 (Note: the image outlines shown in Figures 3-12 and 3-13 have been flipped across the vertical centre line from the originals shown in Figures 3-9 and 3-10).

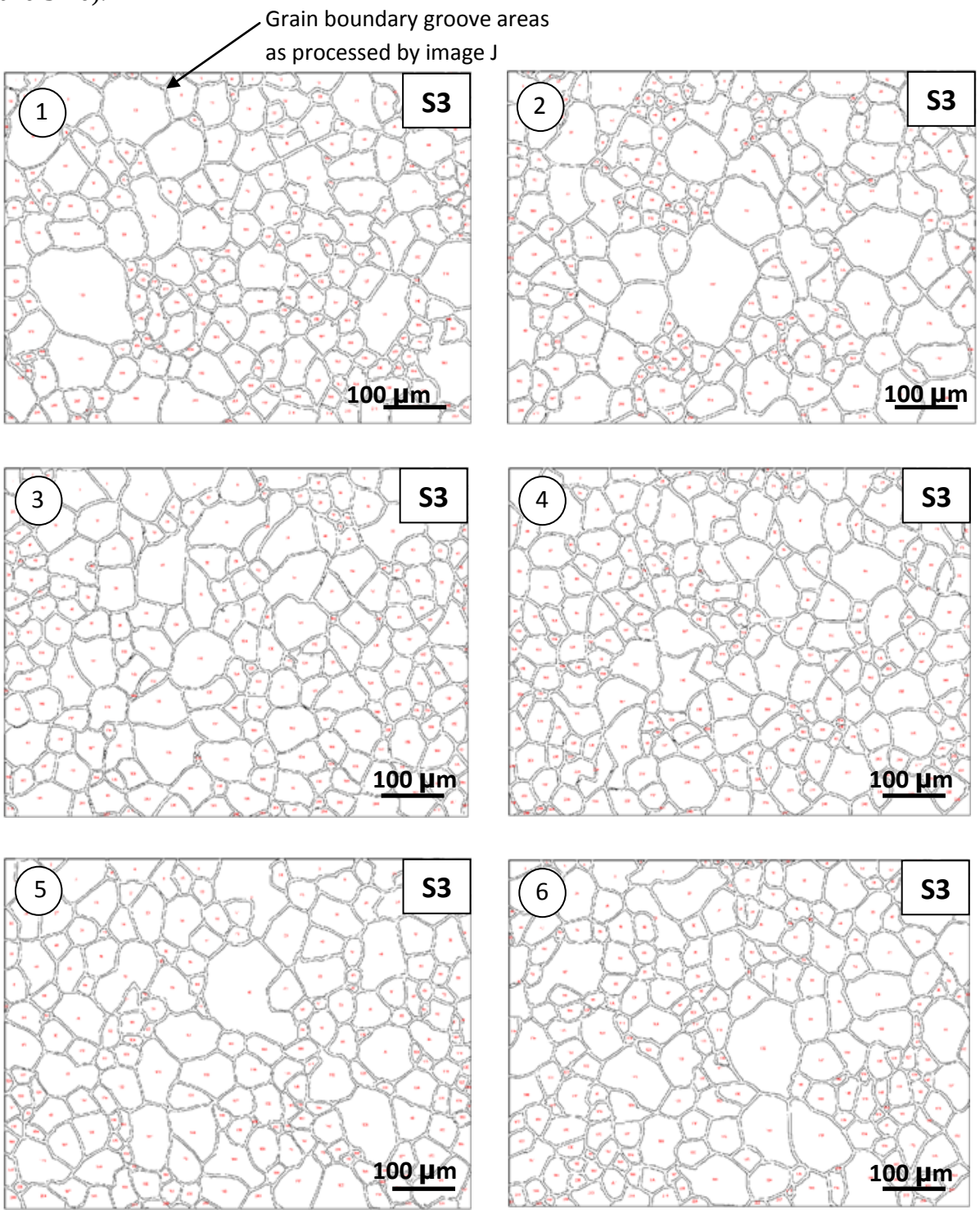

Figure 3-12 Grain outlines produced by image J software from the six fields of view from outside the streak region from sample S3

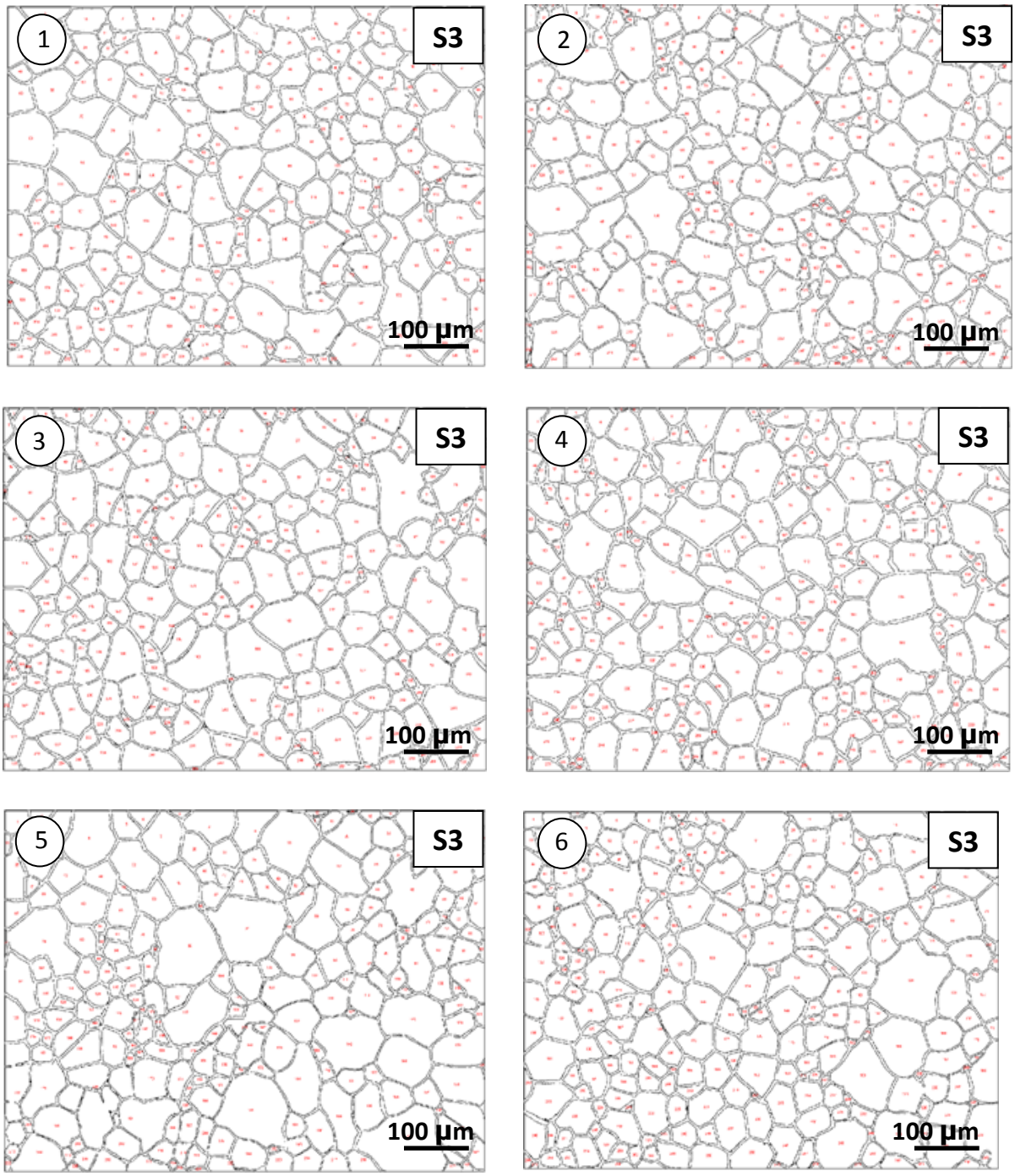

Figure 3-13 Grain outlines produced by image J software from the six fields of view from inside the streak region from sample S3

Figure 3-14 shows the average grain size for each field of view in and out of the streak region as calculated by image J. It can be seen that for all fields of view outside the streak region except view 4 the average grain size is larger across all fields of view. This image J analysis like the Heyn grain size analysis method again shows there is a grain size difference in and out of the streak region.

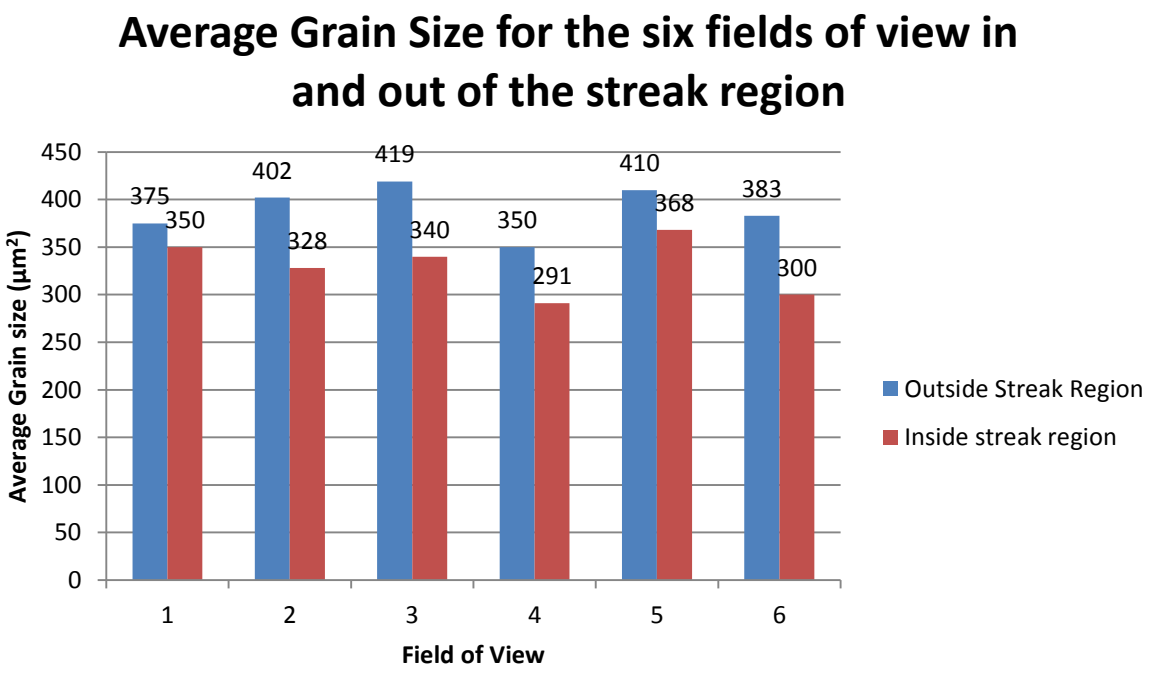

3-14 Average Grain size for the six fields of view in and out of the streak region

Figure 3-15 below shows the average grain size across all fields of view in and out of the streak region. It can be seen overall that the average grain size is smaller inside the streak region.

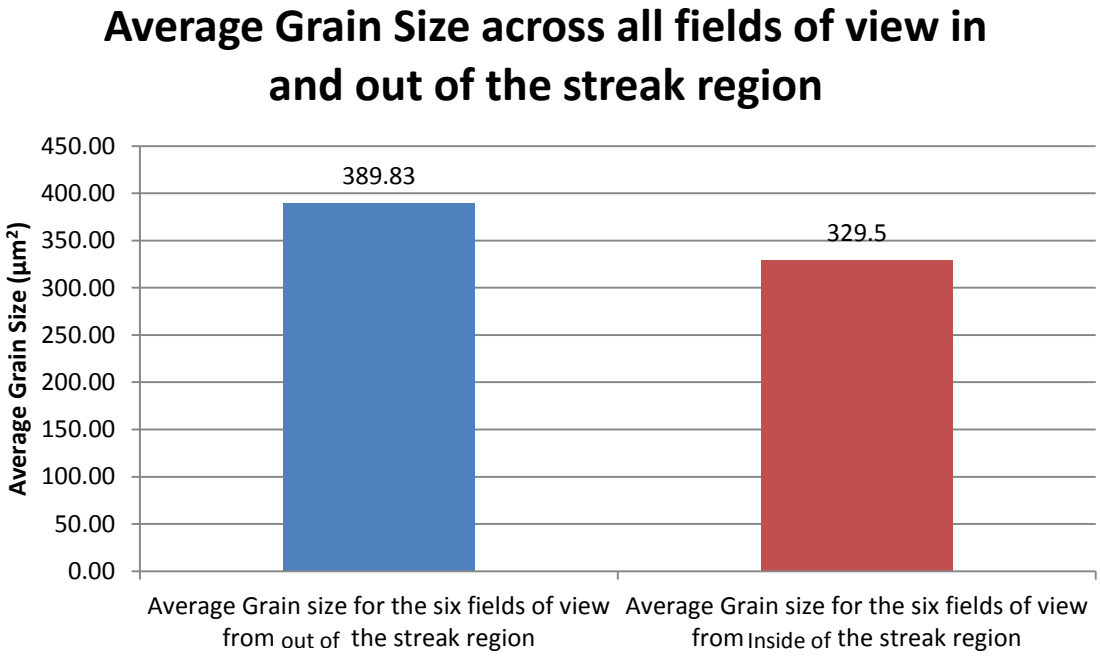

3-15 Average Grain size for the six fields of view in and out of the streak region

For further clarity figure 3-16 compares the average grain diameters in and out of the streak region.

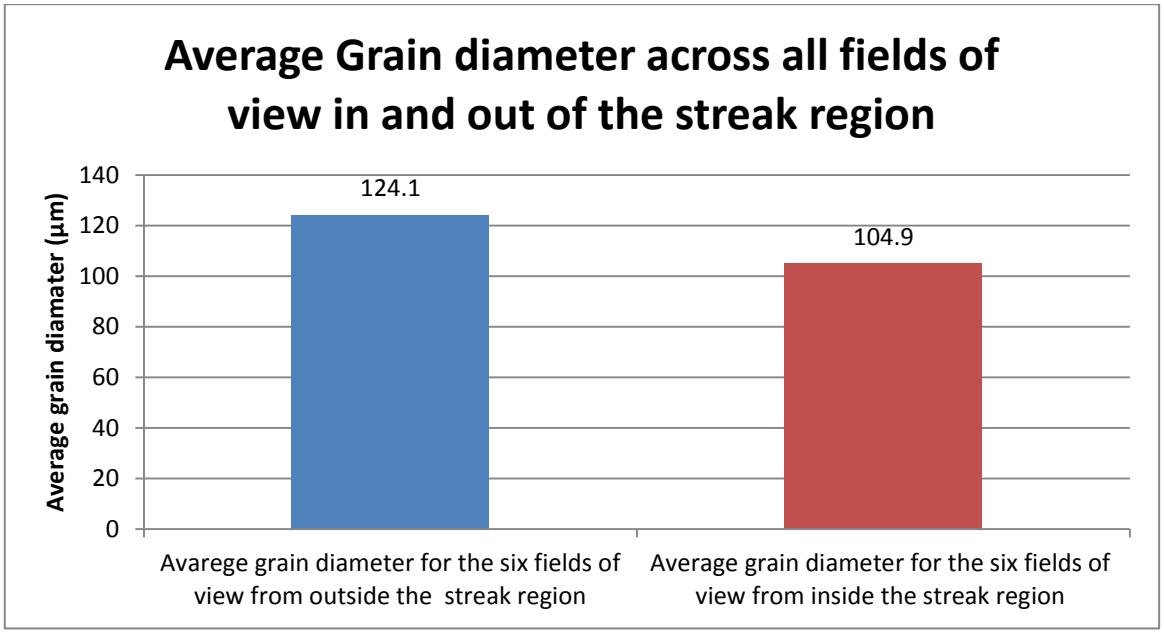

Figure 3-16 Average Grain diameter for the six fields of view in and out of the streak region

3.2.3. Comparison: Heyn and Image J grain size results

Both of these grain size investigations found that over the six fields of view in and out of the streak region that grain size was smaller in the streak region. The average grain size did vary however between methods as can be seen in figure 3-17. However since both methods produced the same result although to varying degrees of difference it can be concluded that grain size does vary slightly in and out of the streak region. It is likely the Heyn method is not as accurate because of the large variance and un-uniformity in grain size which makes this procedure less accurate.

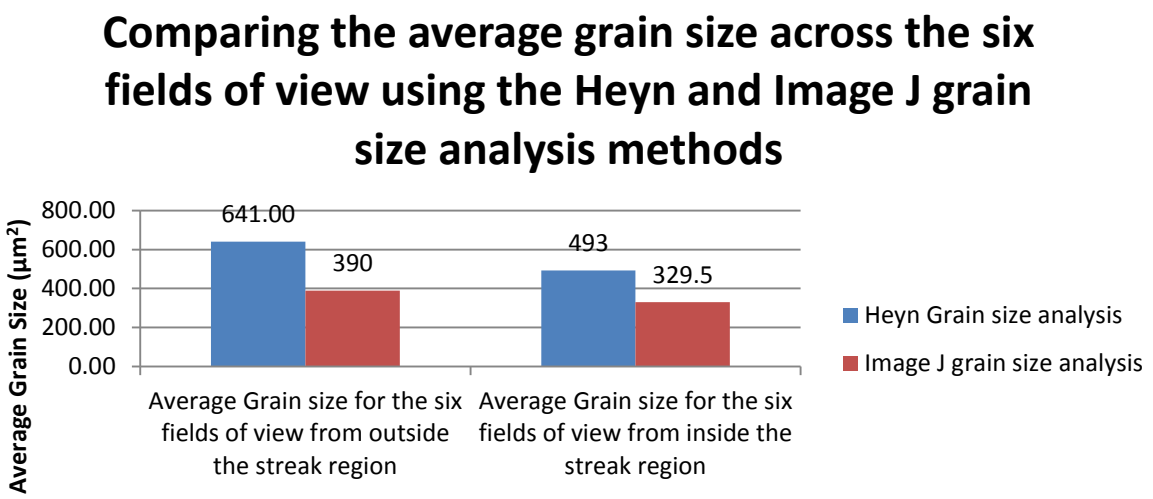

Figure 3-17 Comparing the average grain size across the six fields of view using the Heyn and Image J grain size analysis methods

3.2.4. Grain Boundary Groove Densities Using Image J

Using image J the total fractional percentage of grain boundary areas present in each field of view in and out of the streak region was calculated using the grain and boundary outlines shown in Figures 3-12 and 3-13. This data acquired is shown in Figure 3-18. The blue data labels correspond to the grain boundary groove fraction for each field of view outside the streak region and the red data labels correspond to the grain boundary groove fraction for each view field inside the streak region.

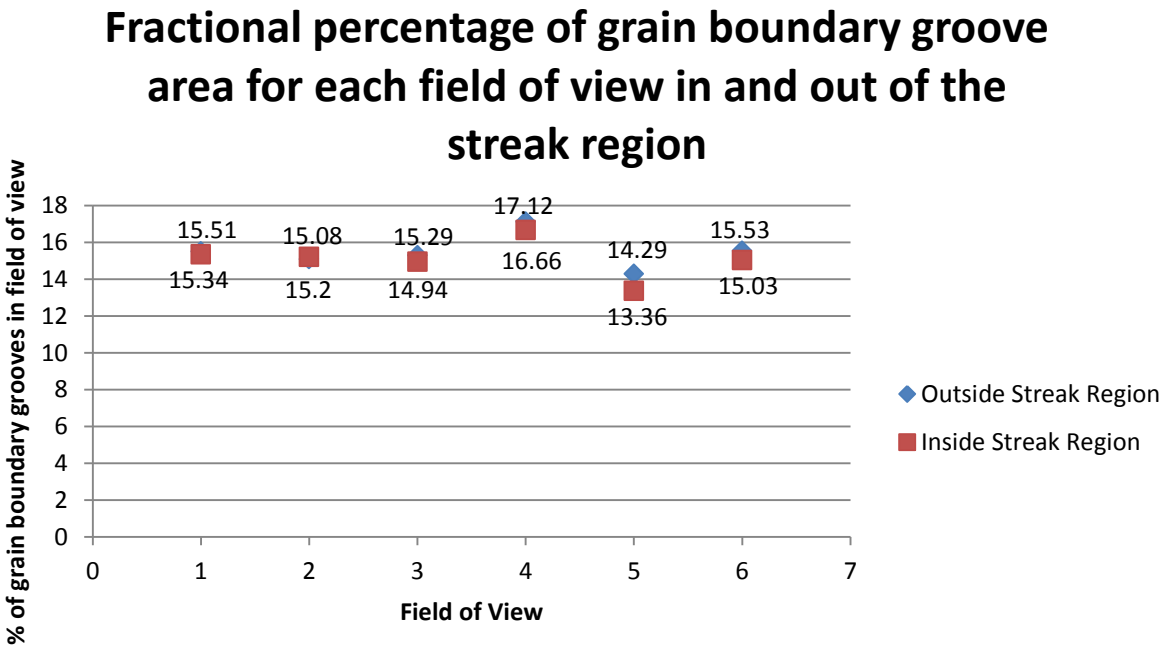

Figure 3-18 Percentage of grain boundary grooves vs. the grain interior for each field of view in and out of the streak region

The average percentage of grain boundary area for the six fields of view in and out of the streak region is shown in Figure 3-19.

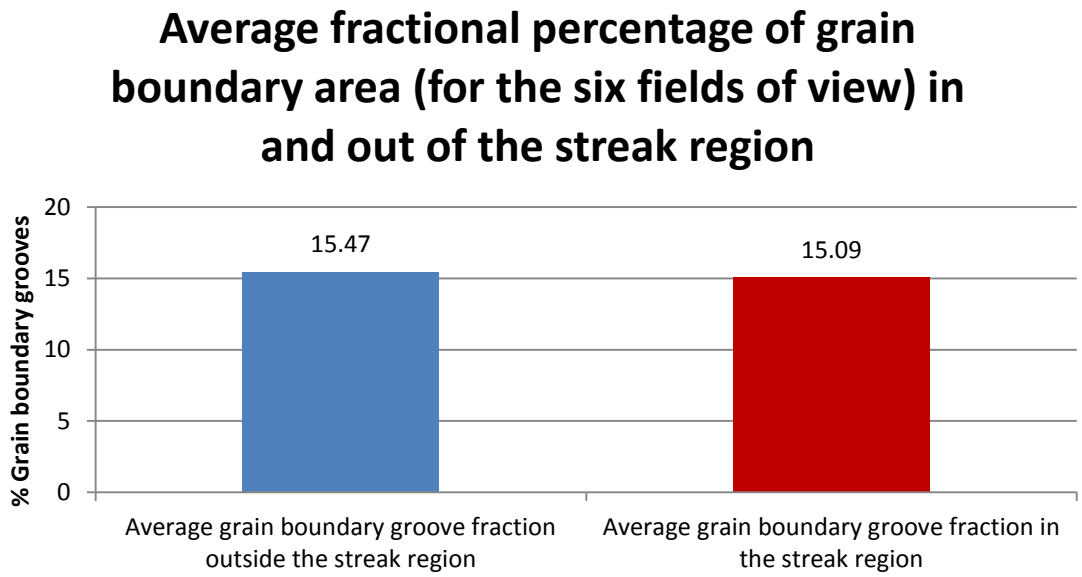

3-19 Average grain boundary groove fraction in and out of the streak region

From Figures 3-18 and 3-19 it can be seen that what would seem logical, in which there is overall a greater distribution of grain boundaries in the streak region due to smaller grain size as identified in sections 3.2.1 and 3.2.2 is not the case. This illogicality may be caused by the following factors:

- The threshold applied in image J means better highlighted features during the grain outlining process may result in a wider grain boundary width when the threshold is applied.
- The outlining of grain boundaries may be uneven in terms of width of grain boundaries causing an error in the results acquired.

From the results obtained and when taking into account the above points which would cause some degree of error, and also assuming the fraction of grain boundary grooves in and out of the streak region is very small (one or two % difference in and out of the streak region) it is concluded that the fraction of grain boundary grooves Vs. grain interiors cannot be accurately identified using image J software

3.2.5. Grain boundary Groove Densities by Calculation

Because Image J is not accurate enough to accurately identify the fractional difference in grain boundary densities due to differences in grain size in and out of the streak region an analytical method has been developed.

The following assumptions have been made regarding the grain structure:

- The grains are equal six sided hexagons
- Each grain is equal to the average grain size found using image J analysis
- Grain boundaries are an average width of 3 microns as outlined in appendix B

Using these assumptions a method as described in appendix B was developed to analyse the degree of effect that grain size has on the area of grain boundary grooves. Figure 3-20 below shows the percentage difference in grain boundary groove area in and out of the streak region as the percentage difference in grain size increases in and out of the streak region. It was found that grain size differs by a minimum of 16% in and out of the streak region as found using image J analysis software which only corresponds to approximately 7.1% difference in grain boundary groove area in and out of the streak region. To get a 20% difference in grain boundary groove area in and out of the streak region there would have to be a 65% difference in grain size in and out of the streak region. Overall from figure 3-20 it can be noted that a significant difference in grain size in and out of the streak region is necessary for a significant difference in grain boundary groove density in and out of the streak region. Thus the possibility of a significant difference in surface roughness and thus an altered reflectance of light and streaking to occur would only be possible with a large difference in grain size in and out of the streak region.

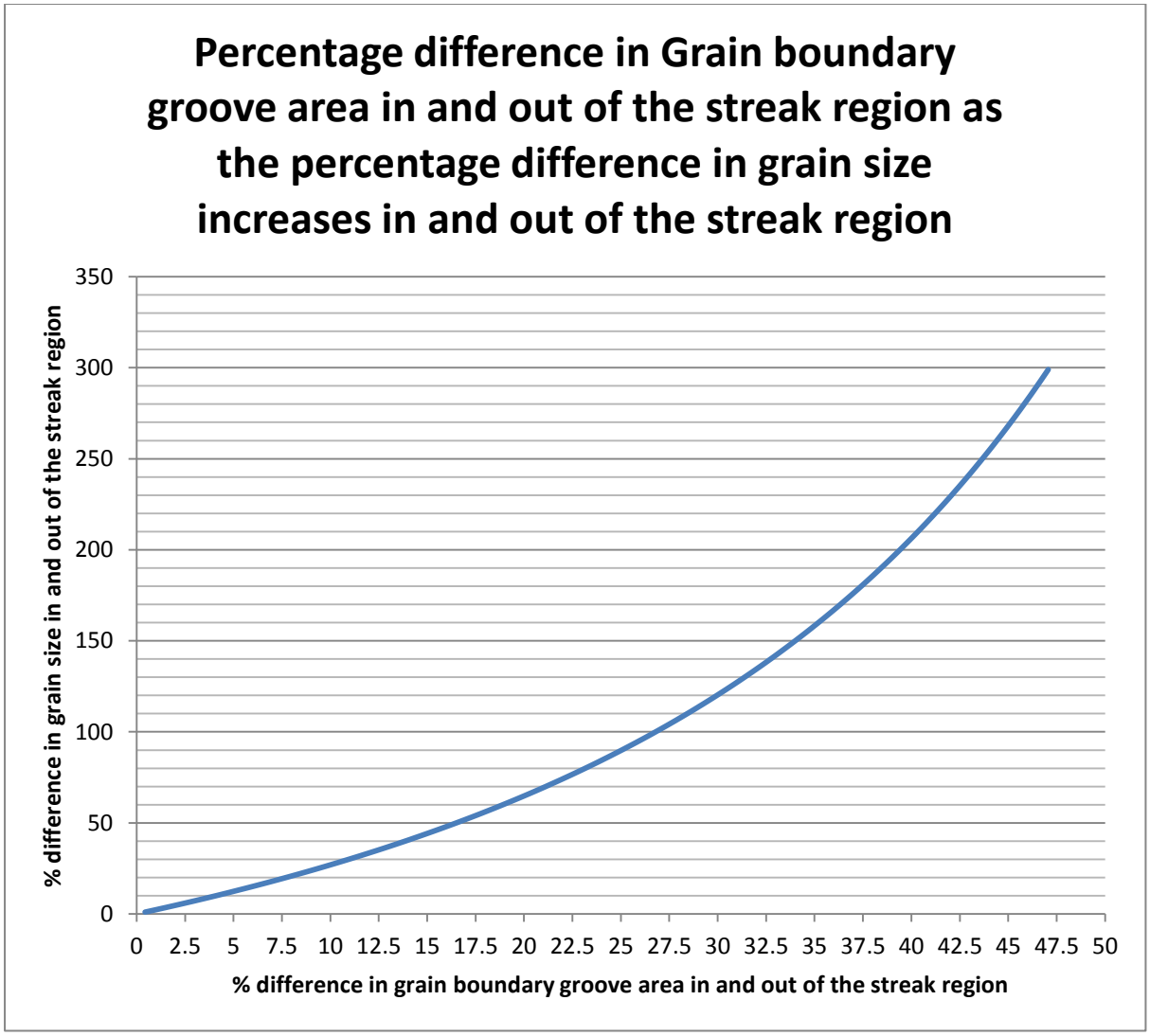

Figure 3-20 Percentage difference in grain boundary groove area in and out of the streak region as the percentage difference in grain size increases in and out of the streak region

3.2.6. Summary of Findings for the Effect of Grain Size on Streaking

Overall it was identified that grain size does differ in and out of the streak region. It was also found that for the area of grain boundary grooves to differ significantly in and out of the streak region the difference in grain size would have to be extremely significant in the region of 65% + as can be seen from figure 3-20. If the grain size and grain boundary groove area did differ enough in and out of the streak region it may then cause an altered surface roughness, reflectance of light and streaking to occur.

3.3. The Effect of Surface Pitting on Streaking

To study the effect that pitting on the surface of the extrudate may have on streaking a series of etching experiments were conducted on the streak prone product 605344. The reason etching was carried out is due to the fact that etching causes intermetallics or other inclusions to etch out forming pits. In addition some etchants can matte the surface causing a honeycomb like pit structure on the surface. If these pit features differ in and out of the streak region a subsequent altered reflectance of light and ultimately streaking may occur.

3.3.1. The Evolution of Streaking Using a Laboratory Etching Simulation

The following etching investigation was carried out from samples S4 to S10 which treatments and analysis methods have been outlined in Table 2-1. Figure 3-21 shows a series of images from the surface of etched samples which were etched for different durations. This figure shows the streaking development after different levels of material removal of the surface layer. Four stages of streaking appear:

1. Low level metal removal of the surface – No streaking
2. Medium level metal removal of the surface – Parallel band streaks
3. Med-High level metal removal of the surface – Single band streaking
4. High level metal removal of the surface – Narrowing of single band streak

In addition to showing the evolution of streaking it is pinpointed that the mechanism in the extrusion manufacturing process which causes streaking to appear is etching. It is also likely that this etching process causes topographical differences in and out of the streak region which will be investigated using optical and scanning electron microscopy in latter sections.

(a) Sample S4 - Electro-polish 1min and 18min etch

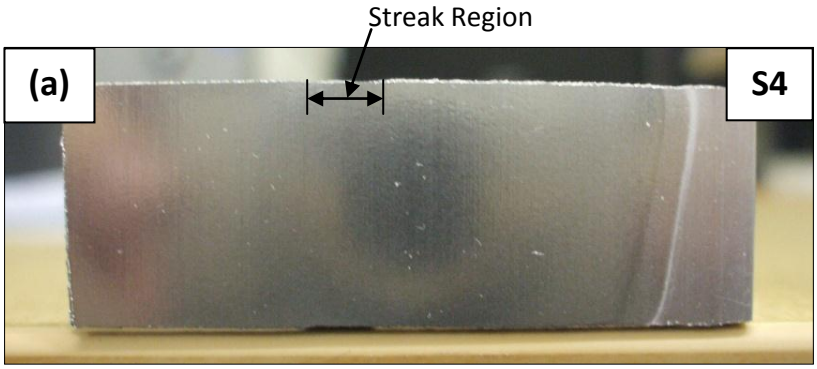

(b) Sample S5 - Electro-polish 1min and 26min etch

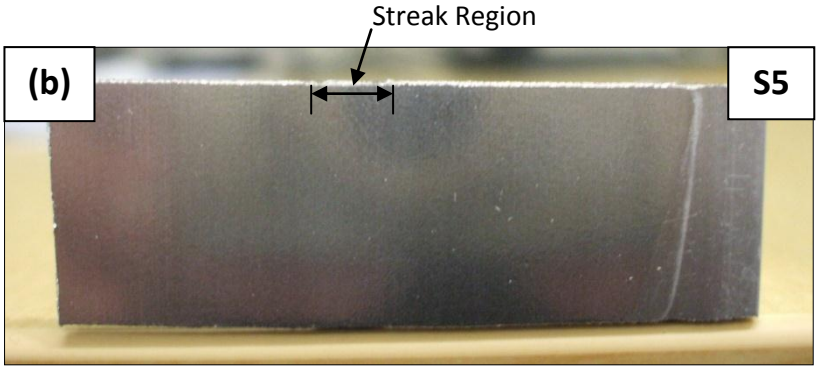

(c) Sample S6 - Electro-polish 1min and 36min etch

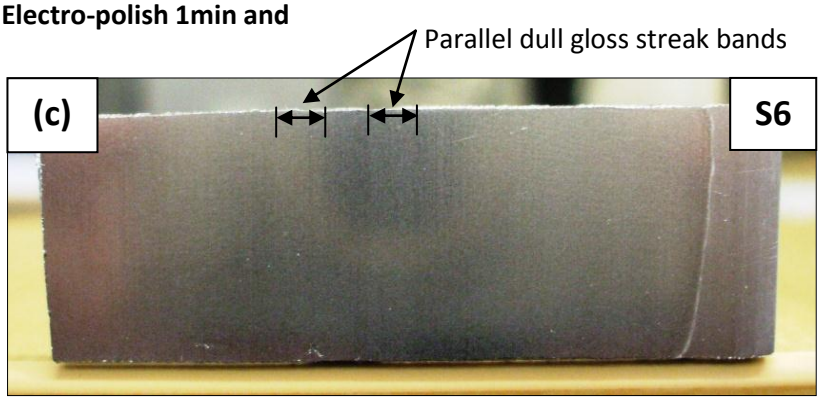

Figure 3-21 Series of samples electro-polished and etched in Graff and Sargent's etchant for different durations

Figure 3-21 continued on the following page

(d) Sample S7 - Electro-polish 1min and 48min etch

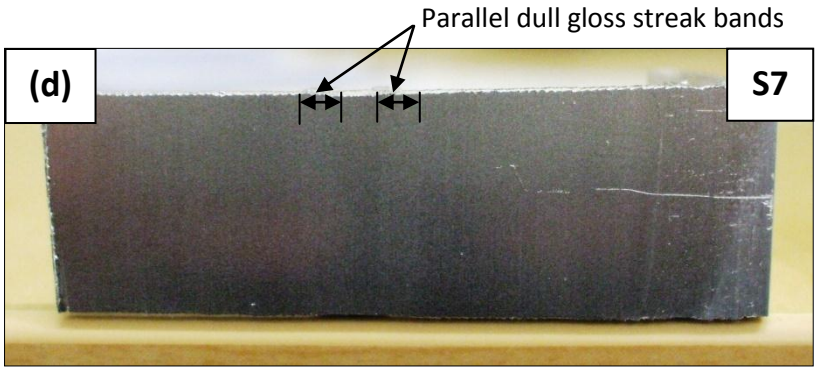

(e) Sample S8 - Electro-polish 1min and 62min etch

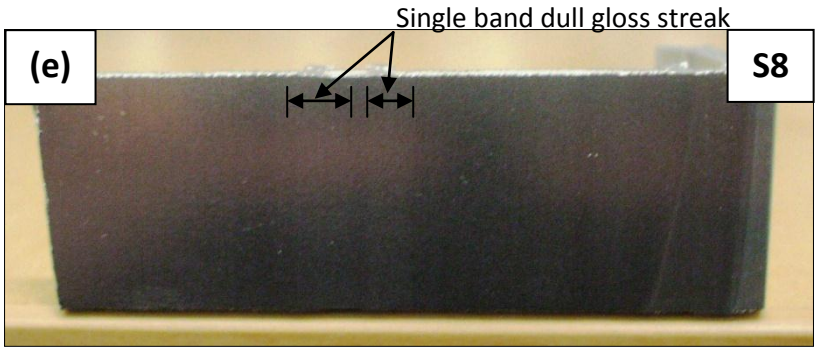

(f) Sample S9 - Electro-polish 2min and 48min etch

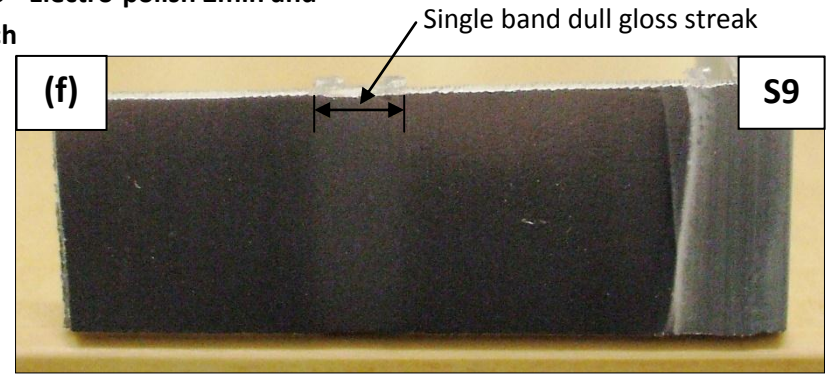

(g) **Sample S10** - Electro-polish 2min and 62min etch

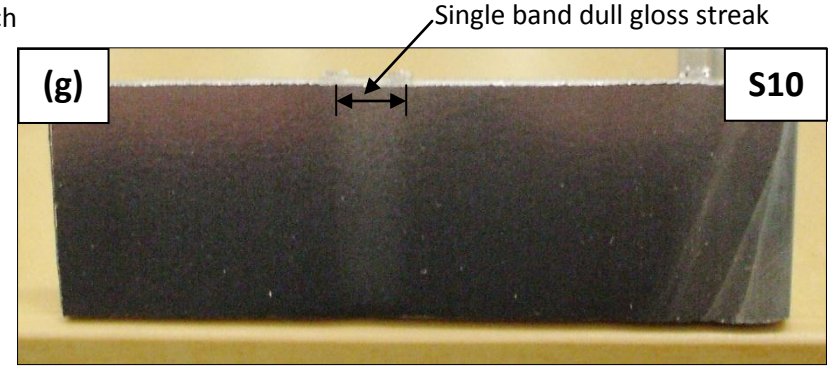

Figure 3-21 Series of samples electro-polished and etched in Graff and Sargent's etchant for different durations

3.3.2. A Model for the Evolution of Streaking – Part 1

From the macroscopic observations made of the streaking occurring after different etch durations and hence different degrees of metal removal using Graff and Sargent's etchant in a laboratory etching experiment, the following model for how the different types of streaking are induced after different etch durations can be established for product 605344. This streaking model is shown in Figure 3-22(b) represented schematically at the cross section in Figure 3-22(a) (Although not to scale). Area 1 is the zone which makes up the bulk of the extrudate in which streaks do not appear. Area 2 is the zone at the cross section in which double band streaking occurs, and area 3 is the zone in which single band streaking occurs.

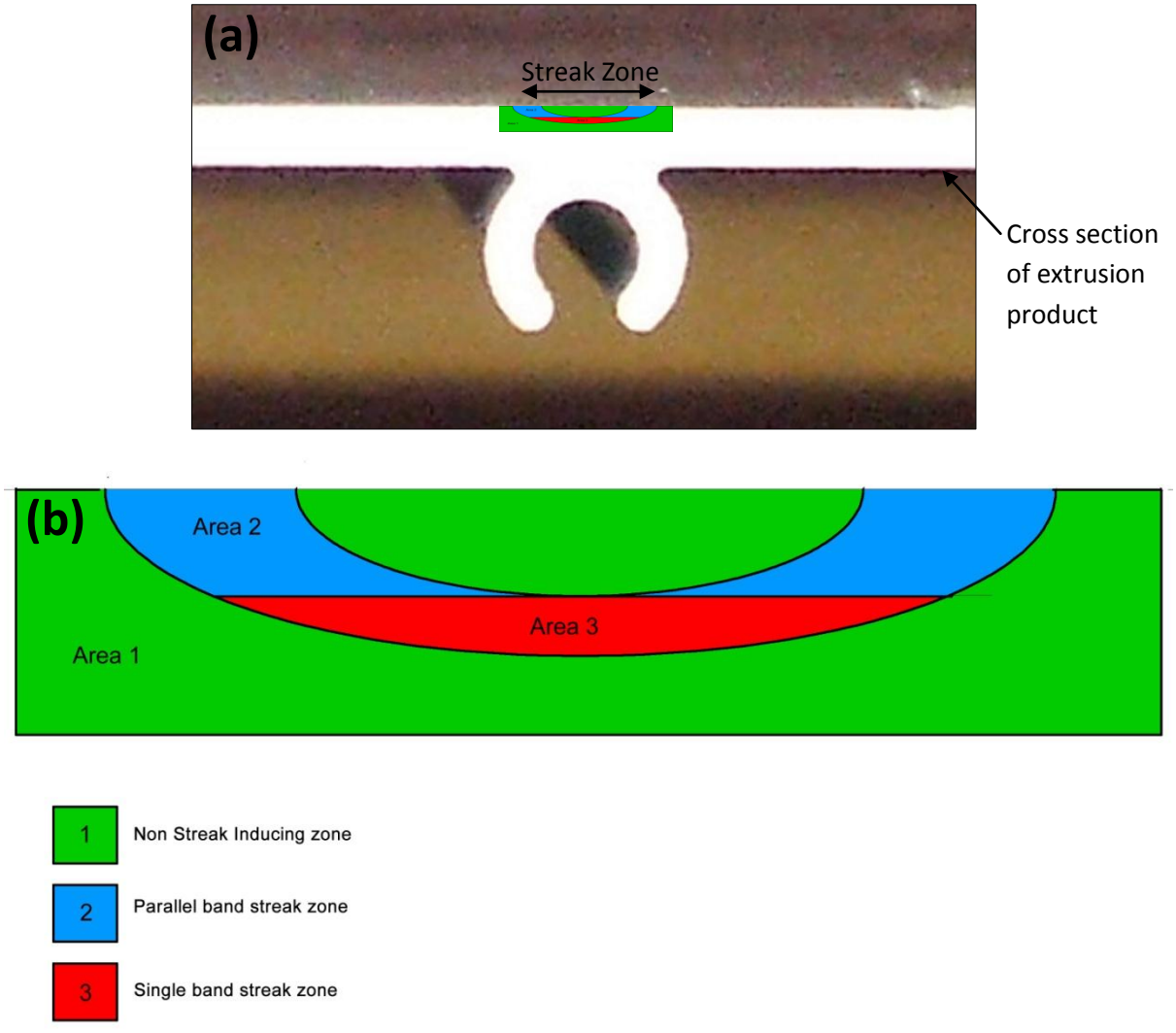

Figure 3-22 Streaking model for product 605344 (a) cross section at streak zone (b) Streaking model

3.3.3. Surface Microstructure of Etch Induced Streak Samples- Laboratory Etching

To examine the etch mechanism or mechanisms which cause an altered surface gloss and ultimately streaking, the Graff and Sargent's etched streak induced samples must be examined microscopically to identify differences in microstructure in and out of the streak region. To investigate differences in surface microstructure of Graff and Sargent's etched samples, images were taken in and out of the streak regions and then analysed using image J.

To examine the surface microstructure differences which are causing streaking the first sample investigated was sample S7 which was etched for 48 min (Please refer to Table 2-1 for further information on sample treatment) and showed faint double parallel band streaks as shown in Figure3-23. The numbered points shown on Figure 3-23 represent the approximate points at which the images shown in Figure 3-24 were acquired across six fields of view.

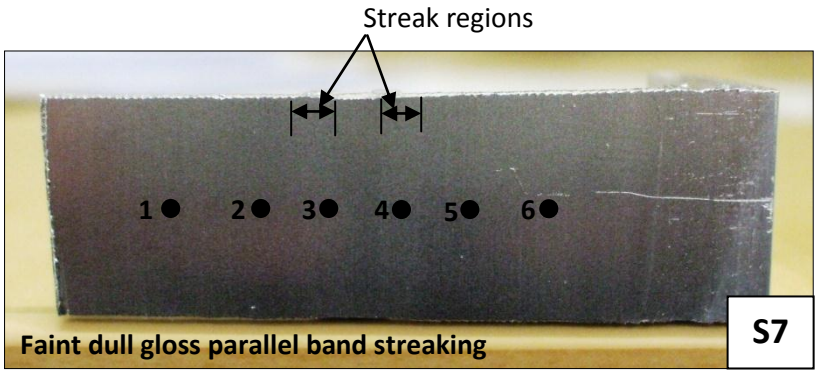

Figure 3-23 Surface of sampleS7 which was electro-polished for 1min and etched for 48min. The numbered points represent the locations at which the images shown in Figure 3-24 were acquired from.

On visual inspection of the images acquired shown in Figure 3-24 there is many circular features which are most likely pits. Because specimen S7only shows faint streaking, differences in microstructure features in and out of the streak regions should be minimal. Visually inspecting images 3 and 4 from inside the streak region with images 1, 2, 5 and 6 from outside the streak region it seems there may be slightly more circular pit like features from fields of view 3 and 4 from inside each parallel band streak region.

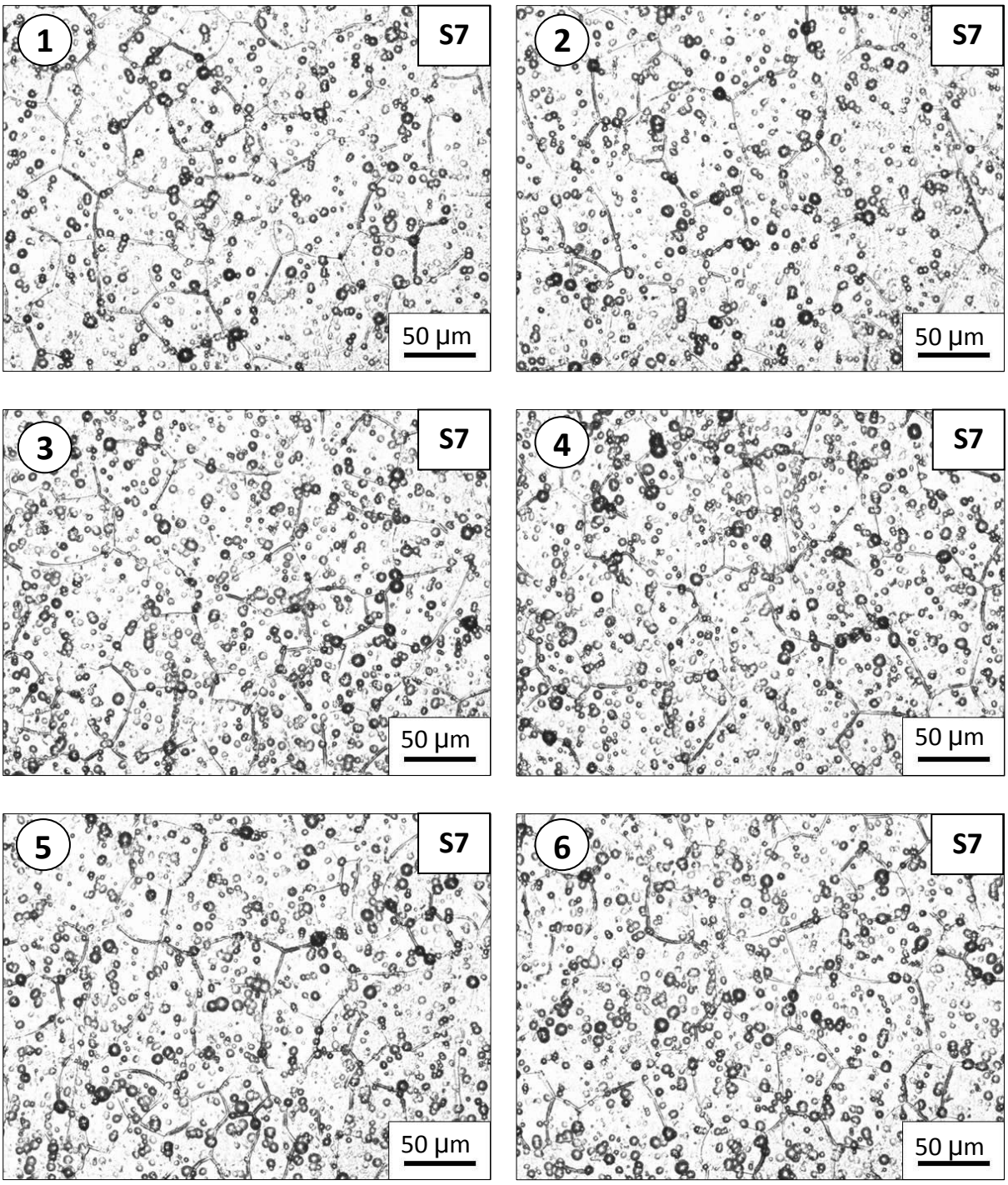

Figure 3-24 Microscopic images for sample S7 taken at the approximate points as specified in figure 3-23

The main features of the surface microstructure images shown in Figure 3-24 as previously mentioned are the circular pit like features. To quantify if the distribution of these pit like features differs in and out of the streak region Image J software was used to quantify the number of pit like features for each field of view shown in Figure 3-24. Figure 3-25 shows the pit count for each field of view shown in Figure 3-24. It can be seen that fields of view 3

and 4 from inside the streak region had a slightly increased number of pit features compared to fields of view 1, 2, 5 and 6. It must be noted however before further analysis of samples that have been etched for longer durations that the image J analysis would have some inaccuracy but provides further proof beyond visual inspection of images that differences are present in and out of the streak region.

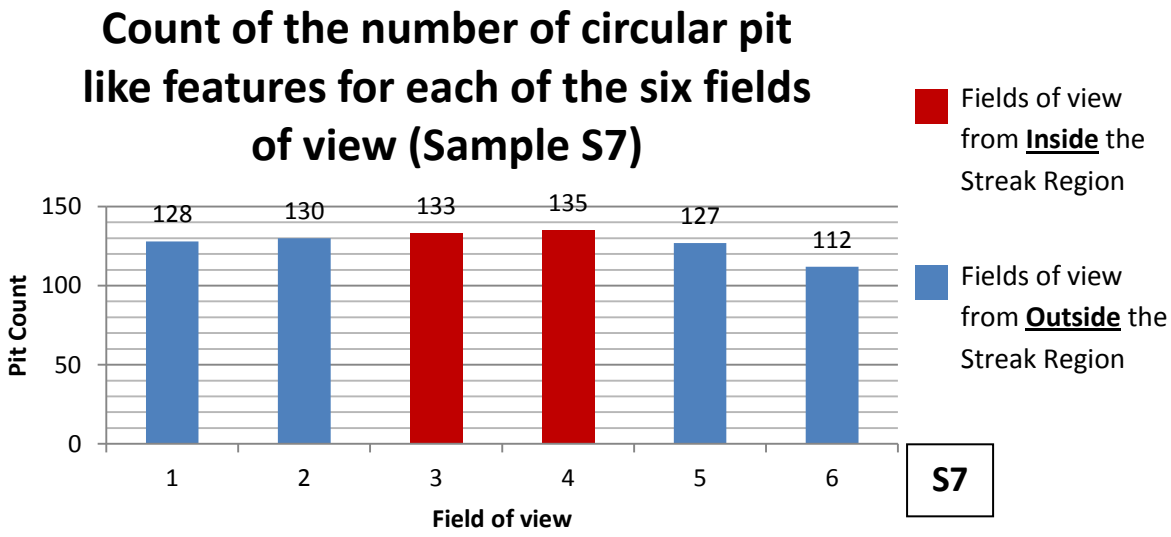

Figure 3-25Count of the number of circular pit like features for each of the six fields of view shown in Figure 3-24 for sampleS7

Further analysis using image J involved examining differences in pit size across the six fields of view. Figure 3-26 shows the average etching pit size across the six fields of view and shows no definitive differences in average etching pit size in and out of the streak region.

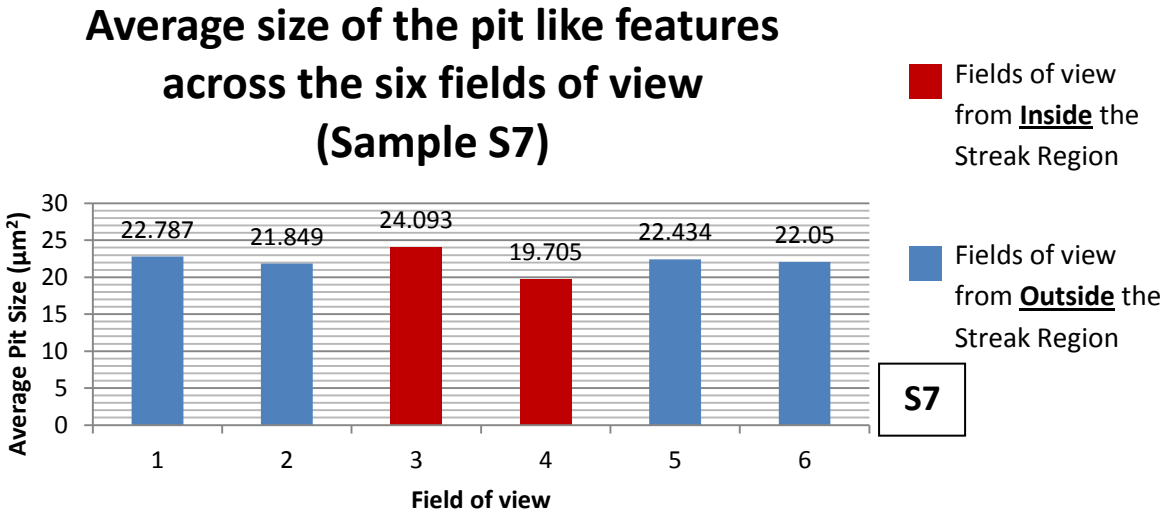

3-26Average Etching Pit Size for each of the six fields of view shown in figure 3-24 for sample S7

The next sample analysed to establish a difference in topographical microscopic surface features in and out of the streak region which could cause streaking was sample S8. Sample S8 like sample S7 showed double parallel band streaks as can be seen in Figure 3-27. The six points are the approximate locations of the six fields of view from which images shown in Figure 3-28 were acquired from.

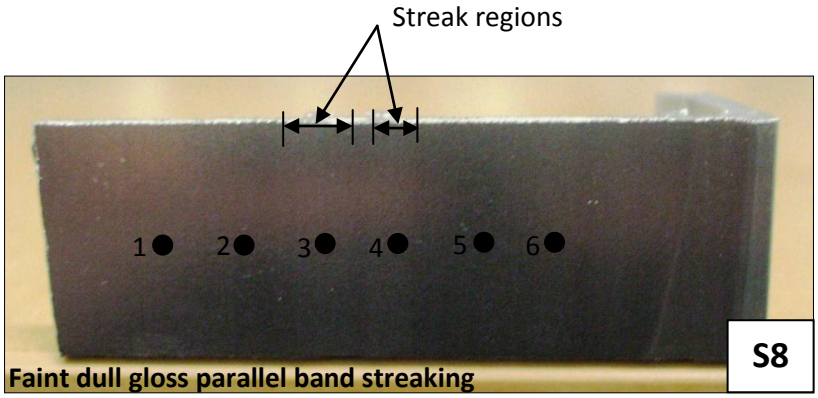

Figure 3-27 Surface of sample S8 which was electro-polished for 1min and etched for 62min. The numbered points represent the locations at which the images shown in Figure 3-28 were acquired from.

As can be seen from the six fields of view shown in Figure 3-28 the difference in circular pit like features is more apparent in and out of the streak region in which fields of view 3 and 4 are from inside the streak region and the remaining fields of view from outside the streak region. This is a more apparent difference in circular pit like features when compared to sample S7which most likely correlates to the greater clarity streak bands observed on sample S8. Overall there seems to be an increased distributional presence of circular pit like features for fields of view 3 and 4 which are from inside each parallel streak band. To again better quantify the differences in pit distributions and sizes in and out of the streak zone for each of the six fields of view an image J analysis was carried out using the same settings as for sample S7.

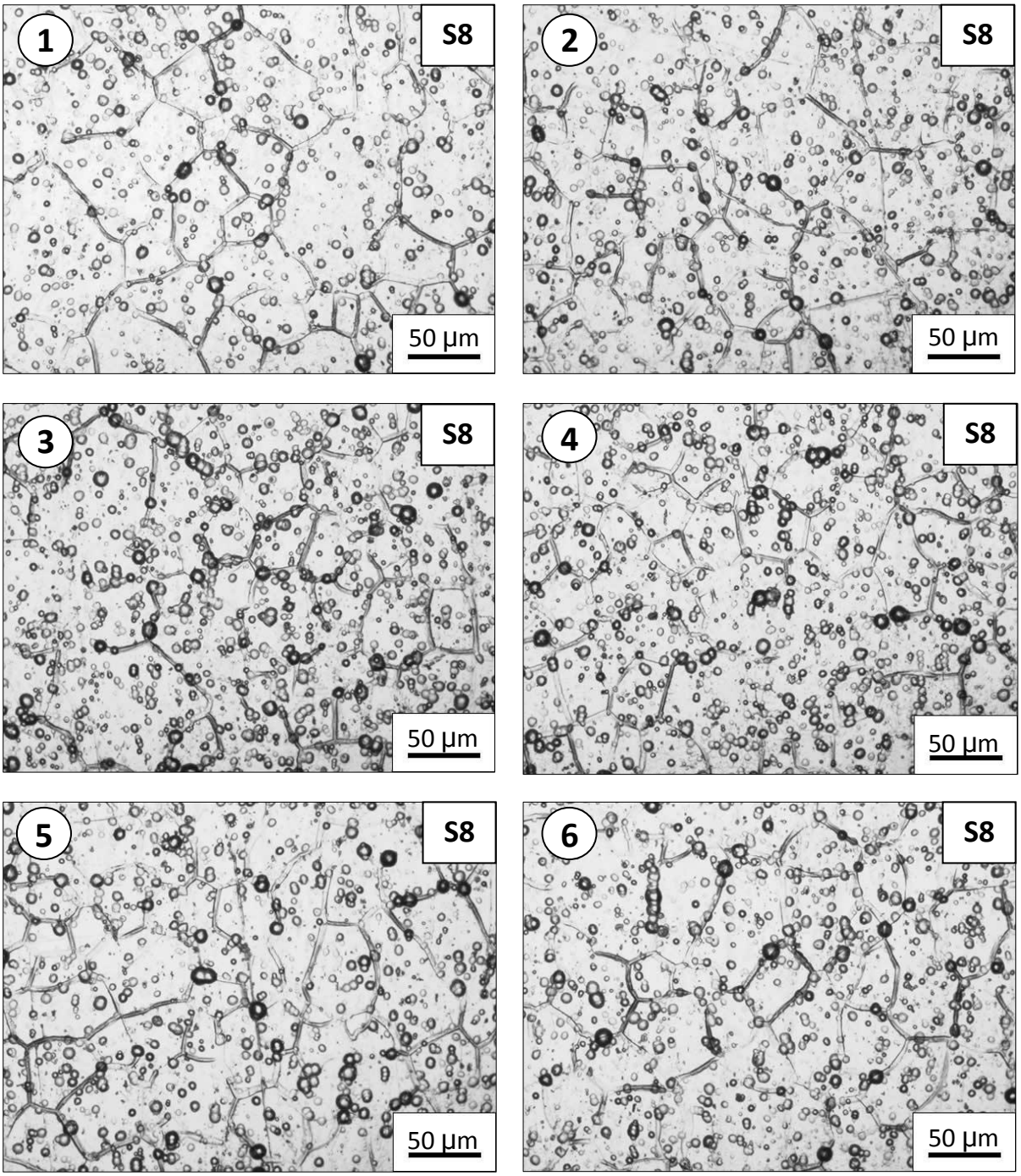

Figure 3-28 Microscopic images for sampleS8 taken at the approximate points as specified in Figure 3-27

Figure 3-29 shows the data obtained using image J regarding the number of circular pit like features for each of the six fields of view shown in Figure 3-28. It can be seen from Figure 3-29 that there is an increased distribution of pit features for fields of view 3 and 4 located in the region of each of the parallel streak bands when compared to the remaining fields of view from outside the streak band regions. Also the difference in the distribution of pit like features has increased in and out of the streak region for sample S8 compared to sample S7.

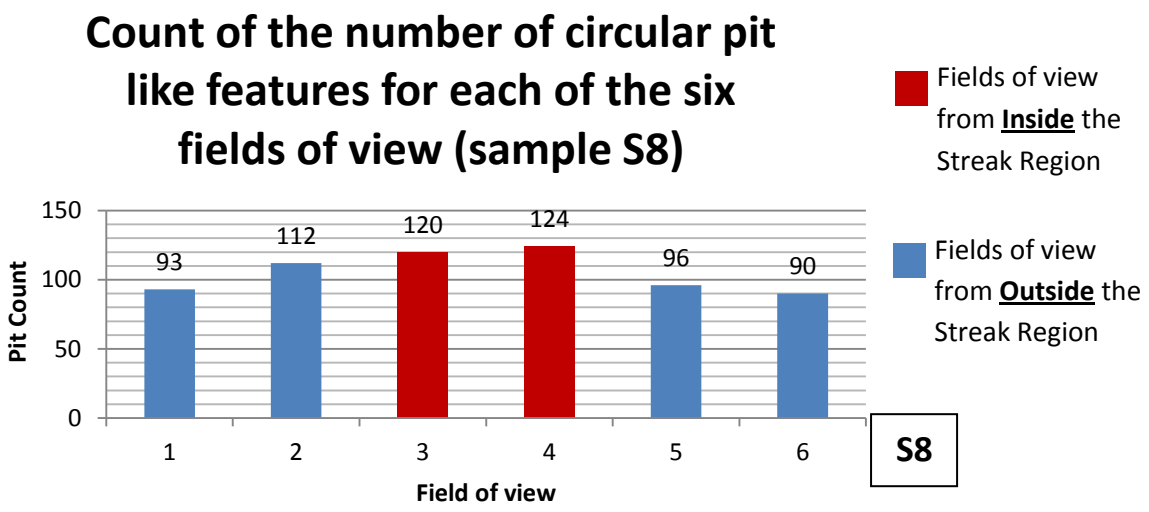

Figure 3-29 Count of the number of circular pit like features for each of the six fields of view shown in figure 3-28 for specimen S8

Further analysis was conducted of etching pit size for each of the six fields of view. This data shown in Figure 3-30 again shows like specimen S7that there was no definitive difference in average etching pit size in and out of the streak region.

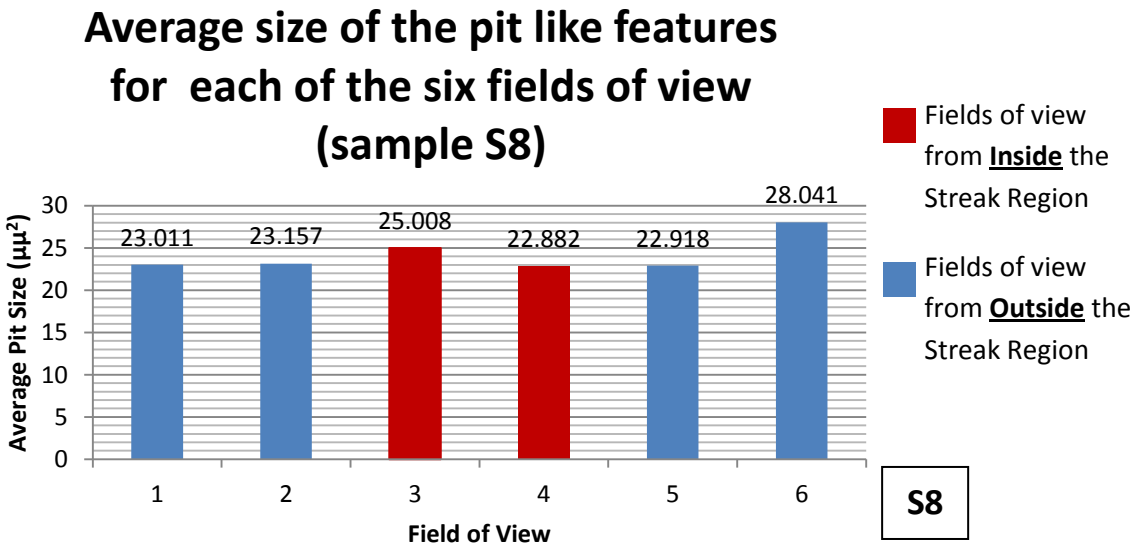

3-30 Average circular Pit like feature size for each of the six fields of view shown in figure 3-28 for specimen S8

The next sample S9 was electro-polished for an increased duration and etched for 48min (see Table 2-1 for sample treatment). Increasing the electro-polishing means more metal removal. When more metal is removed a single band streak will appear according to the model outlined in Figure 3-22. Figure 3-31 shows the surface of specimen S9. The streaking that

occurred for this specimen was a highly visible single band streaking. Microscopic images were acquired from six fields of view at the approximate points shown below in Figure 3-31. Points 1, 2, 5 and 6 are located outside the streak region and points 3 and 4are located inside the streak region.

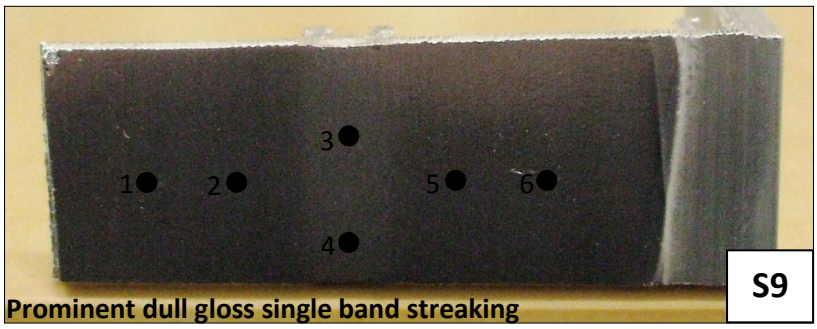

Figure 3-31 View of the surface of sampleS9 which was electro-polished for 2 min and etched for 48 min. The numbered points represent the locations at which the images shown in Figure 3-32 were acquired from.

Figure 3-32 shows microscopic images from the approximate six points outlined in Figure 3-31. It can be seen on visual inspection of these images that there is a significant increase in circular pit like features for fields of view 3 and 4 which are from inside the single band streak when compared to the remaining fields of view from outside the streak region. When visually comparing Figure 3-32 with Figures 3-24 and 3-38 from the previous samples it seems the distribution of circular pit like features in and out of the streak region differs the most for this sample, S9. Interestingly the most visually significant difference in pit like features in and out of the streak region also correlates to the most visually prominent streak yet. Like previous samples further quantification of the differences in etching pit distributions was carried out using Image J software to more accurately quantify the difference in circular pit like features in and out of the streak region.

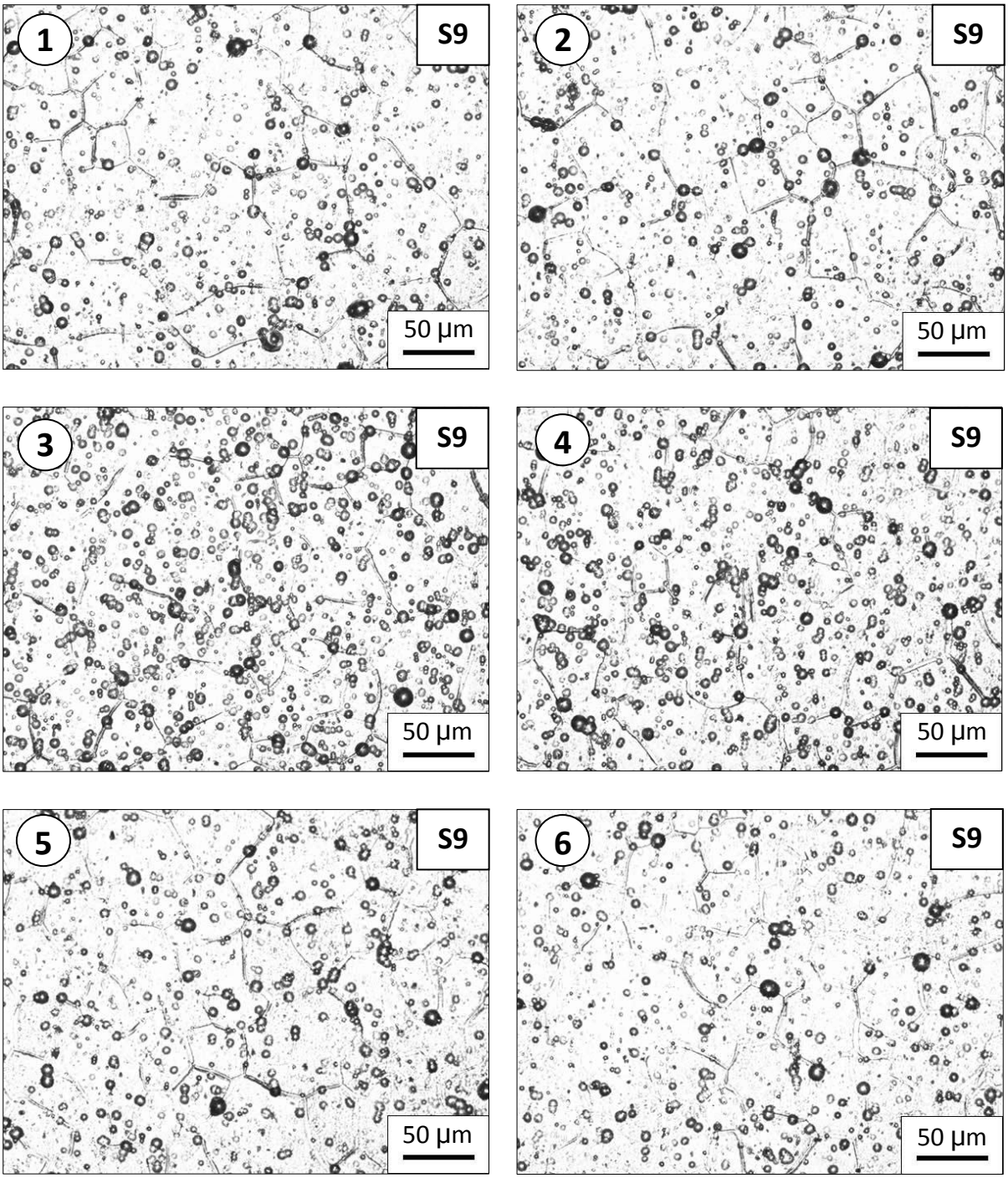

Figure 3-32Microscopic images for sampleS9 taken at the approximate points as specified in Figure 3-31

Using the same Image J processing conditions as was used for samplesS7 and S8a count of the number of circular pit like features was made for each of the six fields of view from Figure 3-32. The data acquired for the number of circular pit features for each field of view is shown in Figure 3-33. When compared to the distribution analysis of circular pit like features for the previous samples the difference in these features in and out of the streak region is the most for this sample, S9. Visually this is what seems apparent and further

concludes that a greater difference in these features in and out of the streak zone will correspond to a more visually prominent streak band.

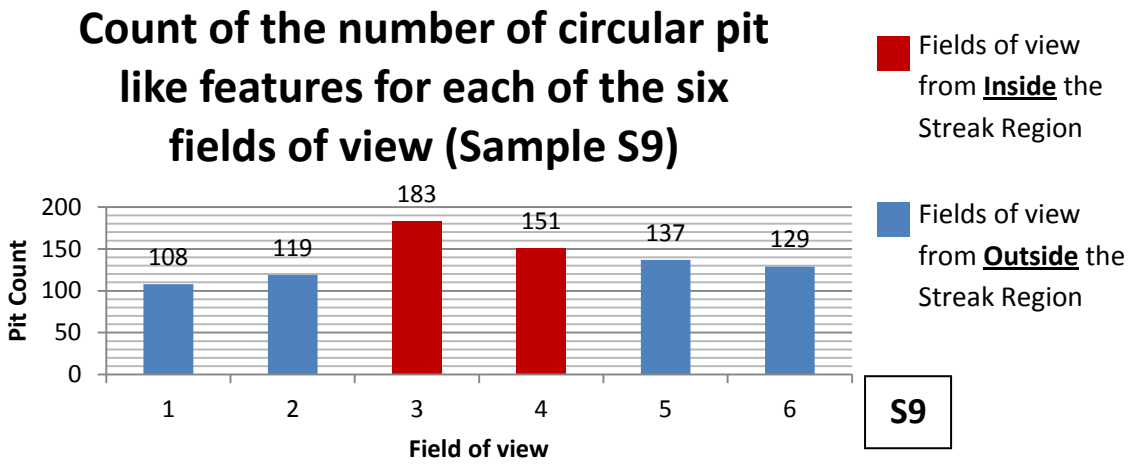

Figure 3-33Count of the number of circular pit like features for each of the six fields of view shown in Figure 3-32 for sampleS9

Like the analysis of the average size of the pit like features for the previous samples there was again no definite difference in the area of these pit like features in and out of the streak region as can be seen from the data shown in Figure 3-34.

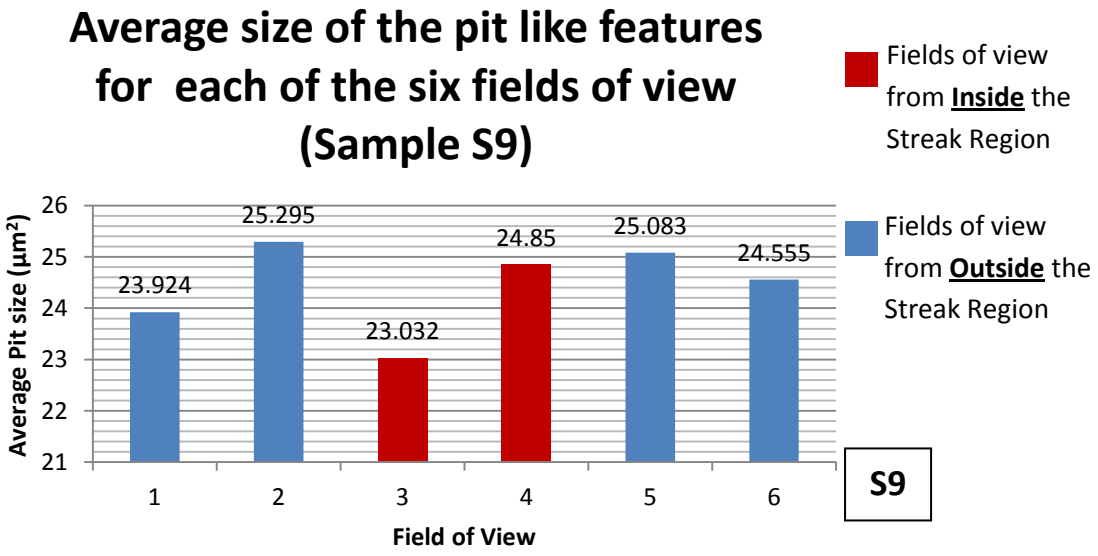

3-34Average size of the pit like features across the six fields of view shown in Figure 3-32

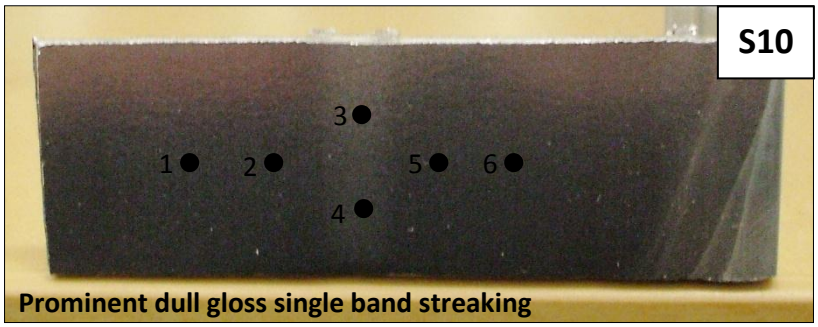

Figure 3-35Surface of sample S10 which was electro-polished for 2 minutes and then etched for 62min. The numbered points represent the locations at which the images shown in Figure 3-36 were acquired from.

Figure 3-36 shows optical microscopy images from six fields of view located at the approximate points shown in Figure 3-35. Fields of view 3 and 4 are from inside the streak region and the remaining fields of view are from outside the streak region. Visually it can be seen that circular pit like features are more densely distributed for fields of view 3 and 4 from inside the streak region when compared to the remaining fields of view from outside the streak region.

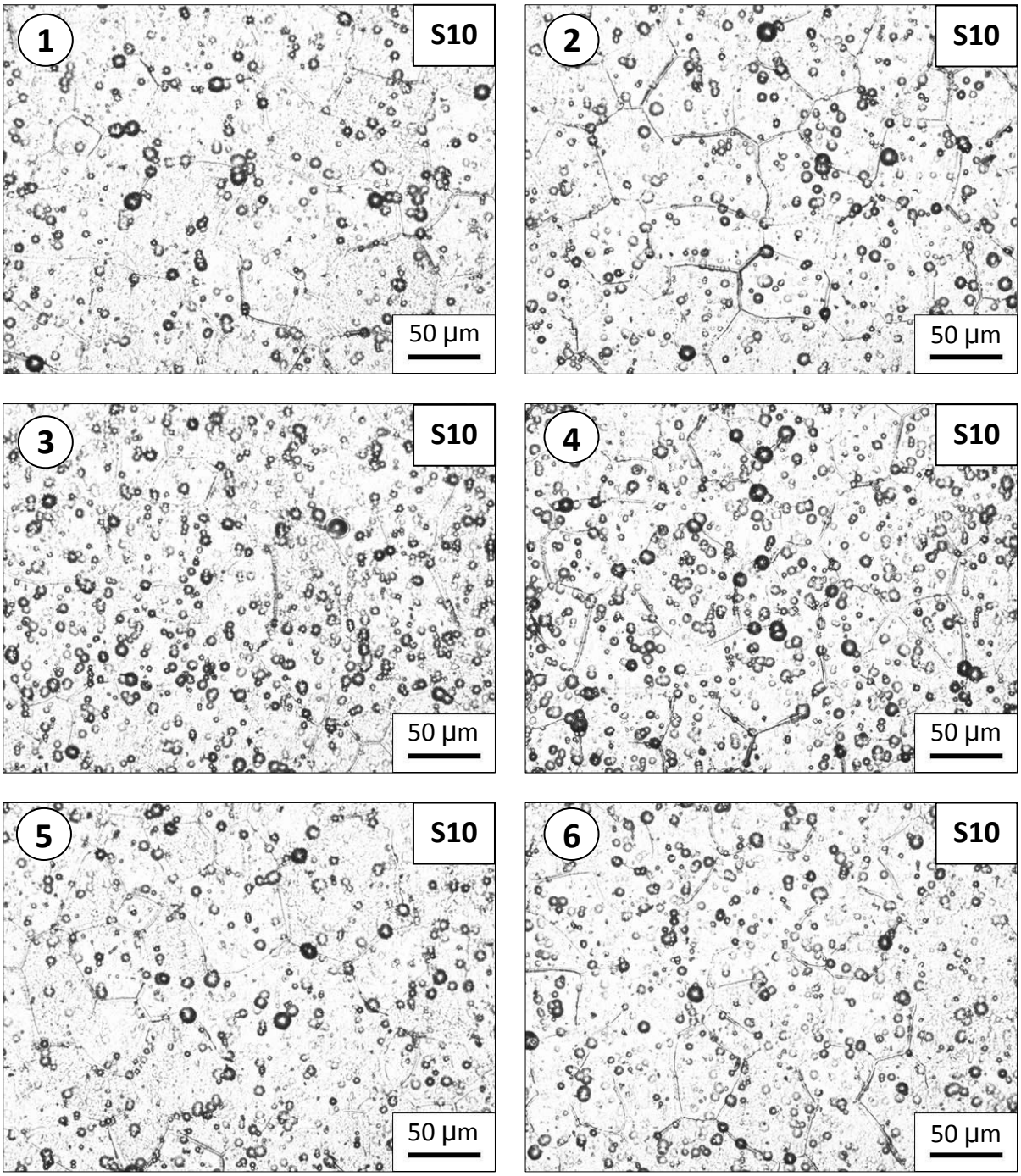

Figure 3-36Microscopic images for sample S10 taken at the approximate points specified in Figure 3-35

Like previous samples, sample S10 showed there was an increase in the distribution density of circular pit like features for the fields of view inside the streak region. The data obtained confirming this is shown in Figure 3-37.

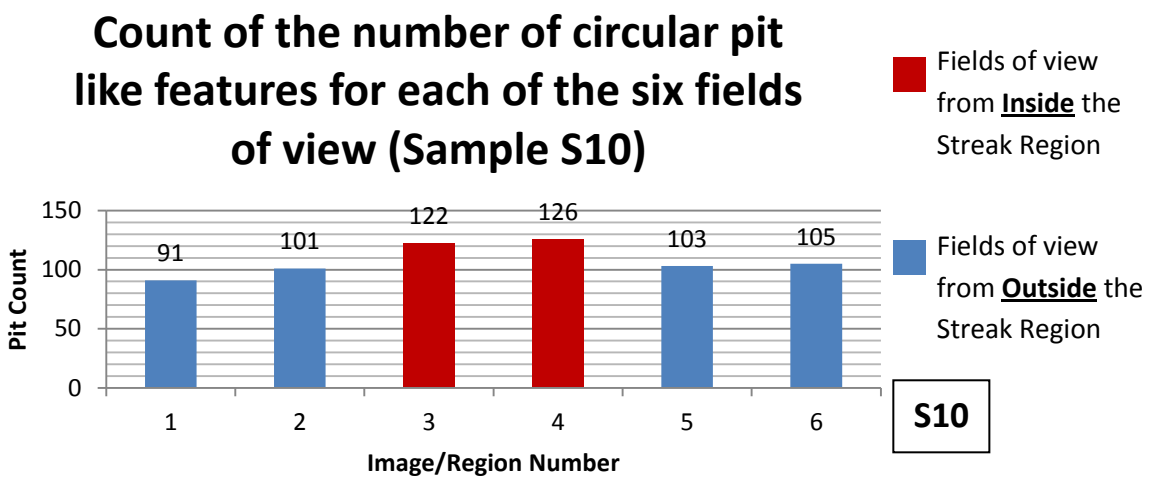

Figure 3-37 Count of the number of circular pit like features for each of the six fields of view shown in Figure 3-36 for sampleS10

Figure 3-38 shows the average etching pit size for each of the six fields of view shown in Figure 3-36. Like previous streak induced specimens there is no definite difference in the circular area of the pit like features.

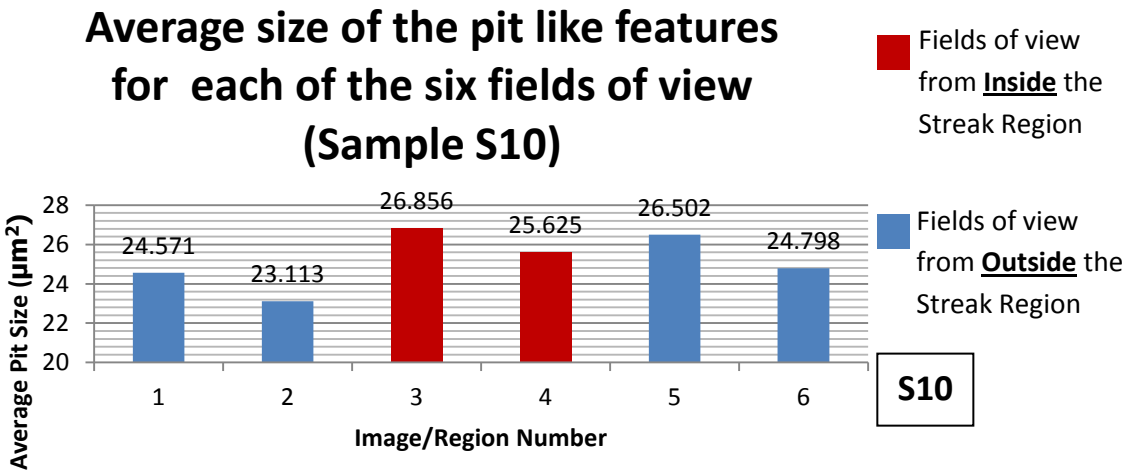

3-38Average circular pit like feature size for each of the six fields of view shown in Figure 3-36 for specimen S10

Overall it can be seen from the data obtained in this experiment that after etching in Graff and Sargent's etchant streaking was induced on the electro-polished surface. Furthermore microscopic analysis has identified circular etch pit like features on the surface which vary in distribution density in and out of the streak region. However the area or size of these circular features does not seem to vary conclusively in and out of the streak region. In addition it seem only a small variation in and out of the streaked regions in terms of distributional density of these pit like features can cause regions of differing surface gloss to appear and ultimately streaking.

3.3.4. The Evolution of Streaking – Manufacturing Etching Simulation

To check the relevance of previous etching results found using Graff and Sargent's etchant which was used to simulate etching in a laboratory, an experiment was conducted using the etching solution and conditions used at Falum. A series of samples were etched for different durations and the streak formations observed to see if they correlate to the findings made using Graff and Sargent's etchant and if any new findings could be made. Four modes of streaking appeared on the surface of the sample after different etching durations as can be seen from images a-h shown in Figure 3-39 for samples S11-218. These modes of streaking are tabulated in Table 3-3 below:

Table 3-3 Mode of streaking for each of the samples shown in figure 3-41

Etch Duration	Type of streaking	Samples	Figure showing streaking
Low etch duration	Single band glossy streaking	S11, S12, S13	Figure 3-39 (a), (b), (c)
Medium etch duration	Parallel band dull Gloss streaking	S14,S15,S16	Figure 3-39 (d), (e), (f)
Medium – High etch duration	Single band dull gloss streaking	S17	Figure 3-39 (g)
High etch duration 20min+	Single band faint streak - disappearing	S18	Figure 3-39 (h)

It must be noted that compared to the samples electro-polished and etched in Graff and Sargent's etchant that the streaking is not as prominent. This can be attributed to the chemical formula of the etchant which is designed to matte the surface and actually mitigate the appearance of surface defects such as streaking. The etchant is known as P3 etch manufactured by Henkel. This etch contains additives such as fume suppressant and sorbitol to stop the alumina from precipitating from the caustic solution. Other unknown additives are added to mitigate defects but these additives are commercially sensitive and were not given.

(a) Sample S11 – etched 2.5

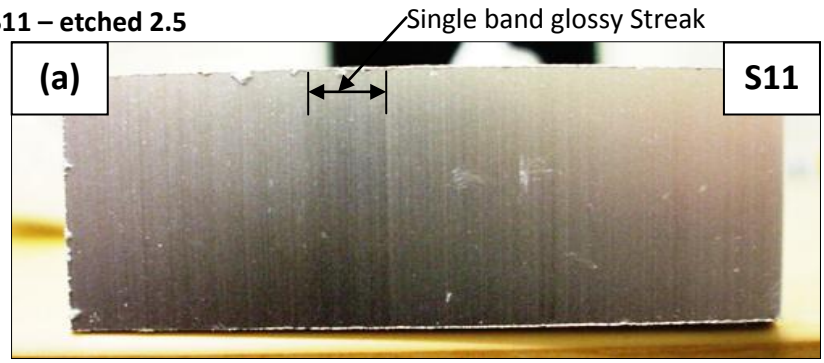

(b) Sample S12 – etched 5 min

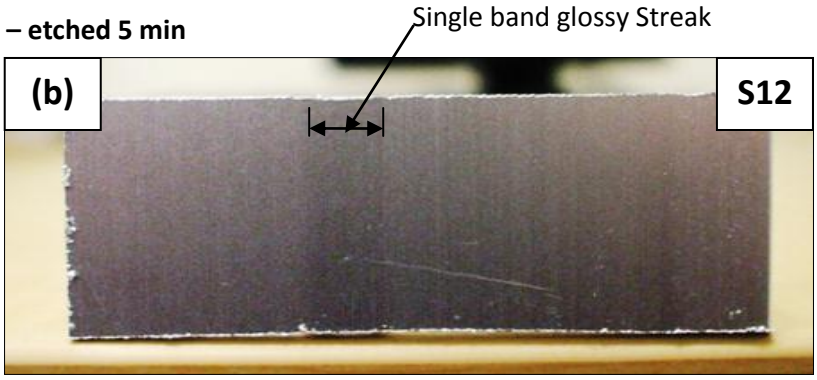

(c) Sample S13 – etched 7.5

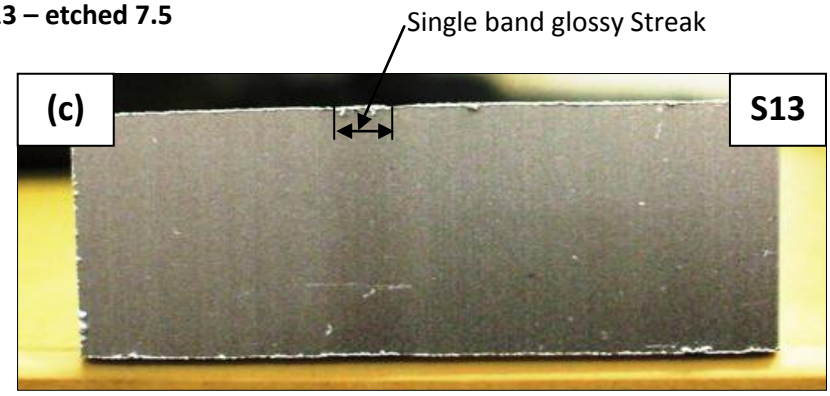

(d) Sample S14 – etched 10 min

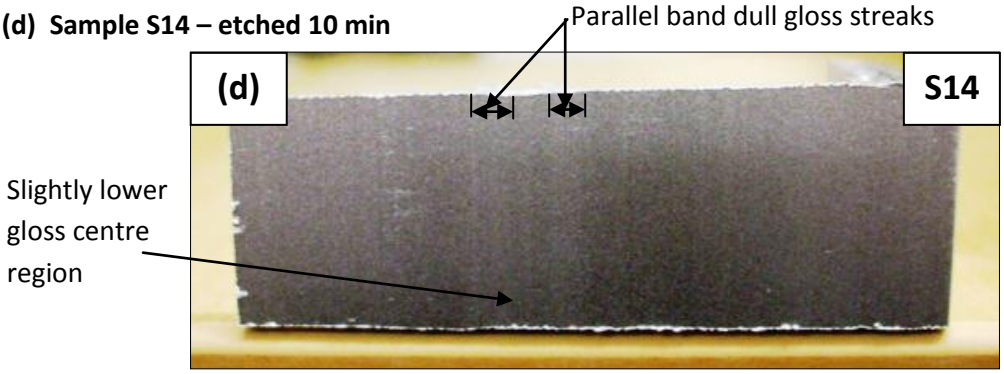

3-39 - Series of samples etched in Henkel etchant (main ingredient sodium hydroxide) for different durations

(e) Sample S15 – etched 12.5

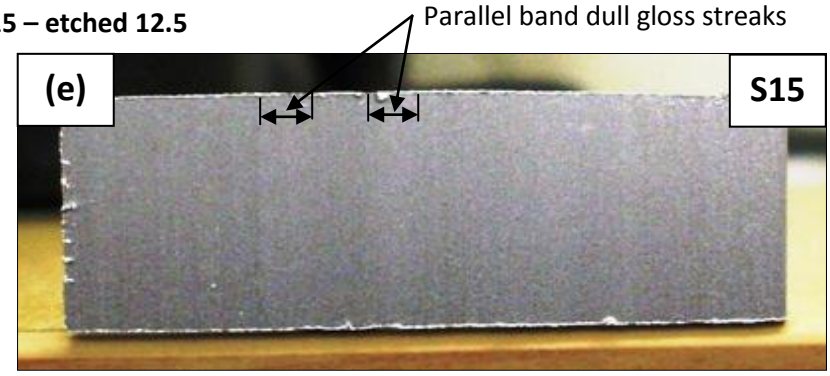

(f) Sample S16 – etched 15 min

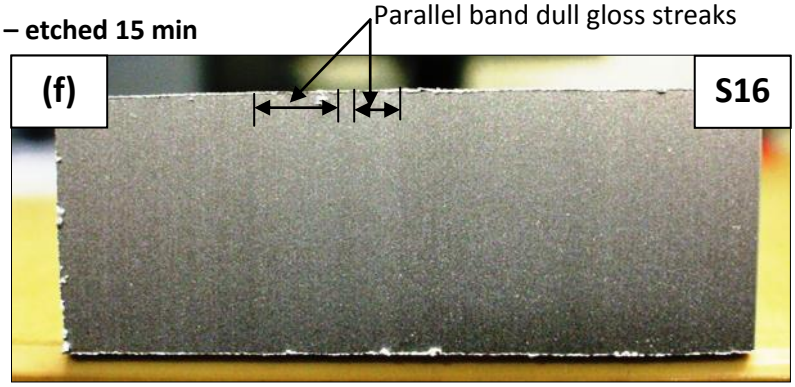

(g) **Sample S17 – etched 17.5**

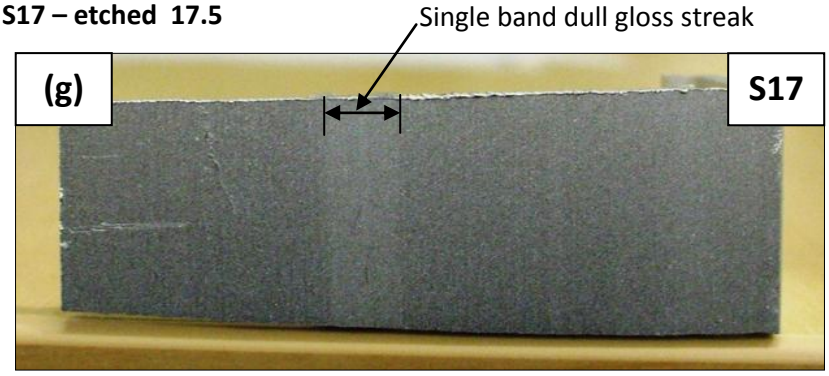

(h) Sample S18 – etched 20 min

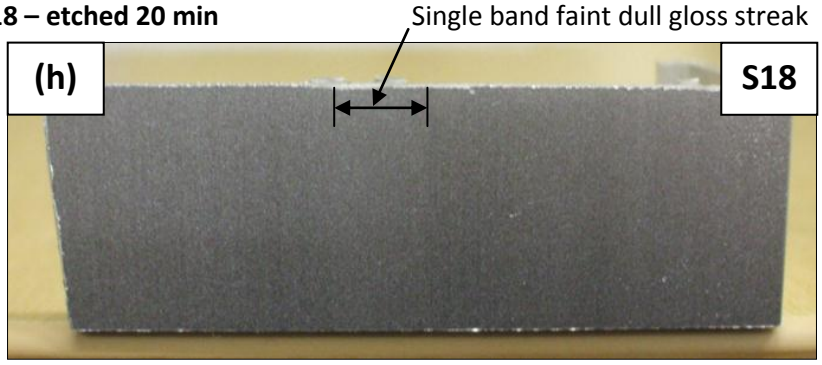

CONTINUED - 3-39 - Series of samples etched in Henkel etchant (main ingredient sodium hydroxide) for different durations

From table 7 there are 2 questions that must be answered:

- Why is the initial streaking after low etch durations glossy?
- Why is streaking after medium and high etch durations a dull gloss?

The following sections will answer these questions.

3.3.5. Reasons for Glossy Streaking After Low Etch Durations

This section will answer the question of why glossy streaking occurs after low etch durations. To answer this question the following topics will be analysed and discussed:

1. The surface microstructure in and out of the streak region to see what differences may be present.
2. An analysis to find if roughness differences on the as extruded product in and out of the streak region may have an effect on etching response and hence mean differences in surface microstructure in and out of the streak region. (Note: Differences in surface roughness in and out of the streak region on the as-extruded product was identified in section 3.1 due to less densely distributed die lines in the streak region)

Starting from point 1 above the surface microstructure of samples S11, S12 and S13 which all exhibited glossy streaks will be analysed to ascertain what microstructural differences exist in and out of the streak region. Summarising from previous analysis it was found that the surface was smoother in the streak region when compared to the surrounding extrudate immediately after extrusion. It was found that after initial low etching durations a highly visible glossy streak appeared while the surrounding extrudate was duller. Based on knowledge that a rougher surface reflects light to exhibit a glossier surface as identified according to the graph shown in Figure 1-9, there should be a smoother surface in the streak region and a rougher surface outside the streak region. Six images were acquired from six fields of view in and out of the streak zone on the surface of sample S11 which was etched for 2.5min as outlined in figure 3-40. The six fields of view are shown in figure 3-41 where fields of view 3 and 4 are located in the glossy streak region.

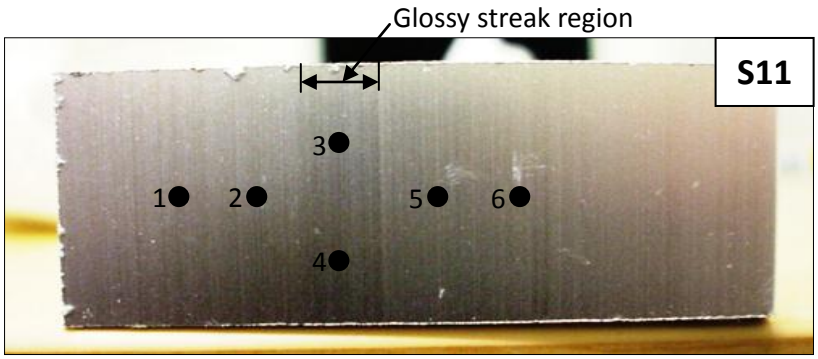

3-40Surface of specimen S11 which was etched for 2.5 minutes. The numbered points represent the locations at which the images shown in figure 3-41 were acquired from.

Figure 3-41 shows the six fields of view acquired from the surface of sample S11. Visually it can be seen that die line features are less densely distributed in the streak region (fields of view 3 and 4) with pitting differences unidentifiable on visual inspection.

For identification of the die like and pit features please note the following: The die line features are the faint black lines which run vertically across the images. These die lines distort the visibility of pitting so no clear visual observational conclusion can be made on the differences in pit like features in and out of the streak region. The features which represent pits are the black circular features which can also be observed in each field of view.

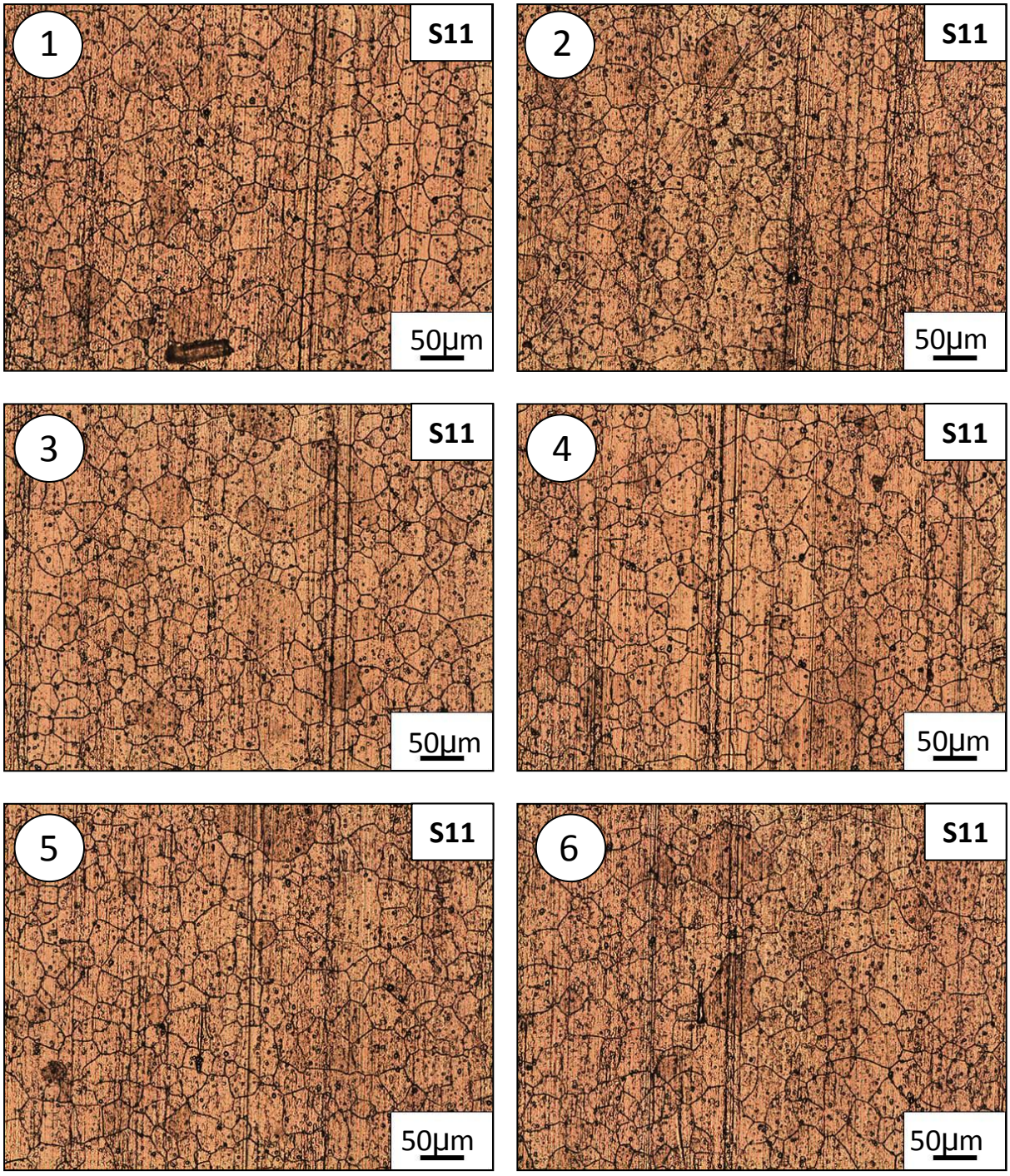

Figure 3-41 Microscopic surface images of sample S11 at the 6 points outlined in figure 3-42

It is clear that die line are less densely distributed in the streak region however pitting differences are unclear on visual observation. If both of these factors differ in and out of the streak region the surface roughness will differ and cause differing surface gloss in and out of the streak region. To further identify that differences in the distributional density of circular pit like features in and out of the glossy streak region is in fact present, the number of these

pits in each field of view shown in Figure 3-41 was analysed using image J. The same analysis procedure was used as for image J analysis of the pit features on Graff and Sargent's etched samples. Figure 3-42 shows the number of circular etch pit like features for each field of view shown in Figure 3-41. It can be seen that image J analysis found a lower distributional density of pit features for fields of view 3 and 4 from inside the glossy streak region. This would cause in combination with a lower density distribution of die lines a lower surface roughness in the streak region. A lower surface roughness hence means a glossier surface according to literature provided in section 1.3. This agrees with the glossy streak and dull surrounding extrudate observed for specimen S11.

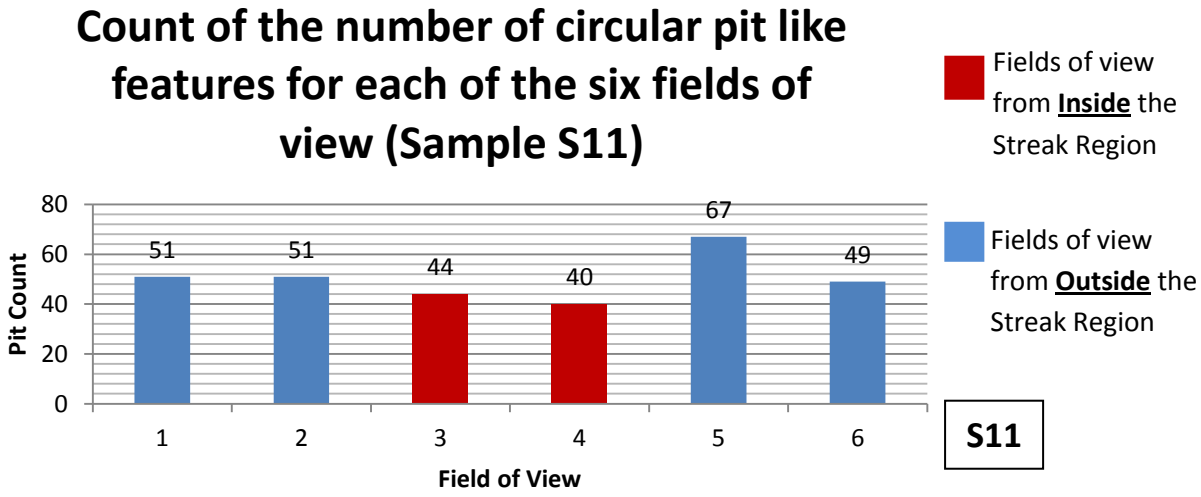

Figure 3-42 Count of the number of circular pit like features for each of the six fields of view shown in figure 3-54 from the surface of specimen S11

The next sample S12 was etched for five minutes. Six images were acquired from six fields of view located at the approximate locations specified in Figure 3-43 across the surface of specimen S12.

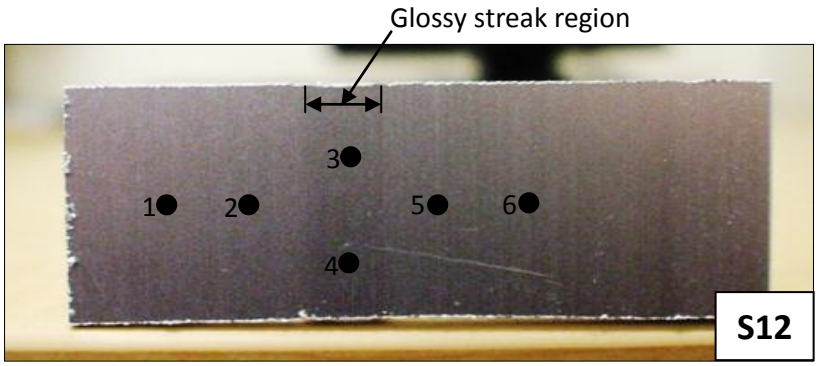

3-43 The surface of sample S12 which was etched for 5 minutes. The numbered points represent the locations at which the images shown in figure 3-44 were acquired from.

Figure 3-44 shows the images across the six fields of view where 3 and 4 are from inside the streak region and the remaining fields of view from outside the streak region. Like sample S11 it can be observed that there are more die line features from the fields of view outside the streak region. Also the density of circular black pit like features seems to be less in fields of view 3 and 4 from inside the streak region.

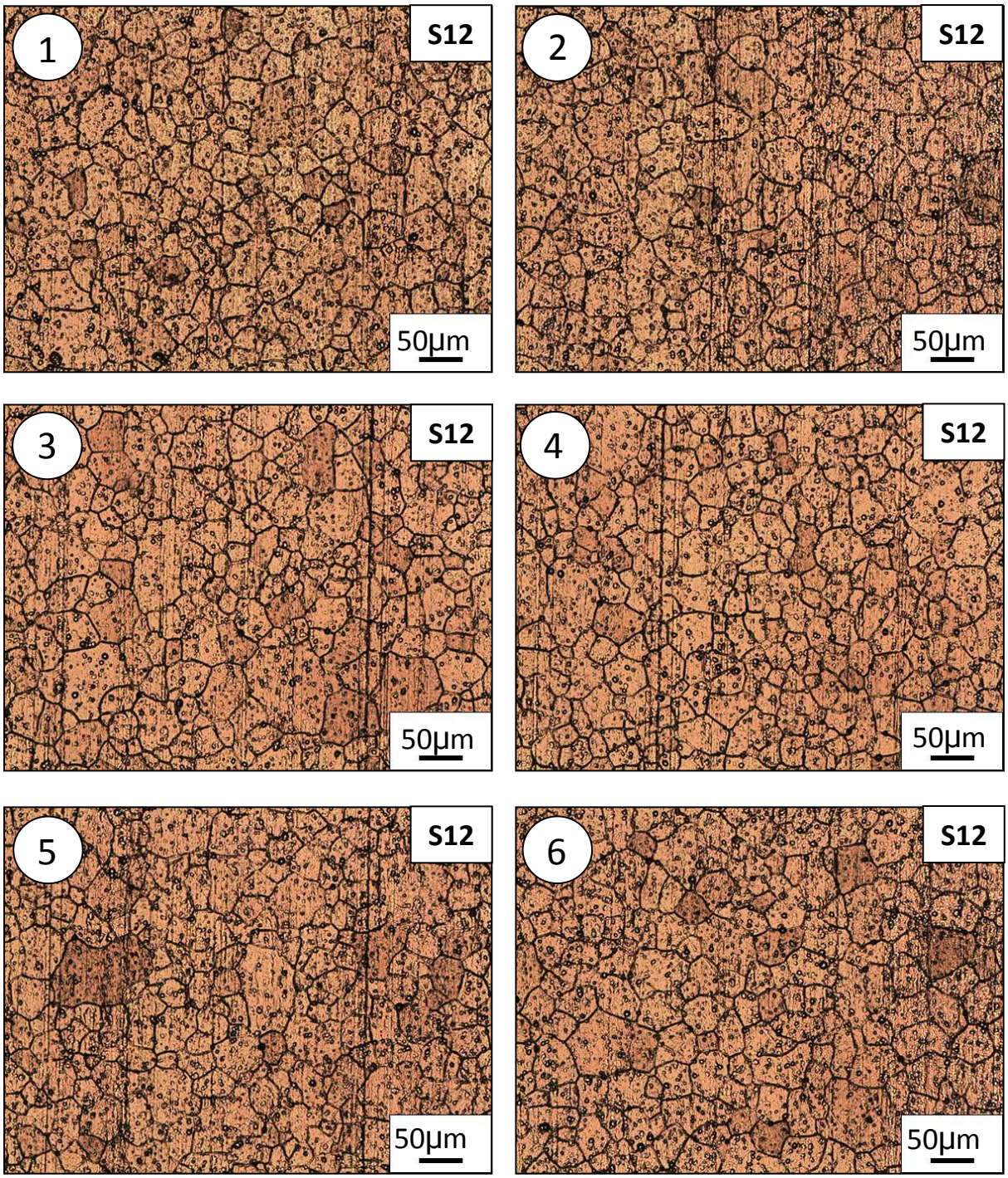

Figure 3-44 Microscopic surface images of sample S12 at the 6 points outlined in Figure 3-43

To confirm that the circular black pit like features are less in fields of view 3 and 4, which would in combination with less densely distributed die lines cause a smoother and glossier surface than outside the streak region, an image J analysis was again carried out for each field of view shown in Figure 3-44 for specimen S12. It can be seen that for fields of view 3 and 4 from inside the streak region there is a significant difference in the distribution density of black circular pit like features when compared to the remaining fields of view from outside the streak region.

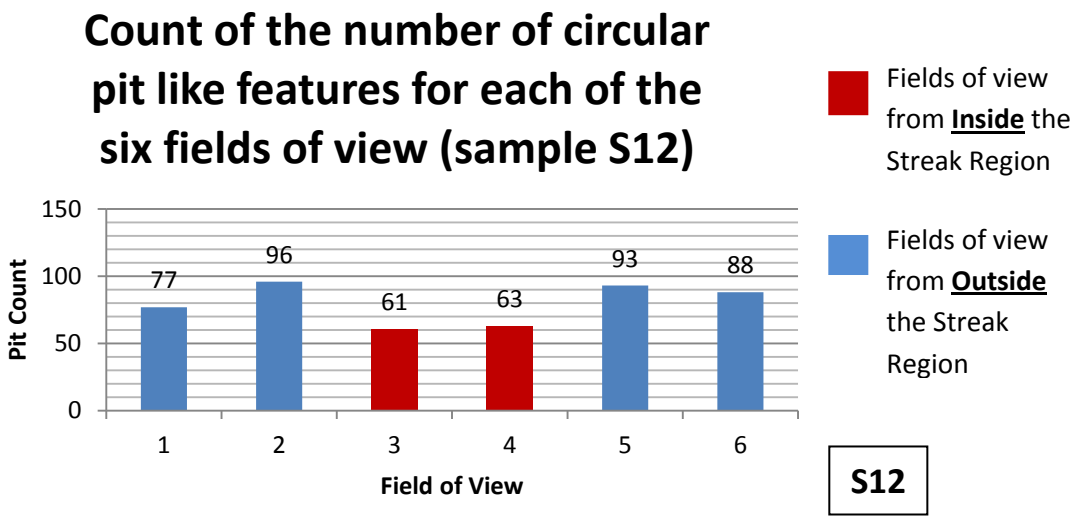

Figure 3-45 Count of the number of circular pit like features for each of the six fields of view shown in figure 3-44 from sample S12

Sample S13 was etched for 7.5min and the surface is shown in Figure 3-46. The six points shown in figure 3-46 represent the six fields of view from which optical microscopy images were acquired from.

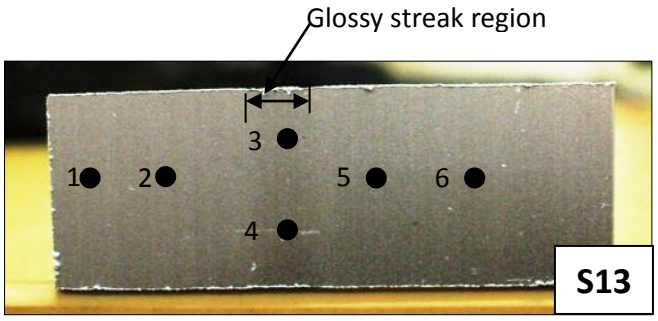

Figure 3-46 Surface of sample S13 which was etched for 7.5 minutes. The numbered points represent the locations at which the images shown in Figure 3-47 were acquired from.

Figure 3-47 shows the images acquired from the six fields of view on the surface of specimen S13 as specified in Figure 3-46. It can be seen that fields of view 3 and 4 from in the glossy streak region are almost free of any die line features running vertically the height of the pictures. Also circular black pit like features appear to be less densely distributed for fields of view 3 and 4 when compared to the remaining fields of view from outside the glossy streak region.

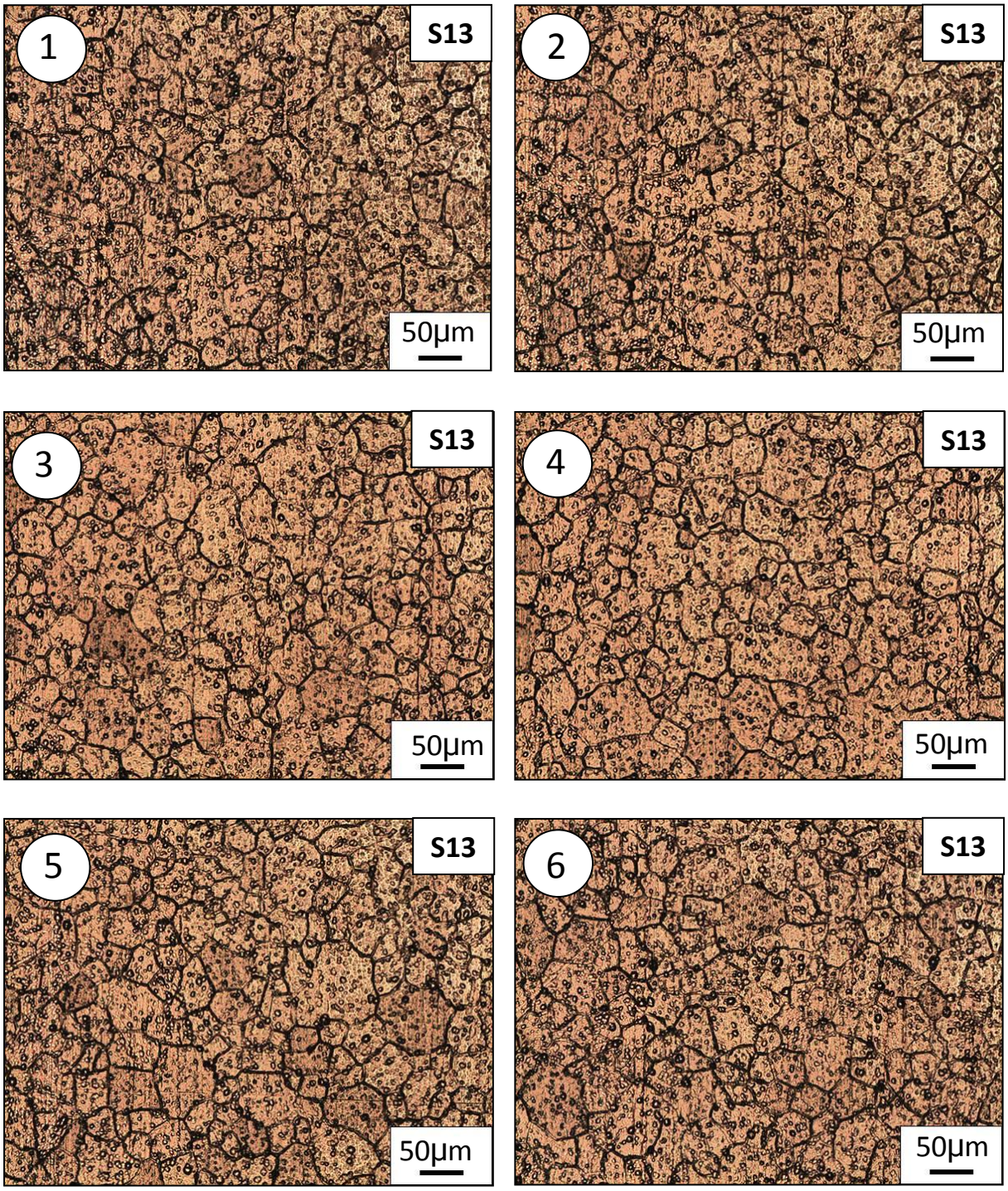

Figure 3-47 Six fields of view taken from the approximate locations specified in Figure 3-46 for sampleS13, Fields of view 3 and 4 are from inside the glossy streak region and fields of view 1, 2, 5 and 6 are from outside the streak region

To further verify that the distribution of black circular pit like features are less in the streak region thereby causing a smoother surface and a higher gloss, the six fields of view shown in Figure 3-47 were analysed using Image J like previous samples. From figure 3-48 it can be seen that image J verifies that there is a lower distribution of circular pit like features in the

streak region (fields of view 3 and 4). The difference in pitting in and out of the streak region has decreased relating to a dulling streak region.

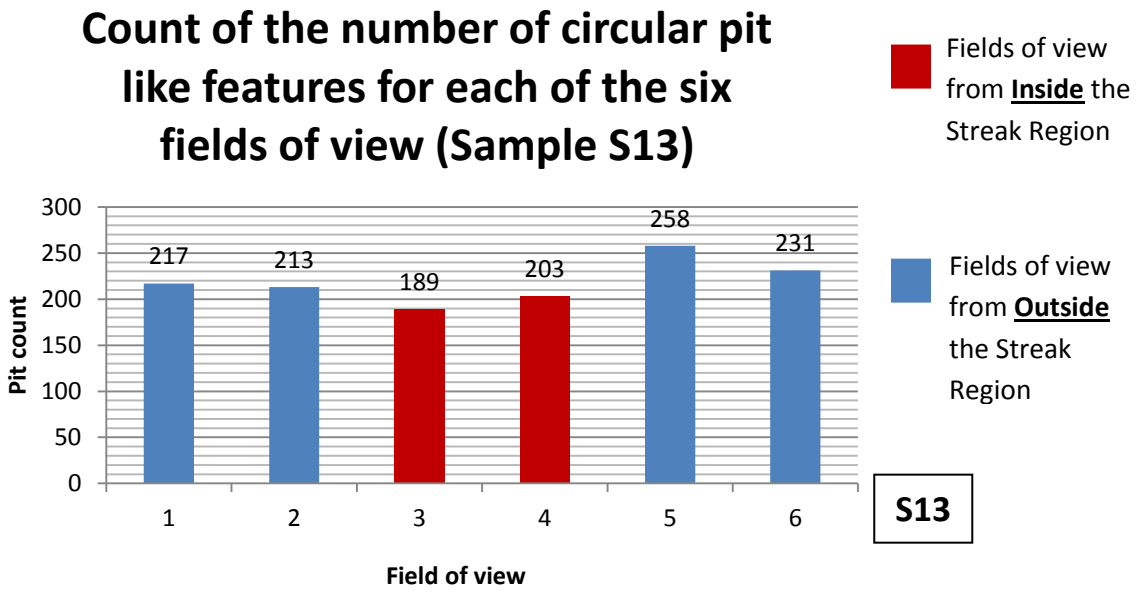

Figure 3-48 Count of the number of circular pit like features for each of the six fields of view shown in figure 3-60 from sample S13

From this above analysis of the surface microstructure of glossy streak samples it is proven that the streak region is less pitted after etching.

For dull streak samples larger levels of surface material removal have occurred than for glossy streak samples. This means the cause of the different etching response in and out of the streak region for the dull gloss streak samples is most likely due to metallurgical differences in out of the streak region. The glossy streaking however is most likely due to mechanical differences in and out of the streak region in the form of less die lines in the streak region.

It was identified that when surface roughness differs in regions so does the etching response. This was identified by mechanically polishing samples to remove die lines and also electro-polish the samples for a short duration. Then by comparing differences in pitting with samples which were only electro-polished for a short duration and not mechanically polished to remove die lines it was established that a differing etching response does occur on samples of different roughness. Therefore this explains the reason for less pitting in the streak region of glossy streaked samples. The following outlines the findings of the samples which were mechanically polished and electro-polished and then a comparison is made of pitting in and out of the streak region with samples which were only electro-polished.

Sample S19 exhibited highly prominent streaking on visual inspection as can be seen from the figures shown in Figure 3-49.

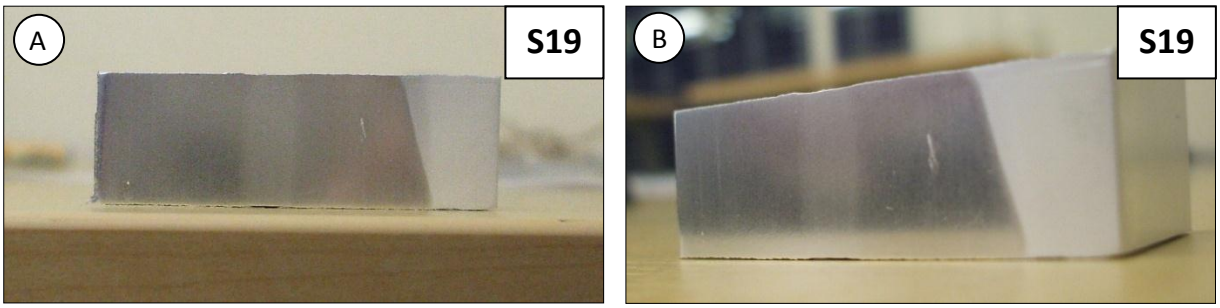

Figure 3-49 Sample S19 mechanically polished, electro-polished and then etched in Graff and Sargent's etchant for 40 minutes (a) Front View (b) Left View

To examine if etching response differs on a rough and smooth surface an optical microscopy and image J analysis will be conducted to determine the degree of pitting in and out of the streak region. The degree of difference will then be compared to the samples (as analysed in section 3.3.3) which were only electro-polished and not mechanically polished also.

Optical microscopy images were taken from six fields of view on the surface of sample S19 where fields of view 3 and 4 are from inside the streak and the remaining fields of view from outside the streak region, either side of the streak band. These images are shown in figure 3-50 and show a significant increase in the density of pits for fields of view 3 and 4 from inside the streak region.

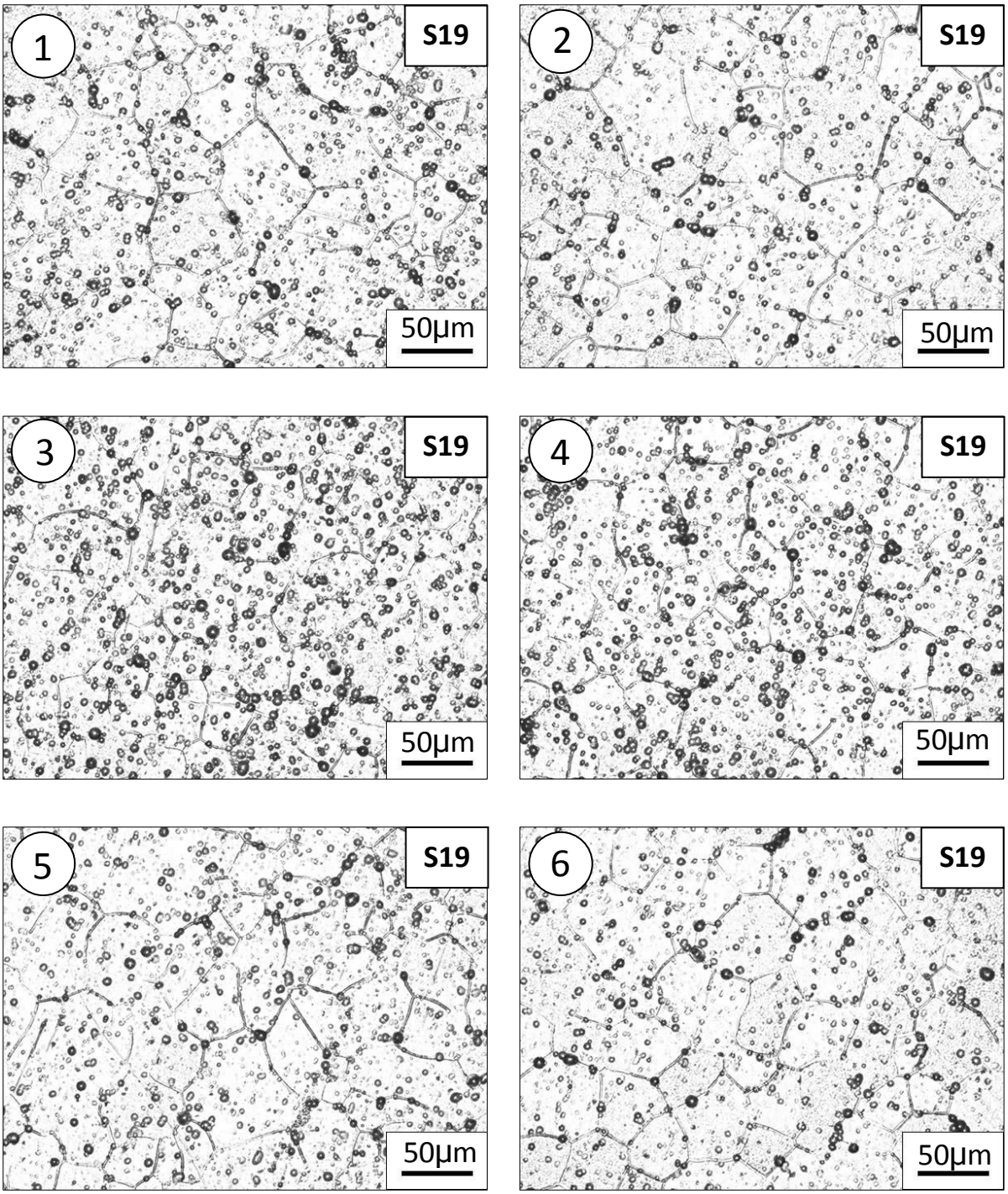

Figure 3-50 Optical microscopy images from along the surface of sample S19, where fields of view 3 and 4 are from inside the streak region and the remaining fields of view are from the surrounding extrudate outside the streak region

Figure 3-51 shows the number of pit features for each field of view shown in Figure 3-50calculated using image J. It can be seen that pitting is significantly increased in the streak region, fields of view 3 and 4.

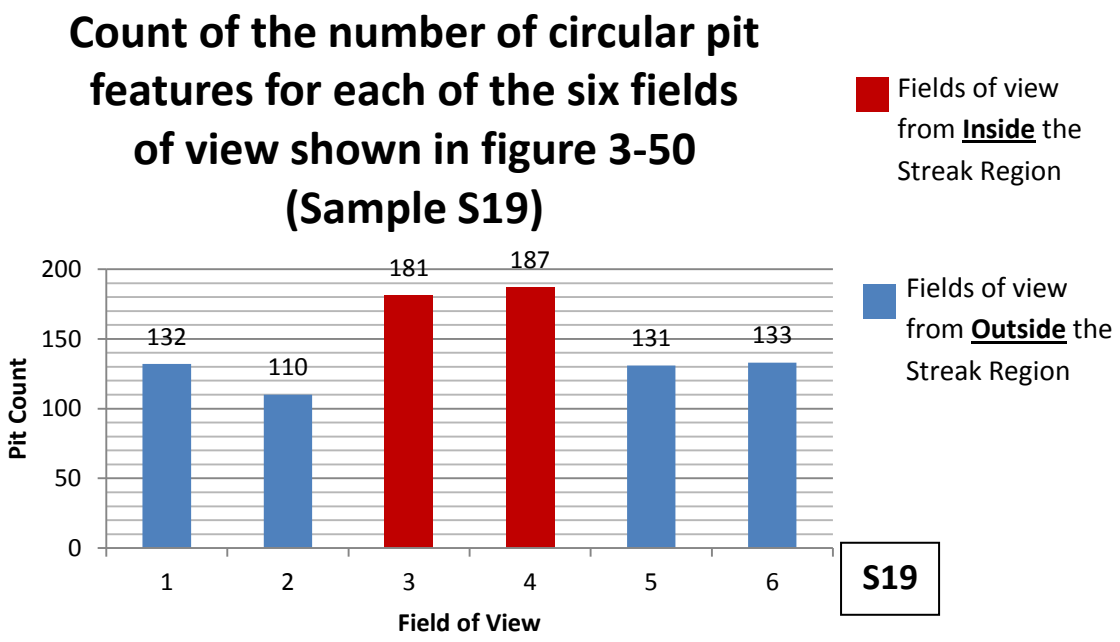

3-51 Count of the number of circular pit features for each of the six fields of view shown in figure 3-50

Sample S20 was polished for an increased duration. Again a highly visible streak is present on the surface as can be seen from macroscopic images shown in Figure 3-52.

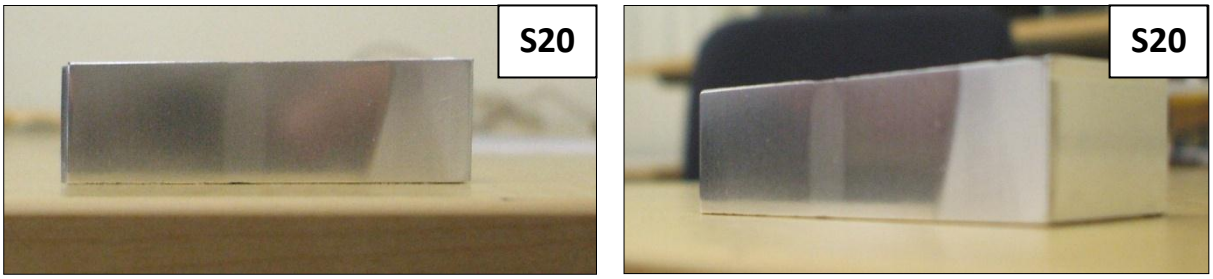

Figure 3-52 Macroscopic view of sample S20 after etching for 40 minutes

Six optical microscopy images from six fields of view were acquired from the surface of sample S20 as shown in Figure 3-53. Fields of view 3 and 4 are from inside the streak region and the remaining fields of view are from either side of the streak region. It can be seen that differences in pitting are even greater in and out of the streak region when compared to the lower polished sample S19.

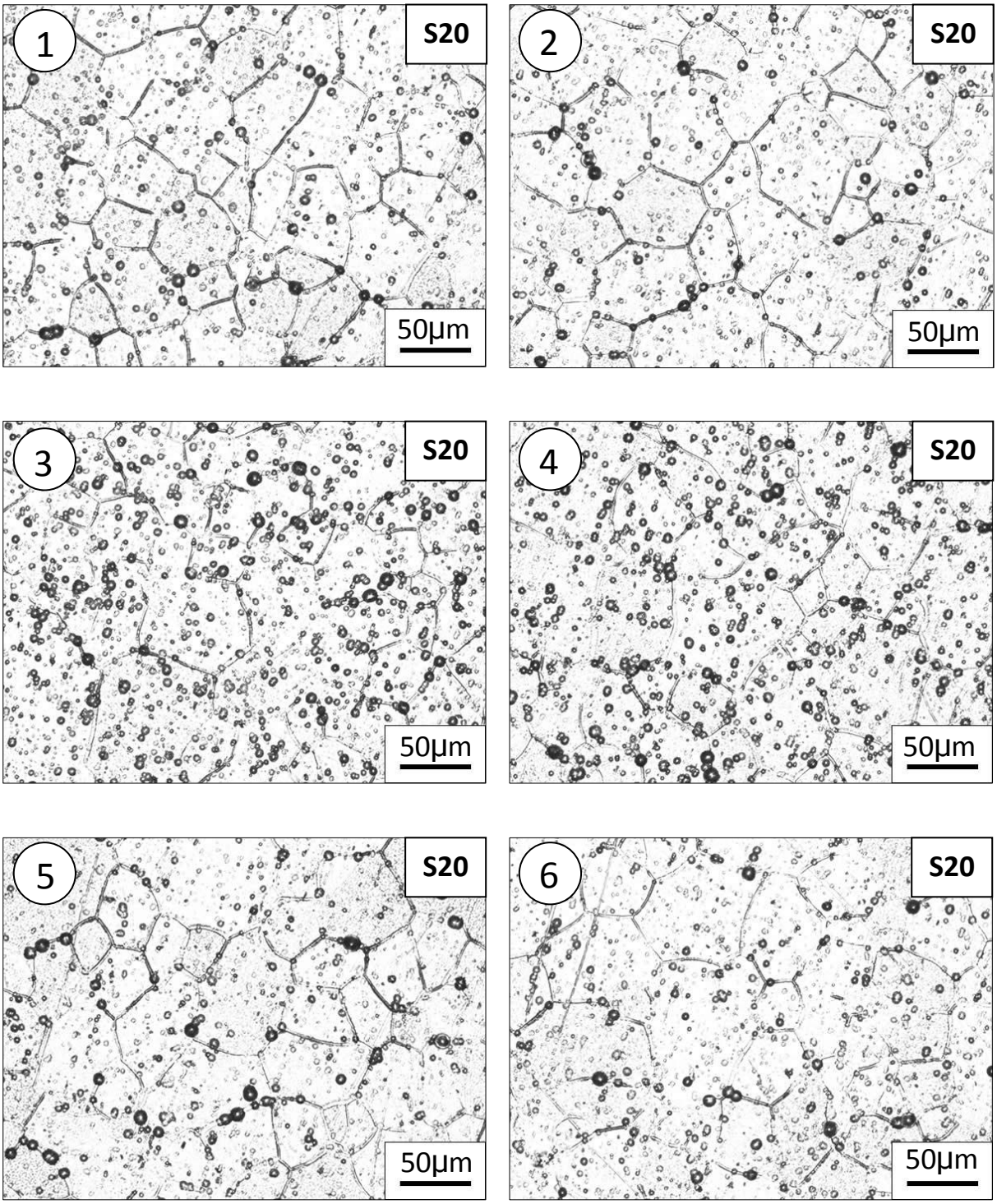

Figure 3-53 Microscopic images for sampleS20 where images 3 and 4 are from inside the streak region and the remaining images are from the surrounding extrudate outside the streak region

Analysing the pit density for each field of view shown in Figure 3-53 using image J with the data shown in Figure 3-54 it can be seen that the degree of pitting in and out of the streak zone is significantly different. This difference is the most significant identified for all etching experiments conducted.

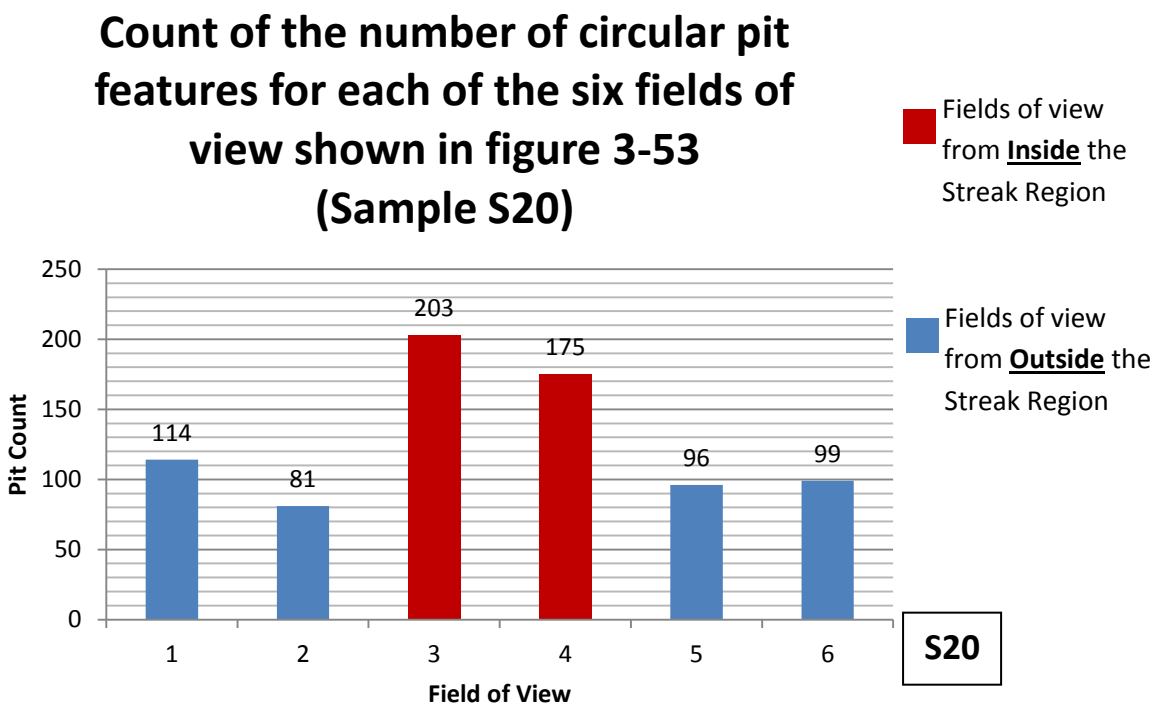

Figure 3-54 Count of the number of circular pit features for each of the six fields of view shown in Figure 3-53

Sample S21 was polished for a further increased duration, as can be seen from Figure 3-55 the streak has narrowed and is also partially removed. This narrowing and partial removal of the streak band further verifies the streaking model shown in section 3.3.2.

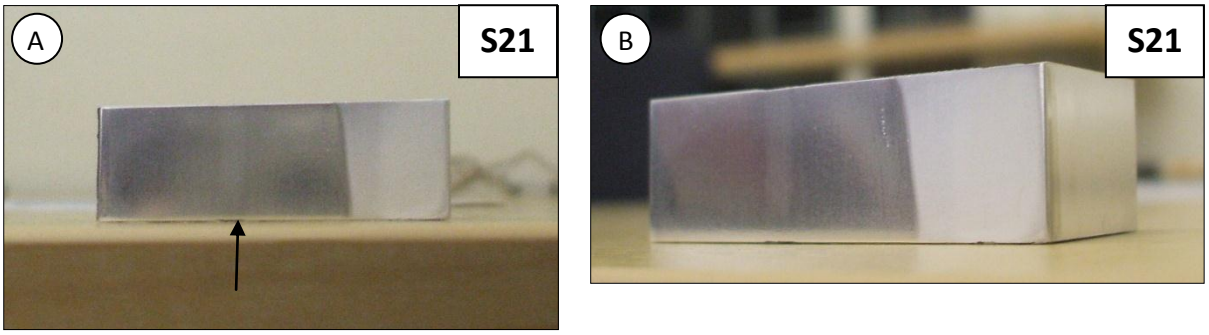

Figure 3-55 Macroscopic view of Specimen S21 after 40 minute etching

Six images were acquired from six fields of view along the surface of sample S21 the same as for samples S19 and S20 as shown in Figure 3-56. The difference in pitting for fields of view 3 and 4 from inside the streak region compared to the remaining fields of view from outside the streak region is again significant on visual inspection of the images.

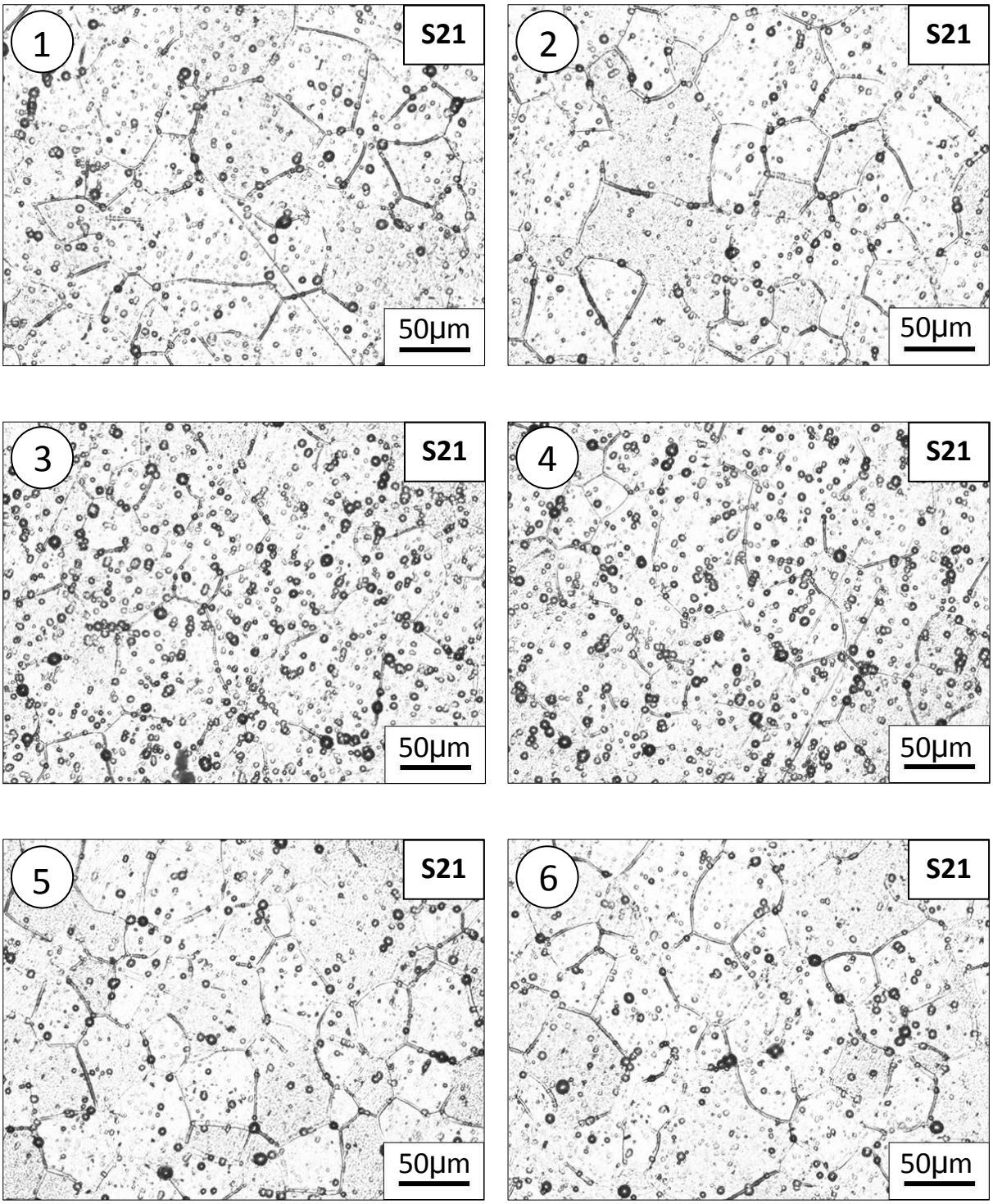

Figure 3-56Microscopic images for sampleS21where images 3 and 4 are from inside the streak region and the remaining images are from the surrounding extrudate outside the streak region

Analysing the six fields of view for the distribution of pitting using image J, it is again found that pitting in and out of the streak region is significantly different as can be seen from Figure-57.

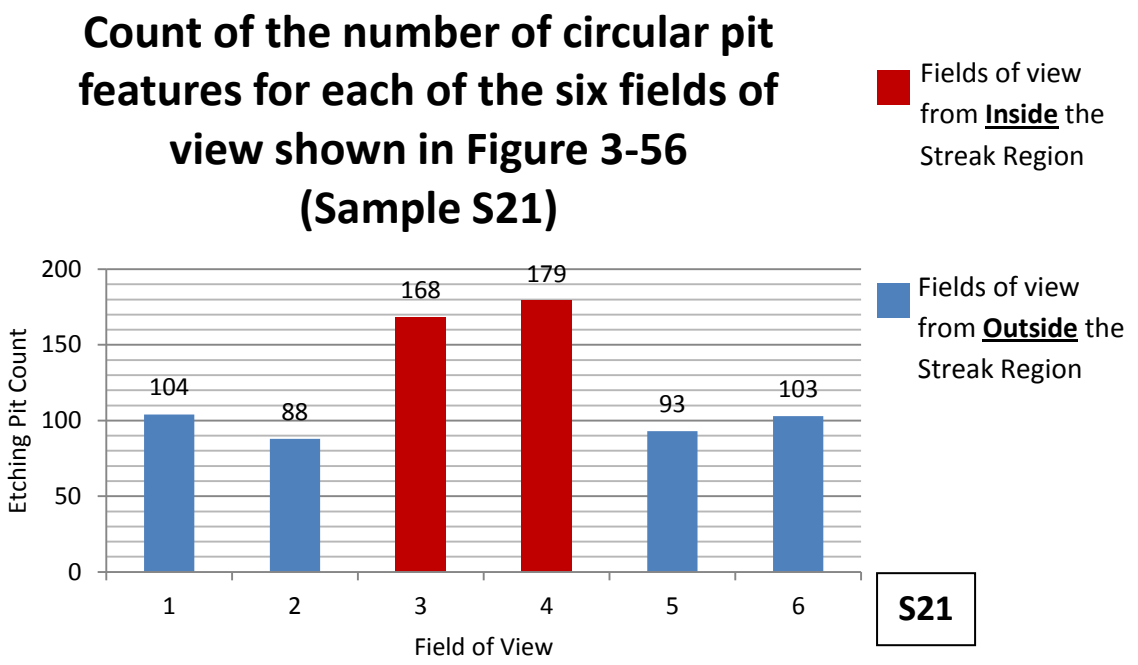

3-57 Count of the number of circular pit features for each of the six fields of view shown in Figure 3-56

To illustrate that a rougher surface has a fast etching attack the average difference in pitting in and out of the streak regions was calculated for all the streak induced specimens which were electro-polished and etched using Graff and Sargent's etchant and streak induced samples S19, S20 and S21 which were mechanically polished, electro-polished and then etched in Graff and sargent's etchant. Figure 3-58 graphs the data obtained showing the average difference in pitting in and out of the streak regions for the mechanically polished, electro-polished and etched specimens S19, S20 and S21 when compared to the electro-polished and etched specimens S14, S15, S16 and S17. It shows the mechanical and electro-polished samples had a greater difference in etching pits in and out of the streak region compared to the only electro-polished specimens.

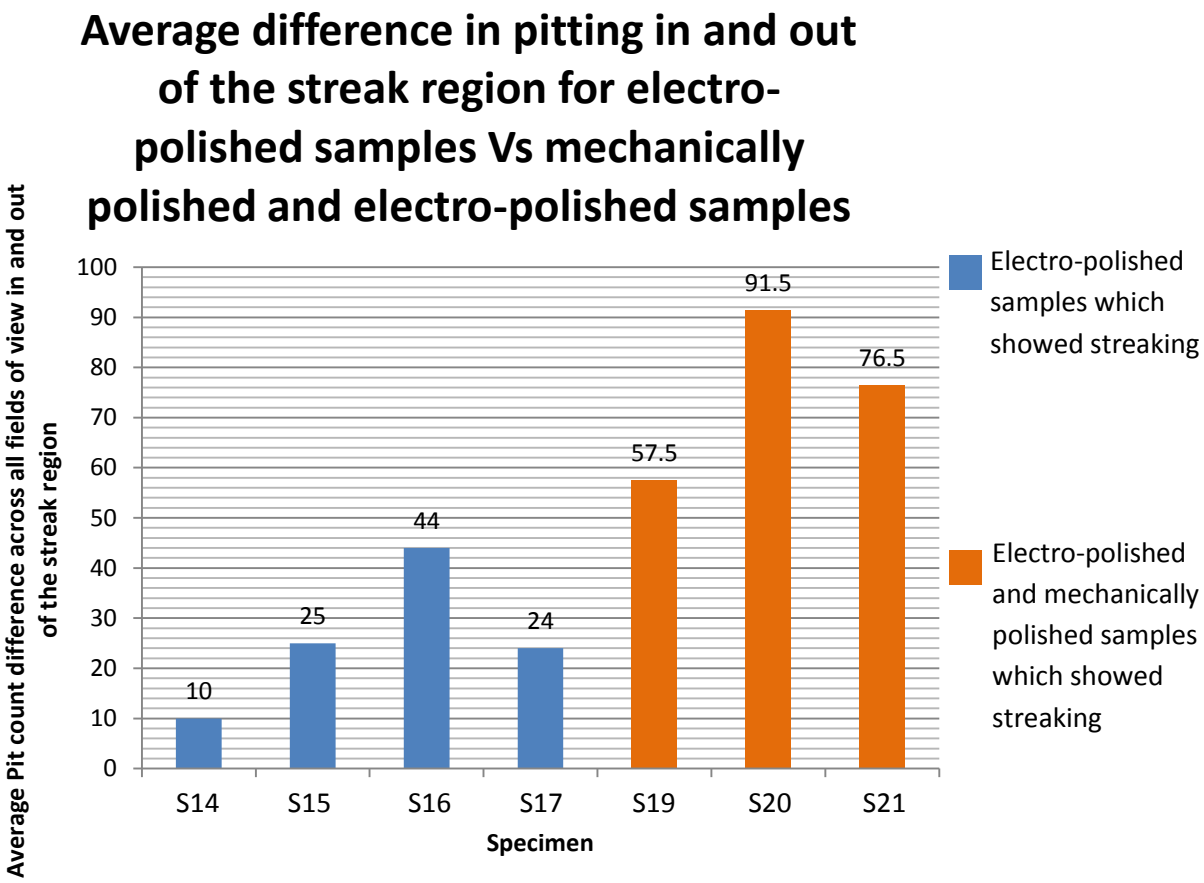

Figure 3-58Average difference in pitting in and out of the streak region for electro-polished samples vs. mechanically polished and electro-polished samples

By measuring the widths of the streak lines the level of metal removal can be established and hence the ranking of the depth at which the streaking was induced established. This data is shown in Table 3-4.

Table 3-4 - Ranking streak width for streak induced specimens

Rank (Greatest Depth – Lowest Depth)	Specimen	Width of streak (mm)
1	S21 – (Mechanical Polish 10 Seconds, electro-polish for 2 min and etch 40 min)	3.5mm
2	S20 – (Mechanical Polish 10 sec , electro-polish for 1 min 30 sec and etch 40 min)	5.5mm ←
2	S17 – (Electro-polish 2 min and etch 62 min)	5.5mm ←
3	S19 – (Mechanical Polish 10 sec ,electro-polish 1 min and etch 40 min)	6.5mm
4	S16 – (Electro-polish 2 min and etch 48 min)	7.5mm
5	S15 – (Electro-polish 1 min and etch 62 min	9.5mm
6	S14 – (Electro-polish 1 min and etch 48 min)	10mm

From Table 3-4 it can be seen that even with the same level of material removal for specimens S20 and S17 specimen S20 has by far a greater difference in pitting in and out of the streak zone when compared to specimen S17. This proves without a doubt that a rough surface with topographical features such as die lines makes the etching attack occur faster than a smoother surface. Therefore the differences in pitting in and out of the streak region occurring for the glossy streak samples are due to mechanical aspects of the as-extruded extrudate surface.

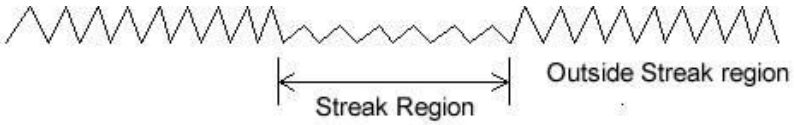

Case 1: Uneven etching attack – Increased distribution of intermetallics or differently oriented grain from outside the streak region causes increased pitting but is mitigated by increased etching response outside the streak region increasing etching response and ultimately pitting also.

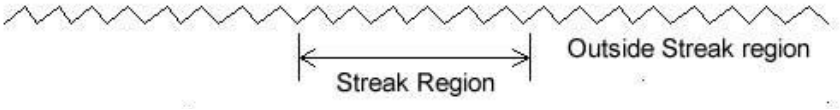

Case 1: Uneven etching attack – Increased distribution of intermetallics or differently oriented grain from outside the streak region causes increased pitting.

3-59 - -Schematic illustrating etching attack

3.3.6. A Model for the Evolution of Streaking – Part 2

The model for the evolution of streaking described in section 3.3.2 (page 62) only takes into account the formation of dull streaks after different levels of material removal. The occurrence of glossy streaks for lower levels of material removal is not accounted for in this model. Therefore a revised model for the evolution of streaking is needed as shown in figure 3-60 below. This model takes into account the glossy streaking seen for low etch durations due to the mechanical effect of die lines and the dull streaking observed after longer etch durations and more material removal which are due to metallurgical differences in the extrudate material.

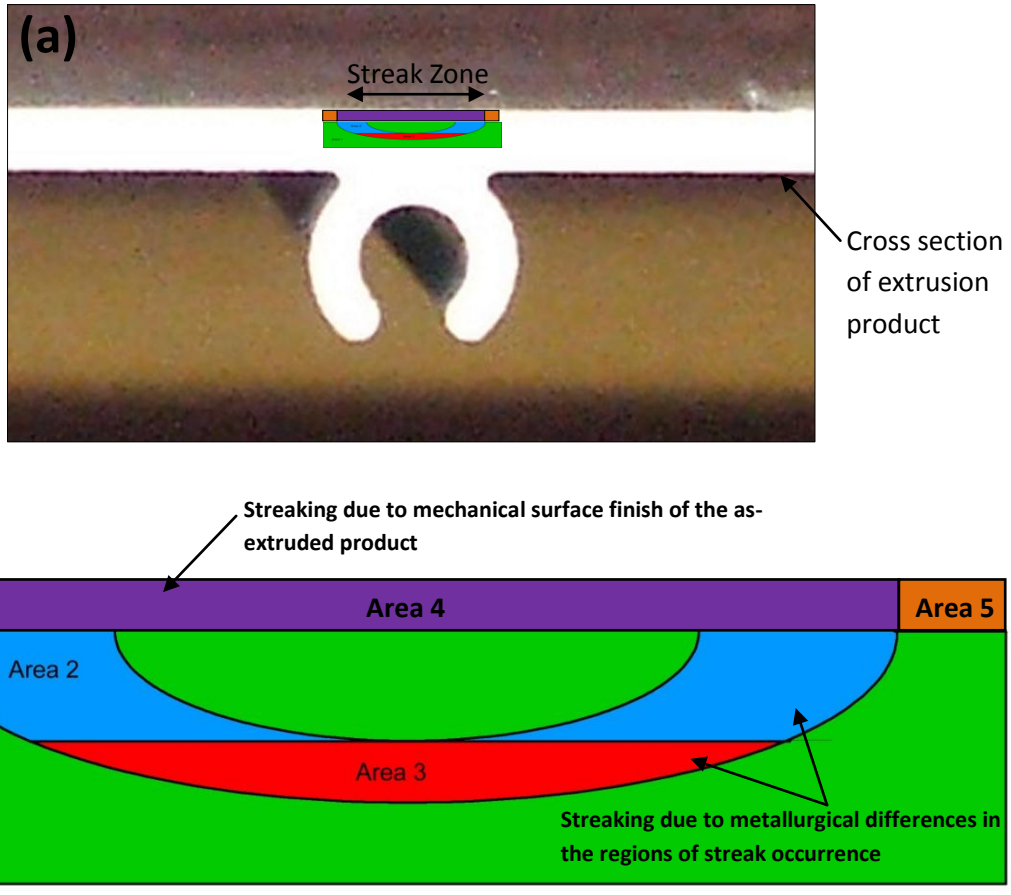

3-60 A model for the evolution of streaking revised

3.3.7. Confirming Why Dull Gloss Streaking Occurs After Medium to High Etch Durations

This chapter will investigate why glossy streaks revert to dull gloss streaking after medium and high etch durations using the same etching process used at Fletcher Aluminium. From etching using Graff and Sargent's etchant it was established that surface topography differences in the form of etching pits caused the streaking which was a dull gloss. To further conclude if the findings made in laboratory simulated etching experiment using Graff and Sargent's etchant correlates to the reason for dull gloss streaks using Henkel P3 etch as used at Falum in their extrusion etching operations a microstructural analysis was conducted. To conduct this analysis the surfaces of samples S14-S17 were analysed using optical microscopy and image J software.

For sample S14(etched for 10 min) the streak pattern is faint parallel band streaking as was also observed on samples with an electro-polished surface and etched in Graff and Sargent's etchant for medium etch durations. Figure 3-61 shows the surface of specimen S14 with eight points which were the locations at which the surface was viewed using optical microscopy. These 8 fields of view are shown in figure 3-62.

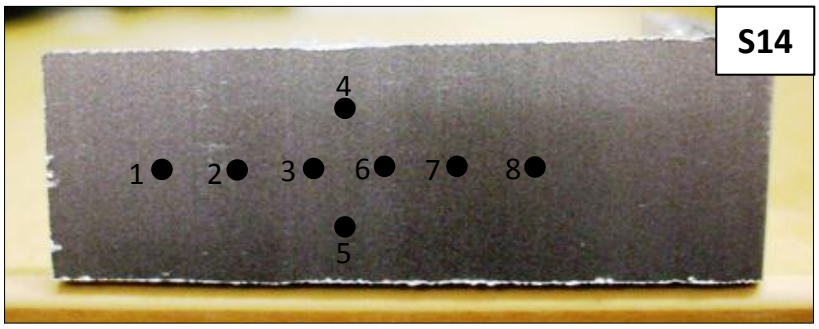

Figure 3-61 Surface points represent the locations at which the images shown in figure 3-62 were acquired from.

On visual observation of the eight fields of view from specimen S14 no clear differences in die lines or circular black pit features in and out of the streak region can be made.

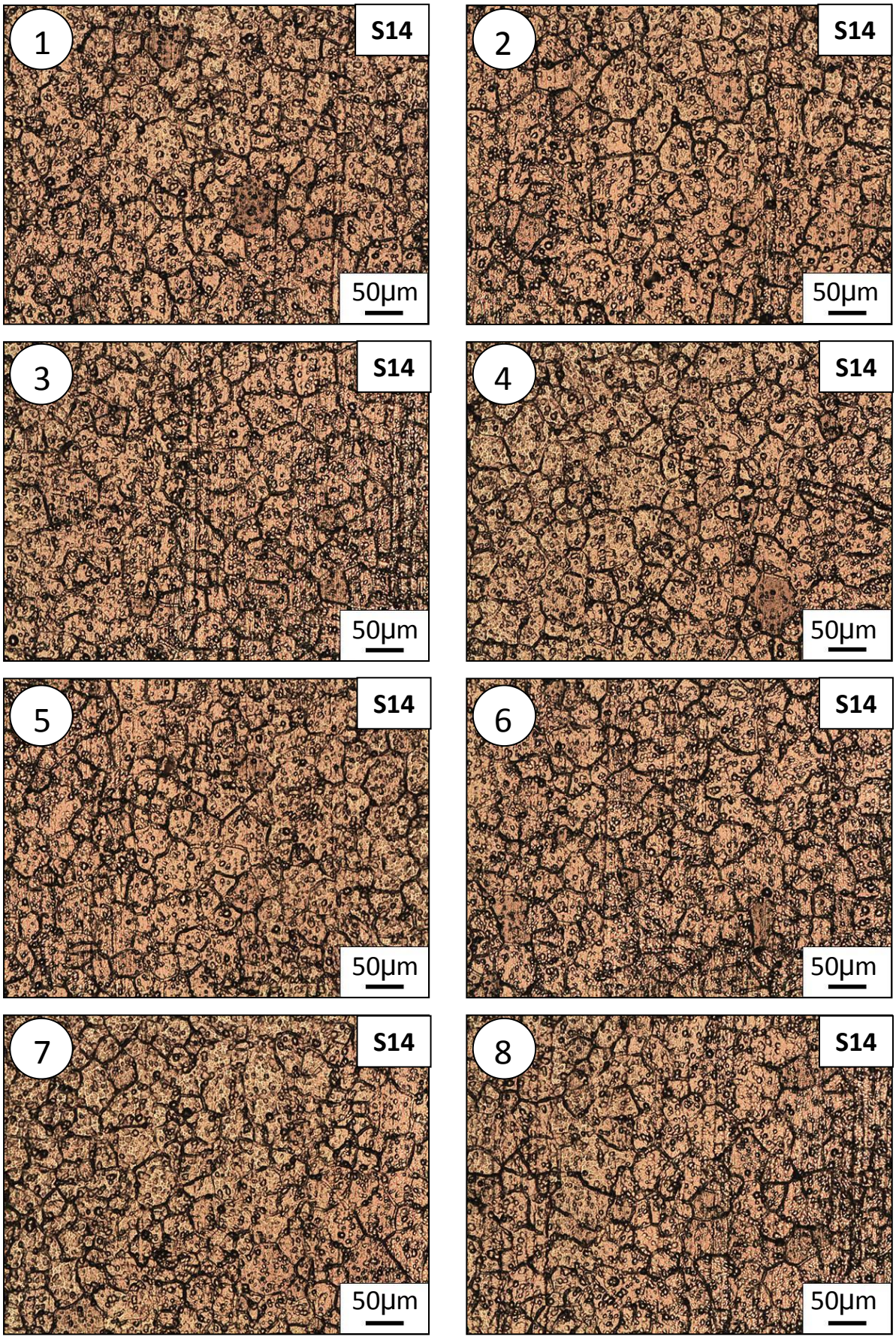

Figure 3-62 Microscopic surface images of specimen S14 at the 8 points outlined in Figure 3-61

Since visual observation does not provide any clear evidence of varying microstructural features in and out of the streak regions an image J analysis was carried out as was done for previous samples. It is worth noting that the microstructural differences not varying to a large degree in and out of the streak region would also relate to the low visibility of the streak features on macroscopic inspection of sample S14. Figure 3-63 shows the pit count for each field of view along the surface of specimen S14. It can be seen that the parallel streak bands (green) had the highest distribution density of circular pit like features. The centre un-streaked region (red) was found to have the lowest distributional density of circular black pit like features.

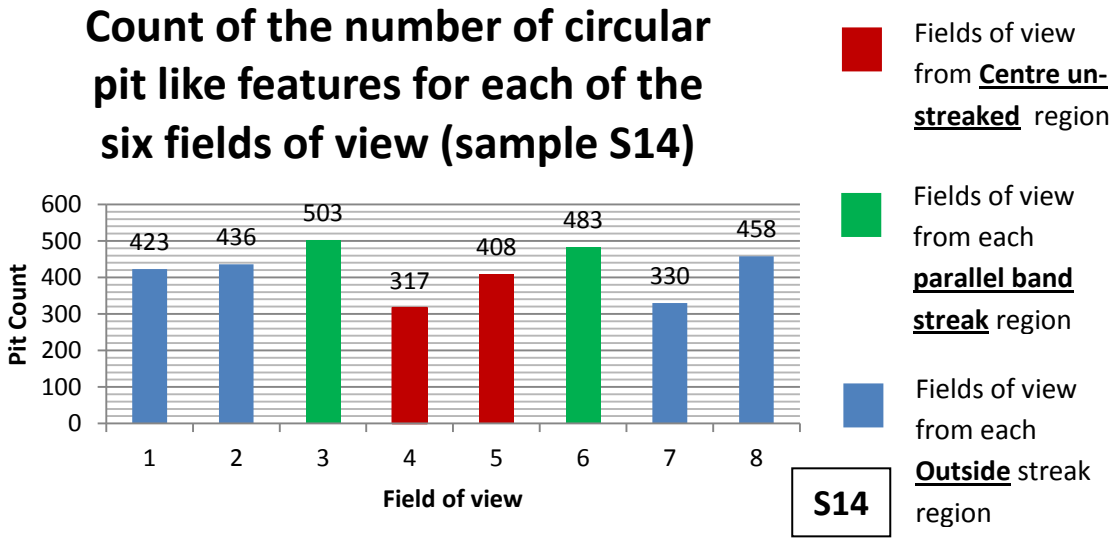

3-63 Count of the number of circular pit like features for each of the six fields of view shown in Figure 3-62 from sample S14

Sample S15 (etched for 12.5min) shows faintly visible parallel streak bands as can be seen from Figure 3-64. Compared to sample 14 the centre un-streaked region is much clearer. Eight fields of view were acquired as outlined on the sample surface in Figure 3-64. The eight fields of view are shown in Figure 3-66.

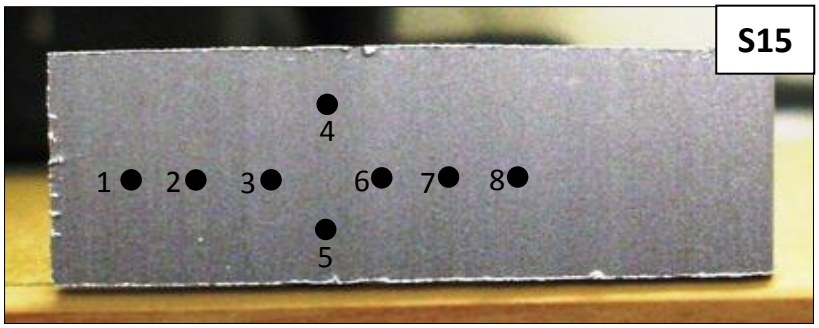

3-64 Surface of sampleS15 which was etched for 12.5 minutes. The numbered points represent the locations at which the images shown in Figure 3-65 were acquired from.

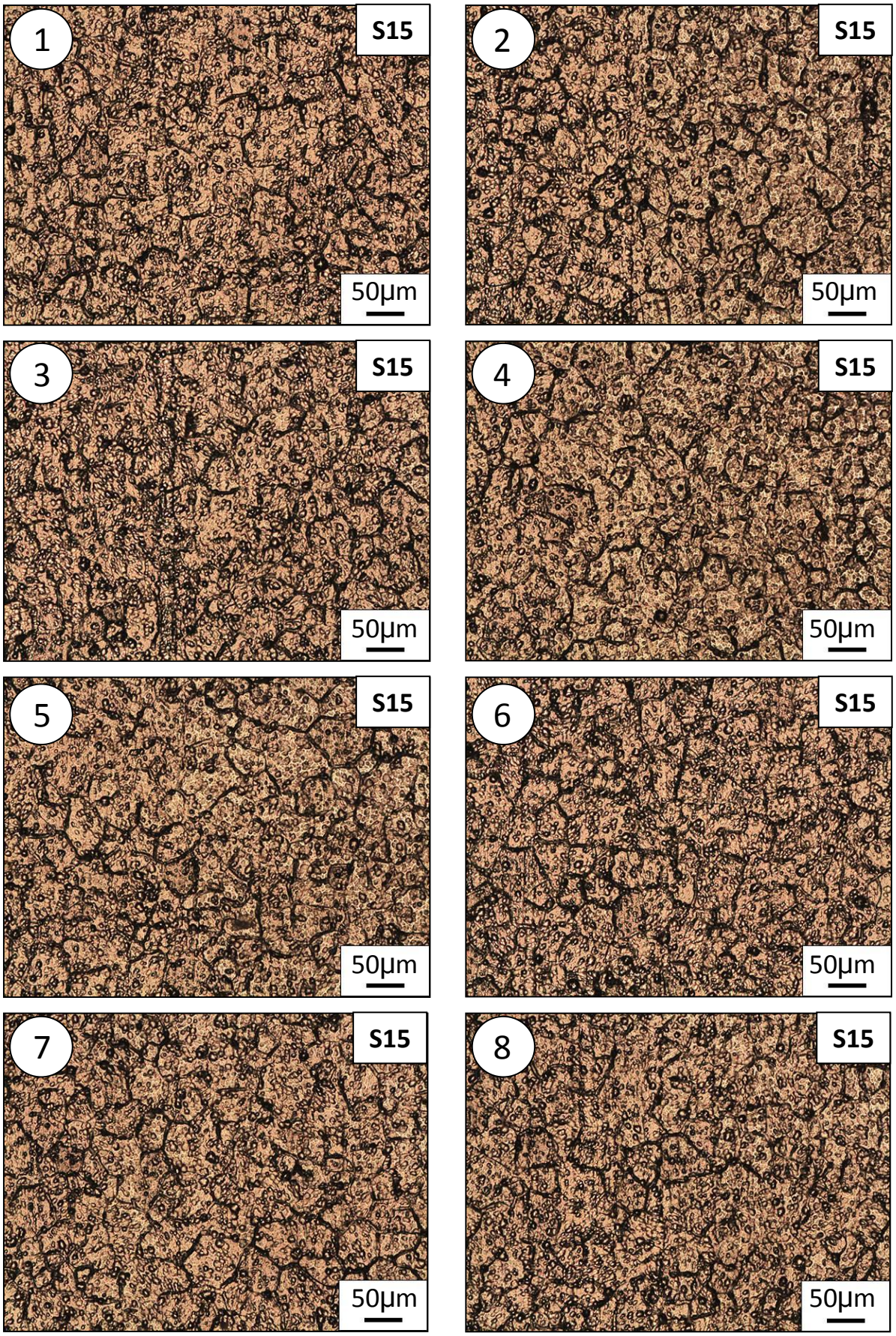

Figure 3-65Microscopic surface images of specimen S15 at the 8 points outlined in figure 3-64

From fields of view 3 and 6shown in figure 3-65 it can be observed that there may be an increased distributional density of circular pit like features in the regions of the parallel streak bands. Furthermore fields of view 4 and 5 from the centre un-streaked region seem to have the lowest distribution of circular pit like features when compared to the other fields of view. To confirm whether this visual observation is correct an image J analysis was again carried out. The data relating to the pit distribution density for each field of view shown in Figure 3-65 is shown in Figure 3-66. Like sample S14 which displayed parallel streaking the fields of view from the centre un-streaked region (red) had the lowest distributional density of circular pit like features, while the fields of view from inside the parallel streak bands (green) had the highest.

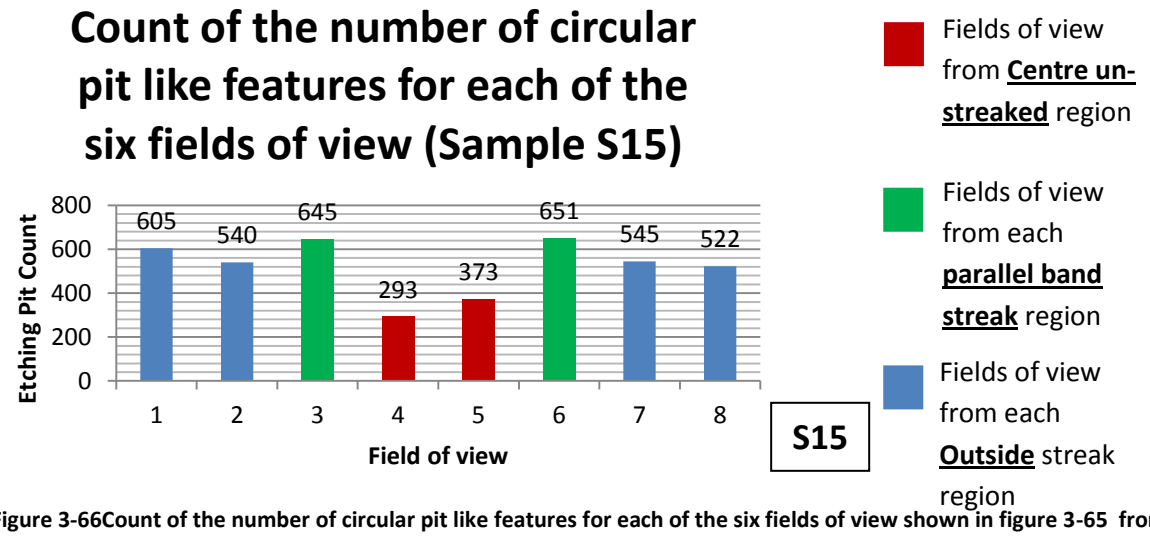

Figure 3-66Count of the number of circular pit like features for each of the six fields of view shown in figure 3-65 from sample S15

Sample S16 (etched for 15min) shows the near complete merger of the two parallel streak bands as can be seen from Figure 3-67. Six images were taken from six fields of view along the surface of sample S16 as outlined in Figure 3-67 and shown in Figure 3-68.

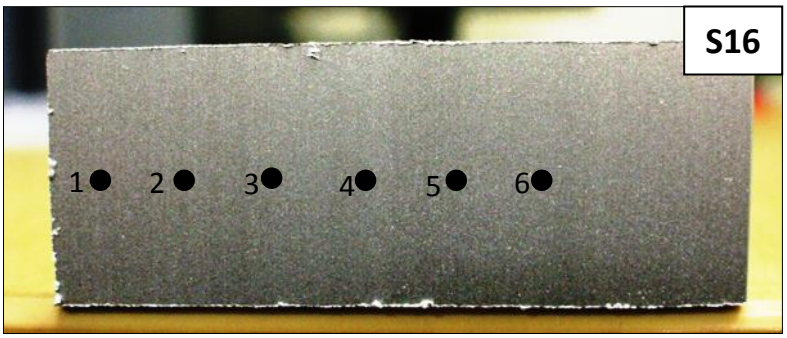

Figure 3-67Surface of sampleS16 which was etched for 17.5 minutes. The numbered points represent the locations at which the images shown in figure 3-68 were acquired from.

From the six fields of view shown in Figure 3-68 it can be visually observed that fields of view 3 and 4 from inside each parallel streak band may have an increased distributional density of circular black pit like features compared to the remaining fields of view from outside the streak region although this is not clear.

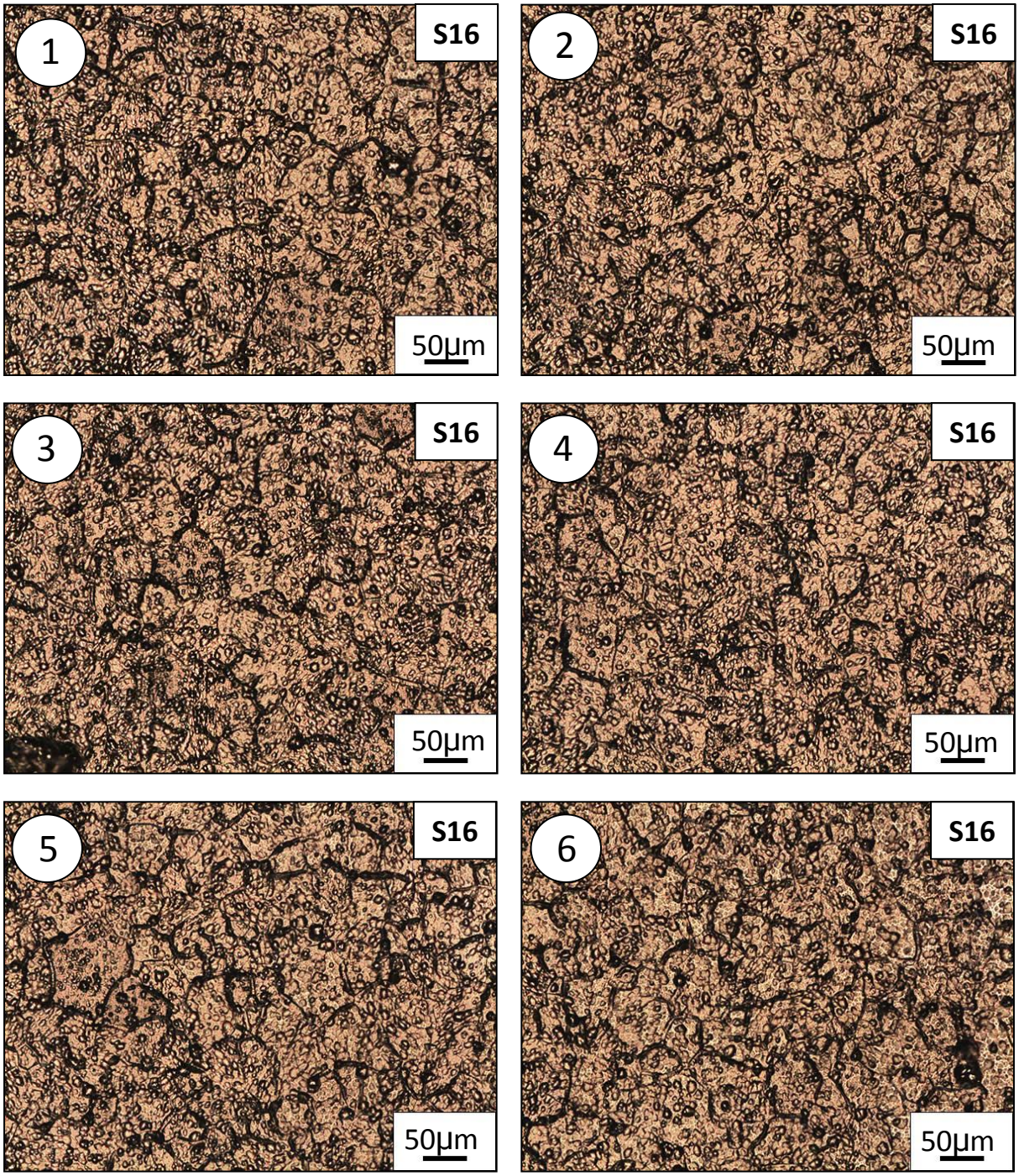

Figure 3-68 Microscopic surface images of specimen S16 at the 6 points outlined in Figure 3-67

Image J analysis data shown in Figure 3-69 confirms that there is a slightly higher density of black circular pit like features for fields of view 3 and 4 (red) from inside the region of the streak bands.

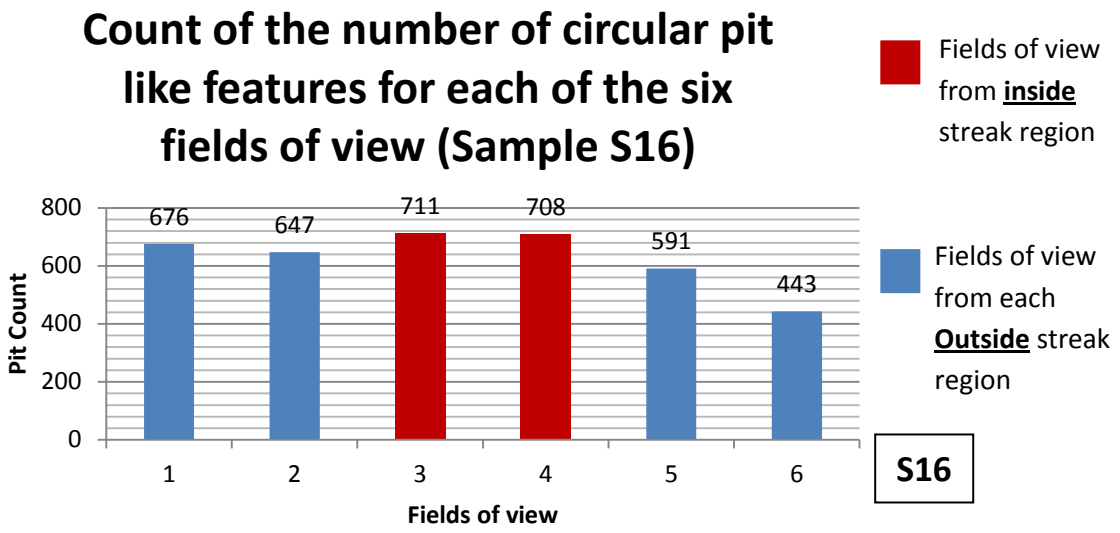

Figure 3-69 Etching Count of the number of circular pit like features for each of the six fields of view shown in figure 3-68 from sample S16

Sample S17 (etched for 17.5min) showed the most visible streaking observed after different etching durations as can be seen from figure 3-70. The parallel streak bands as seen on the previous sample have fully merged into a single narrow streak band. Images were acquired from six fields of view on the surface of sampleS17 as outlined in figure 3-70.

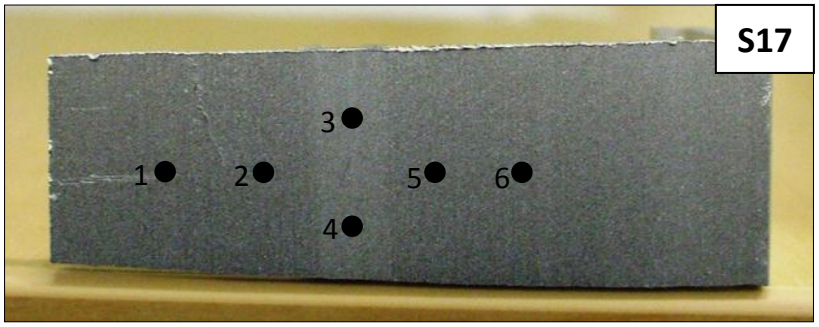

Figure 3-70 The Surface of sampleS17 which was etched for 17.5 minutes. The numbered points represent the locations at which the images shown in figure 3-71 were acquired from.

Figure 3-71shows images acquired from the surface of sample S17 at the points outlined from figure 3-70. It can be seen that there is a clear noticeable difference in the density of circular black pit like features for fields of view 3 and 4 from inside the streak region.

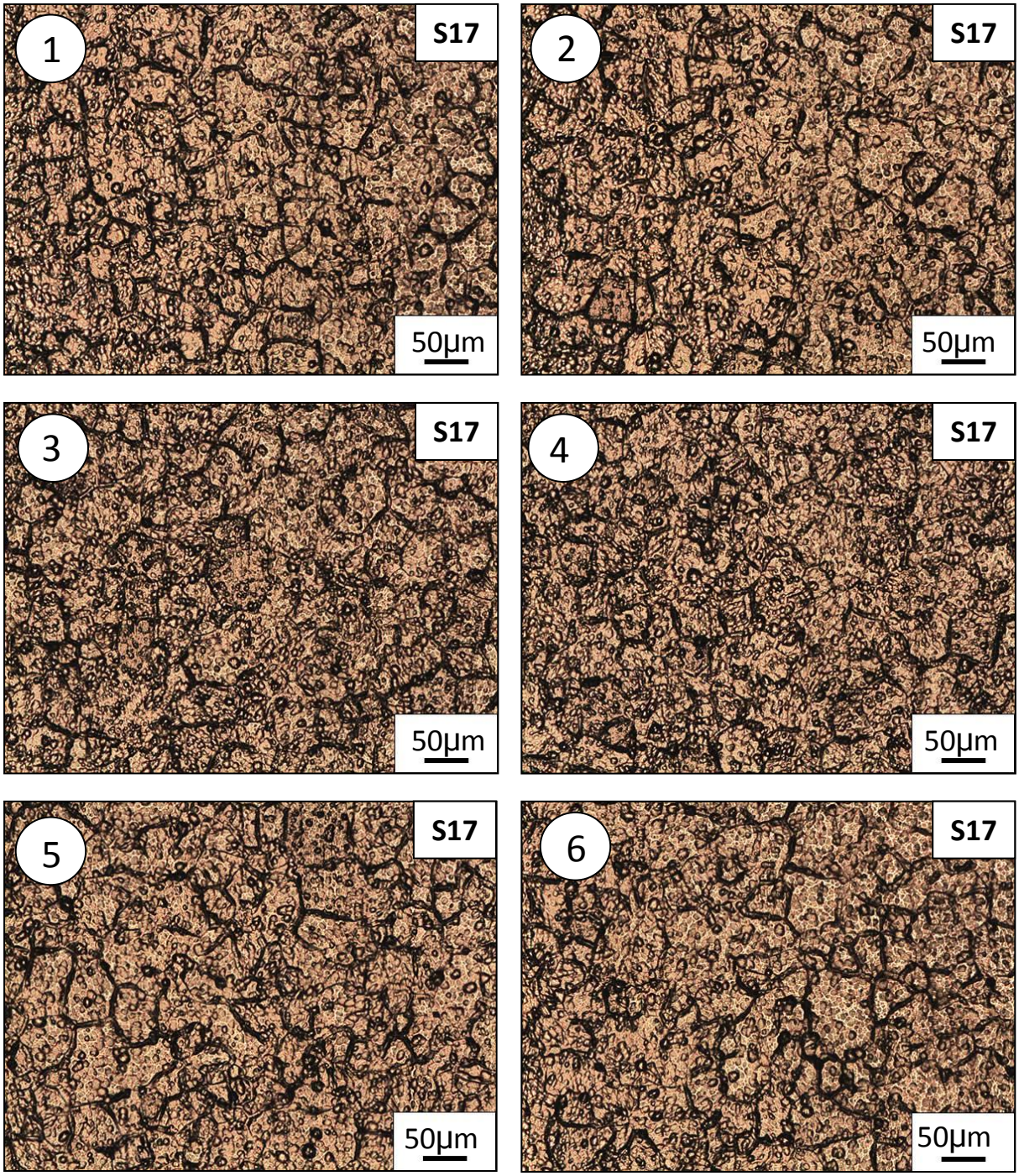

Figure 3-71 Microscopic surface images of sample S17 at the 6 points outlined in figure 3-71

Figure 3-72 confirms the visual observation from the images shown in figure 3-71 that there is an increased density of circular pit like features in the streak region (fields of view 3 and 4 – red) collated through image J analysis.

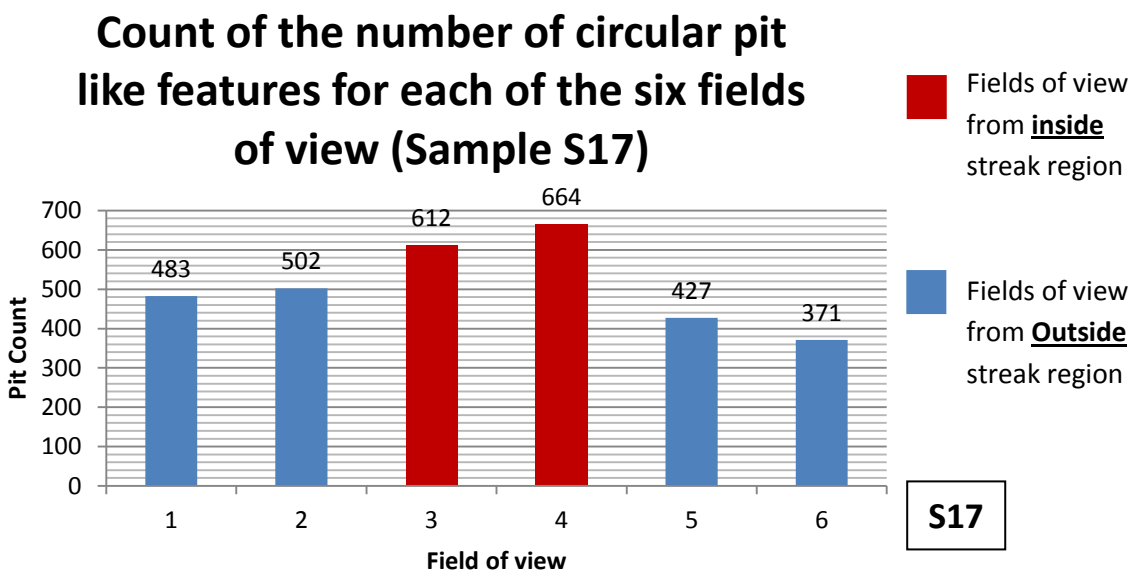

Figure 3-72 Count of the number of circular pit like features for each of the six fields of view shown in figure 3-71 from sample S17

Optical microscopy shows a purely two dimensional view of the surface as can be seen from the images in previous sections of the surface microstructure of the streak induced samples. Examples of these circular black features are highlighted by arrows as shown in Figure 3-74. These circular pit like features are the most likely mechanism which causes an altered reflectance of light and dull gloss streaking when they differ in and out of the streak region thus causing surface roughness difference.

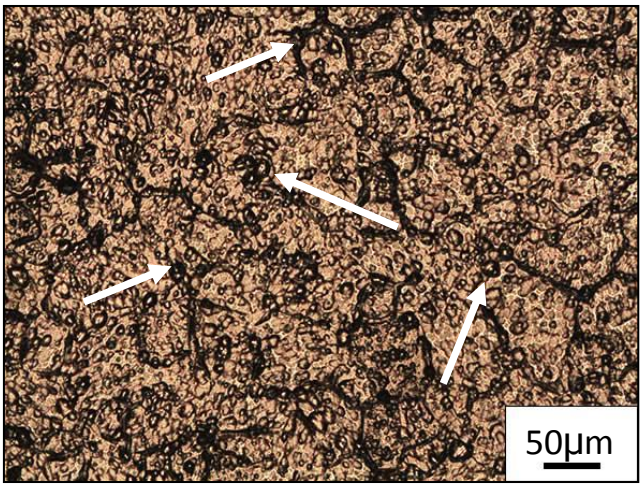

3-73 White arrows identify examples of black circular features seen using optical microscopy

3.3.8. Scanning Electron Microscopy Analysis

Three samples were investigated using scanning electron microscopy. These samples were S12, S15 and S17. The following recaps the streaking seen for these specimens:

- S12 – A glossy single band streak → Figure 3-39 (b)
- S15 – Parallel dull streak bands →Figure 3-39(e)
- S17 – A single band dull streak →Figure 3-39(g)

This analysis using scanning electron microscopy (SEM) was conducted to get a clearer view of the surface topography in the form of pitting and grain boundary grooves. Using Optical microscopy the images are from a 2D viewpoint which makes identifying categorically whether the features observed are etching pits. Scanning electron microscopy produces images with more depth which give a more 3D view point. This enables pitting and grain boundary groove distributions to be more clearly identified. Also the surface topography at a much higher magnification can be identified using SEM. This analysis will further prove the findings made on the reasons for glossy and dull gloss streaking.

For sample S12 (etched for 5min) six fields of view were analysed using SEM as shown in figure 3-74 at a 300X magnification. Fields of view 3 and 4 were located outside the streak region and fields of view 1, 2, 5 and 6 were located from outside the streak region either side of the glossy streak band. The images from the six fields of view shown in Figure 3-74show that overall there is a smoother surface in the streak region (fields of view 3 and 4) compared to the remaining fields of view from outside the streak region. This further confirms the findings made using optical microscopy and image J analysis in the previous section. Also the black circular features can be identified as pits. Therefore the streak region exhibiting a glossier surface after a short etch is caused by a lower incidence of pits and also less die line features in the streak region, fields of view 3 and 4. Outside the streak region there is a higher incidence of pits and more die line features.

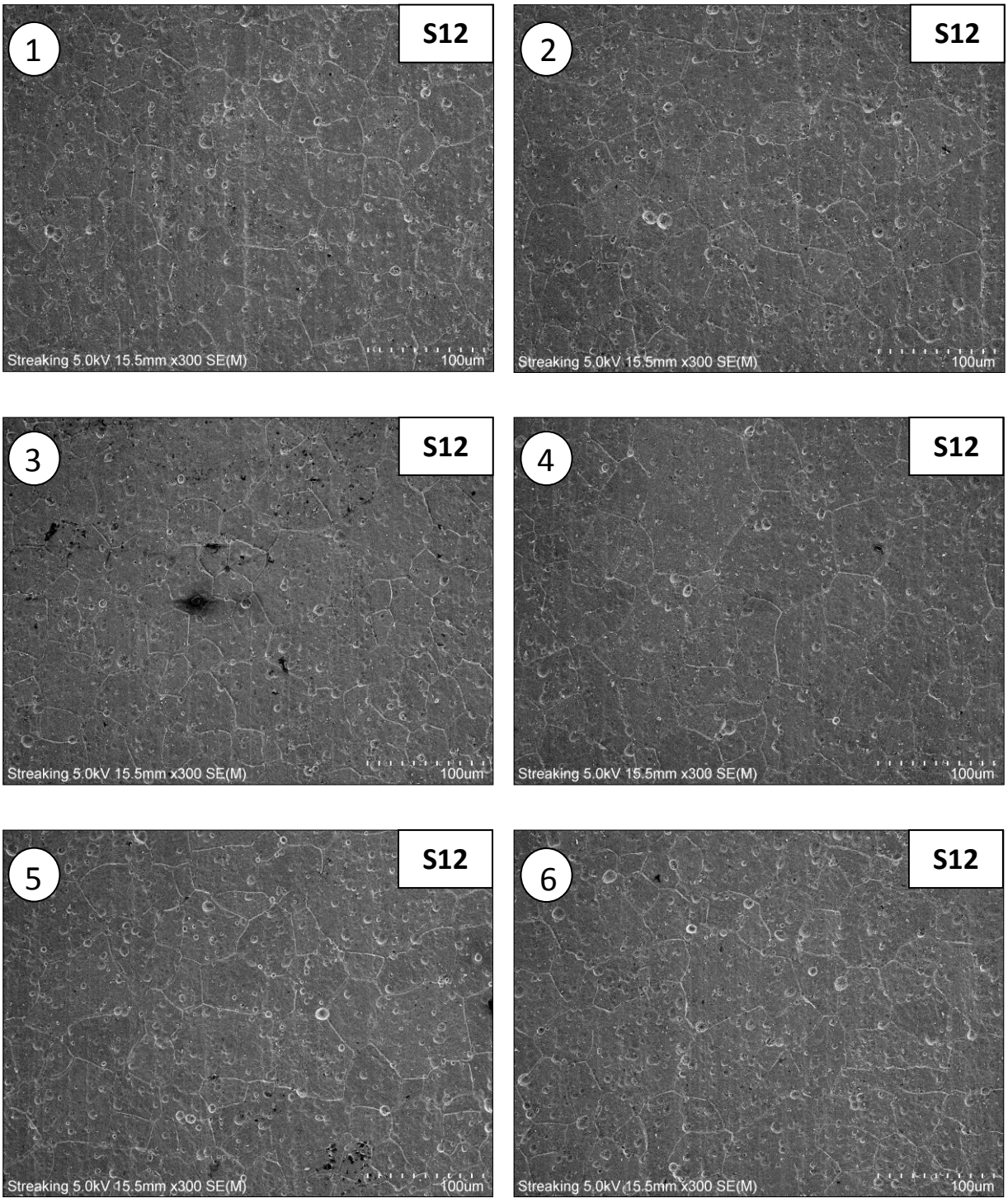

3-74 SEM images taken from six fields of view on the surface of sample S12 at 300X magnification, fields of view 3 and 4 are from inside the single band glossy streak and the remaining fields of view are from outside the streak region

Further SEM images were acquired from six fields of view in and out of the glossy streak band at 1000X magnification as shown in Figure 3-75. From these images it can be seen that surface region surrounding the pit features is smoother or less matte for fields of view 3 and 4 from inside the glossy streak band when compared to the remaining fields of view from outside the streak region. This difference in surface matteness in and out of the streak region

would contribute to a smoother surface with an altered reflectance of light and an ultimately a glossier surface.

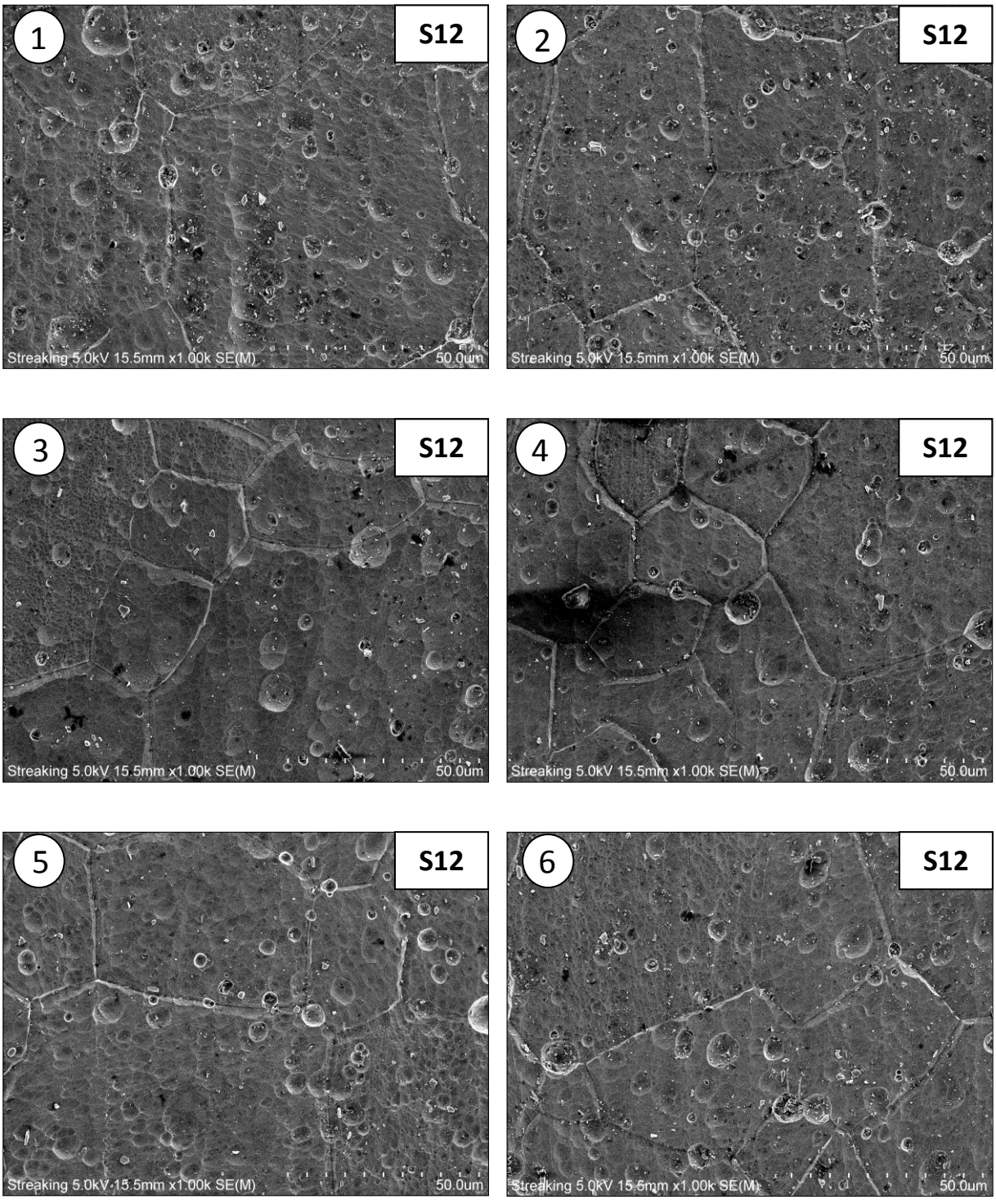

3-75 SEM images taken from six fields of view on the surface of sample S12 at 1000X magnification, fields of view 3 and 4 are from inside the single band glossy streak and the remaining fields of view are from outside the streak region

A further six fields of view were acquired at 4000X magnification as shown in Figure 3-76. From these images differences in surface matteness can be observed in and out of the streak

region. Also for fields of view 3 and 4 from inside the glossy streak region there is a lower incidence of white iron rich intermetallic particles. These white iron rich particles will speed up the etching response hence causing an increased matting of the surface.

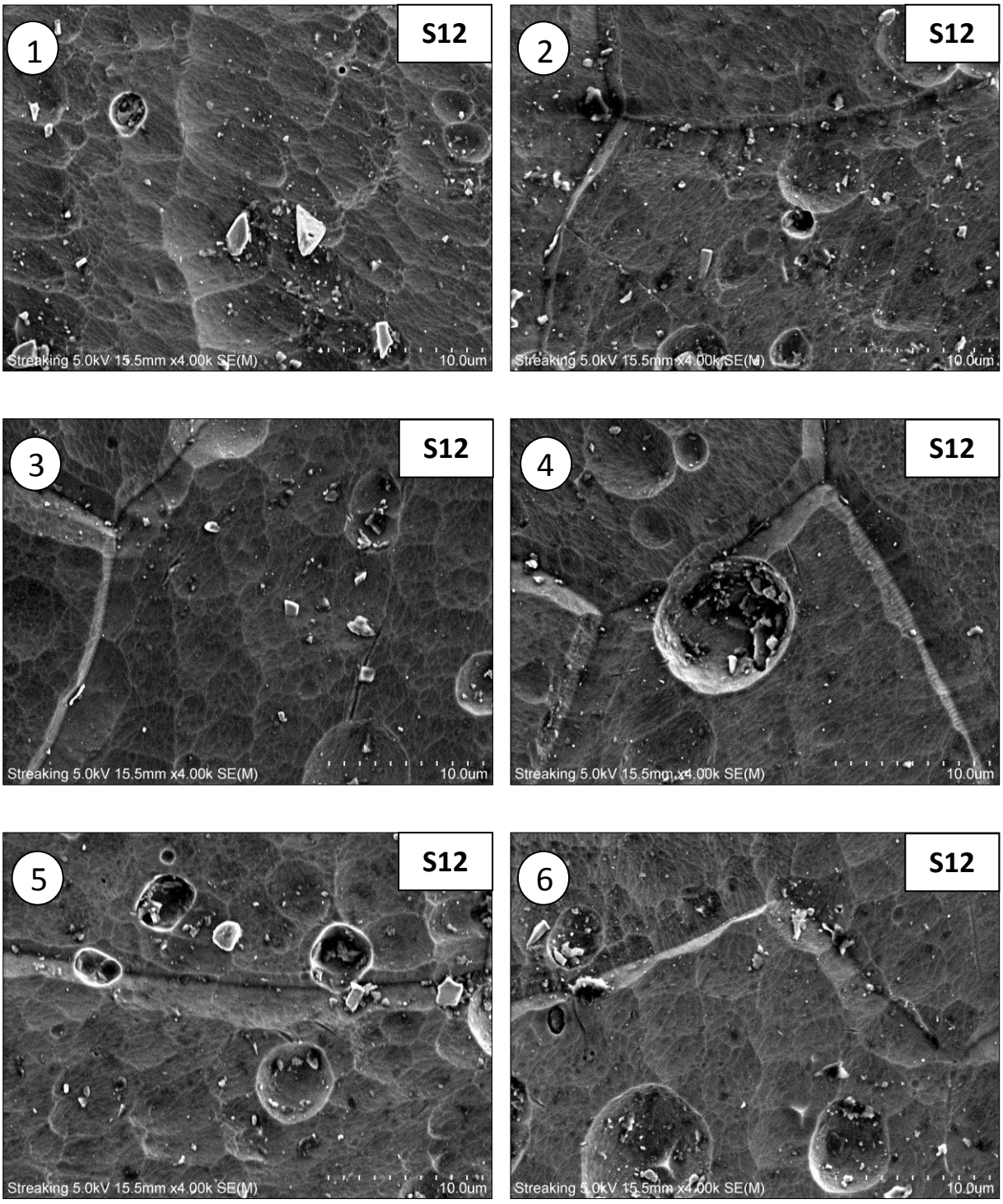

3-76 SEM images taken from six fields of view on the surface of sample S12 at 4000X magnification, fields of view 3 and 4 are from inside the single band glossy streak and the remaining fields of view are from outside the streak region

The next sample S15 analysed using SEM showed faint parallel band streaks as can be seen from Figure 3-39(e) in section 3.3.4. The gloss of these streaks was duller than the surrounding extrudate; this means the surface inside the streaks should be rougher and more heavily pitted than the extrudate surrounding the streak bands. Six images were acquired from six fields of view in and out of the streak region at 300X, 1000X and 3000X magnification. Fields of view 3 and 4 correspond to inside each parallel streak band, fields of view 1 and 2 correspond to the centre un-streaked region and fields of view 5 and 6 correspond to inside the extrudate surrounding the parallel streak bands.

Figure 3-77 shows the six fields of view in the regions as specified above at 300X magnification. It can observed there is a slightly an increased incidence of larger pits in the region of the parallel streak bands (fields of view 3 and 4). However differences between the images from in and out of the streak zone cannot be accurately ascertained at this magnification. This lack of clear identifiable difference would relate to the faintness and low visibility of the parallel streak bands on macroscopic observation of sample S15.

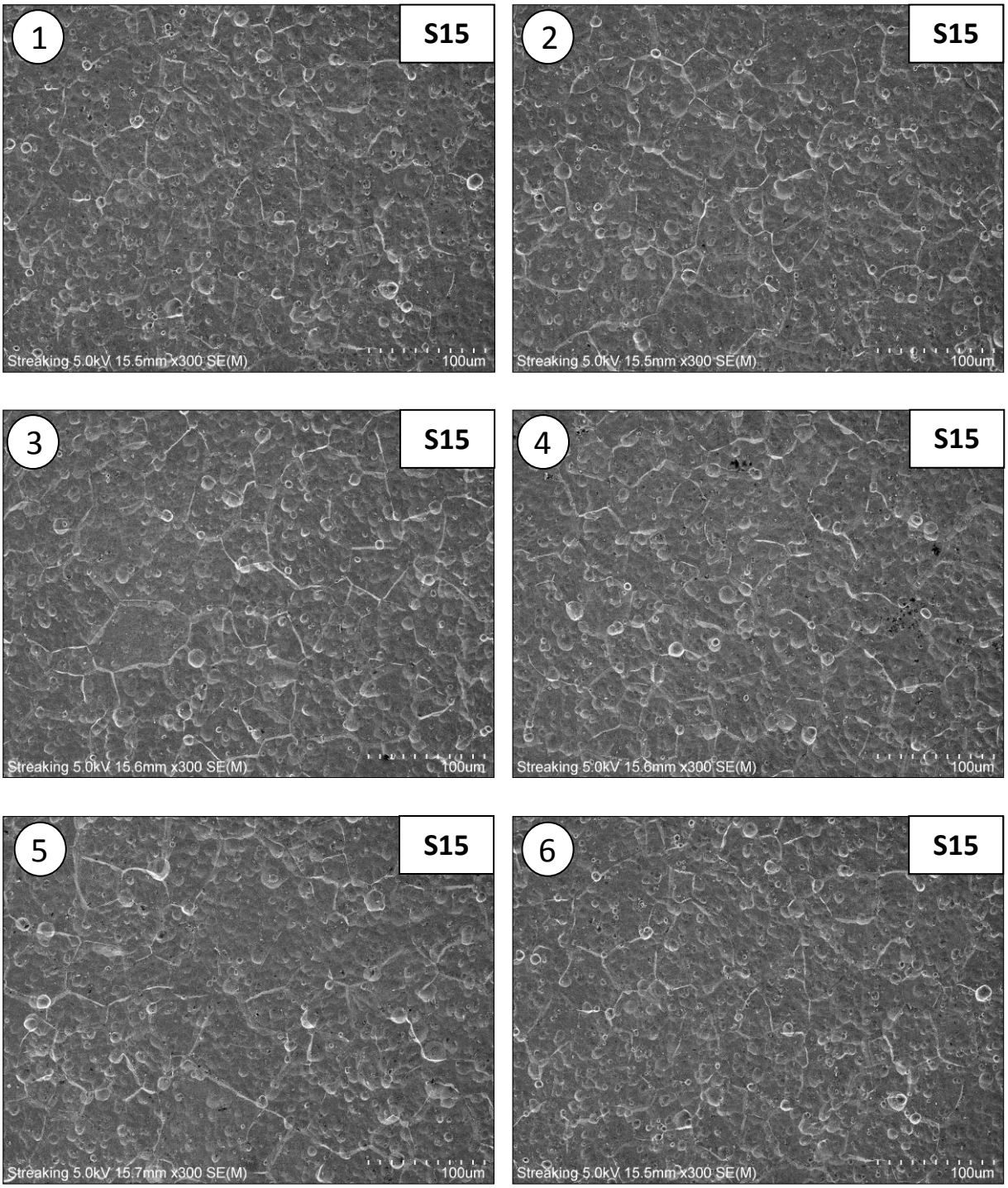

3-77 SEM images taken from six fields of view on the surface of sample S15 at 300X magnification, fields of view 3 and 4 are from inside each of the parallel dull gloss streak band, fields of view1 and 2 are from the centre un-streaked region and fields of view 5 and 6 are from the extrudate surface surrounding the parallel streaks

Six more fields of view were acquired in and out of the streak region in the same manner at an increased magnification of 1000X as shown in figure 3-78. Looking at fields of view 1 and 2 it can be observed that there is an increase in white iron rich particles compared to the remaining fields of view from in the regions of the parallel streak bands and the surrounding extrudate. Also overall there is a higher incidence of small pit features. These small surface

pits may be caused by the increased etching response due to a greater distribution of white iron rich particles. Fields of view 3 and 4 then show a higher incidence of large pits in combination with small surface pits causing the dullest surface. Fields of view 5and 6 from the surrounding extrudate exhibits a relatively smooth surface compared to the other fields of view corresponding to the glossier surface on macroscopic inspection.

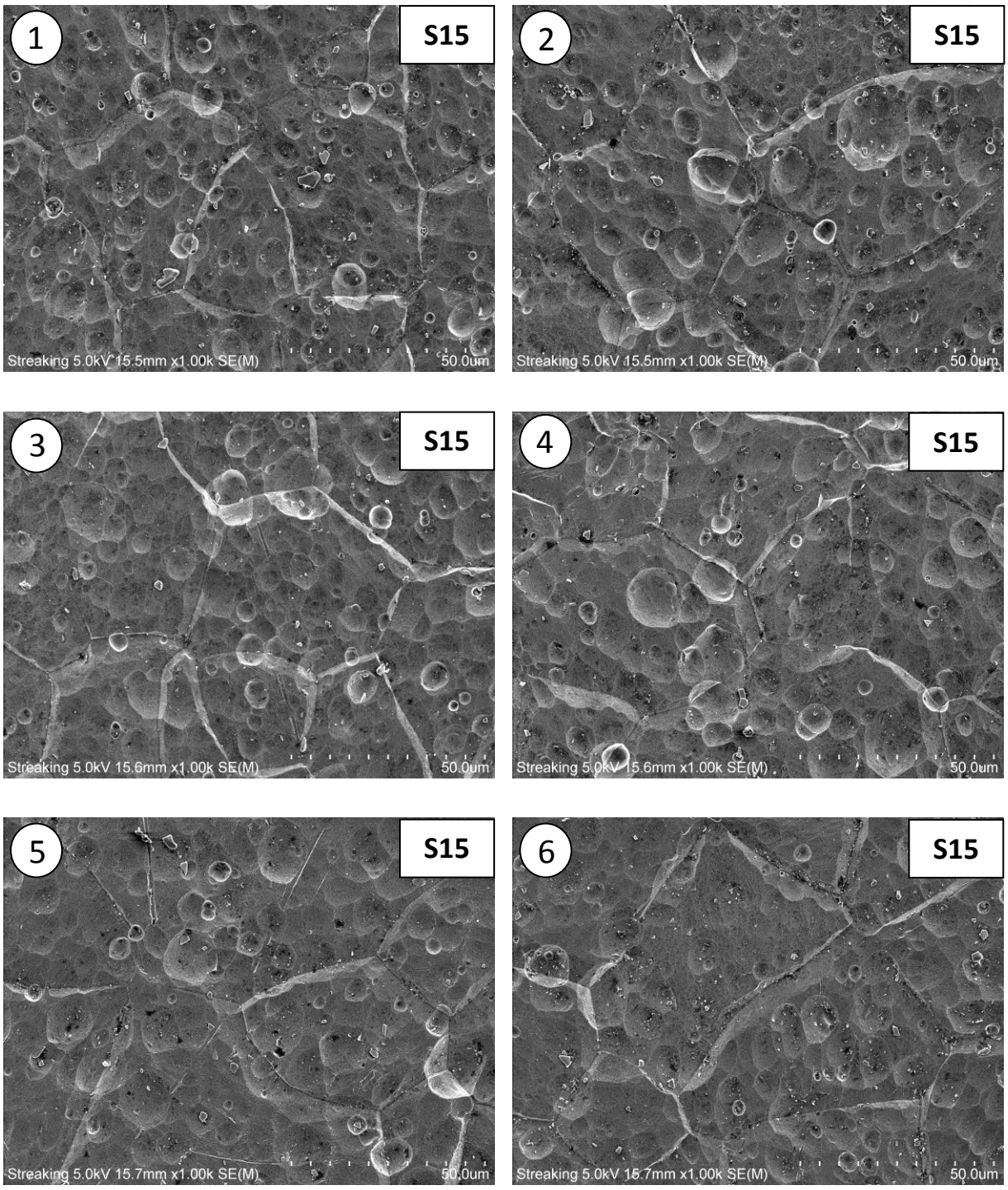

3-78 SEM images taken from six fields of view on the surface of sample S15 at 1000X magnification, fields of view 3 and 4 are from inside the parallel dull gloss streak band, fields of view1 and 2 are from the centre un-streaked region and fields of view 5 and 6 are from the extrudate surface surrounding the parallel streaks

Figure 3-79 shows six fields of view at an increased magnification of 4000X. It can again be observed that fields of view 1 and 2 from in the region between the parallel band streaks have a greater incidence of large iron rich intermetallic particles (white particles). This gives further evidence to the fact that these larger iron rich particles will cause an increased etching response in the centre region after a longer etching duration. These etched out features cause a rougher surface, a duller gloss surface and ultimately a highly prominent single band streak.

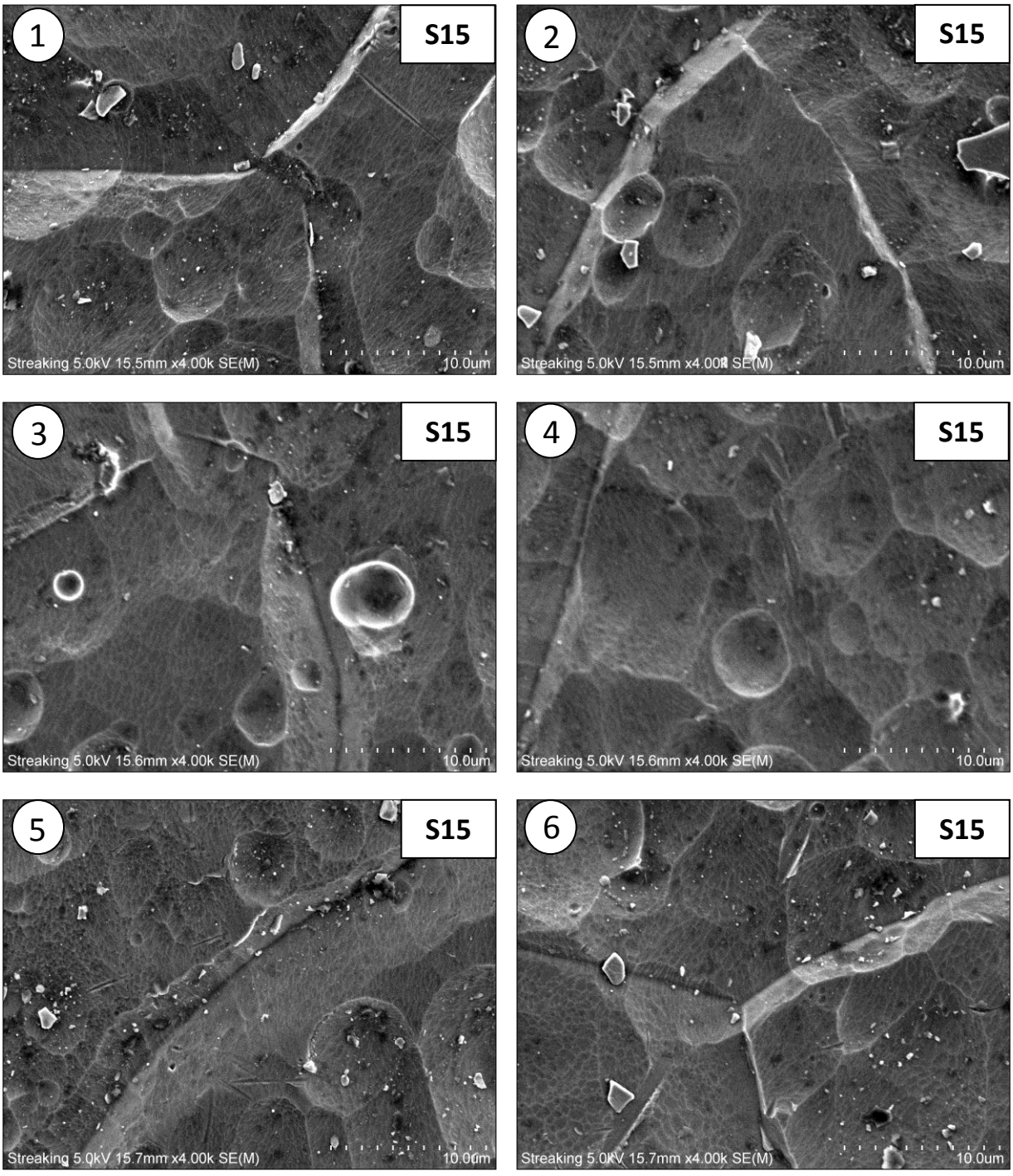

3-79 SEM images taken from six fields of view on the surface of sample S15 at 4000X magnification, fields of view 3 and 4 are from inside the parallel dull gloss streak band, fields of view1 and 2 are from the centre un-streaked region and fields of view 5 and 6 are from the extrudate surface surrounding the parallel streaks

To confirm that the centre region between the parallel streak bands will become more matte and pitted due to a higher concentration of iron rich intermetallic particles after a longer etching duration sample S17 was investigated which exhibited a highly prominent dull gloss single band streak which is situated in the centre region between the parallel streak bands. It can be seen from Figure 3-80 that the streak surface (fields of view 3 and 4) is more heavily pitted when viewed from a 300X magnification.

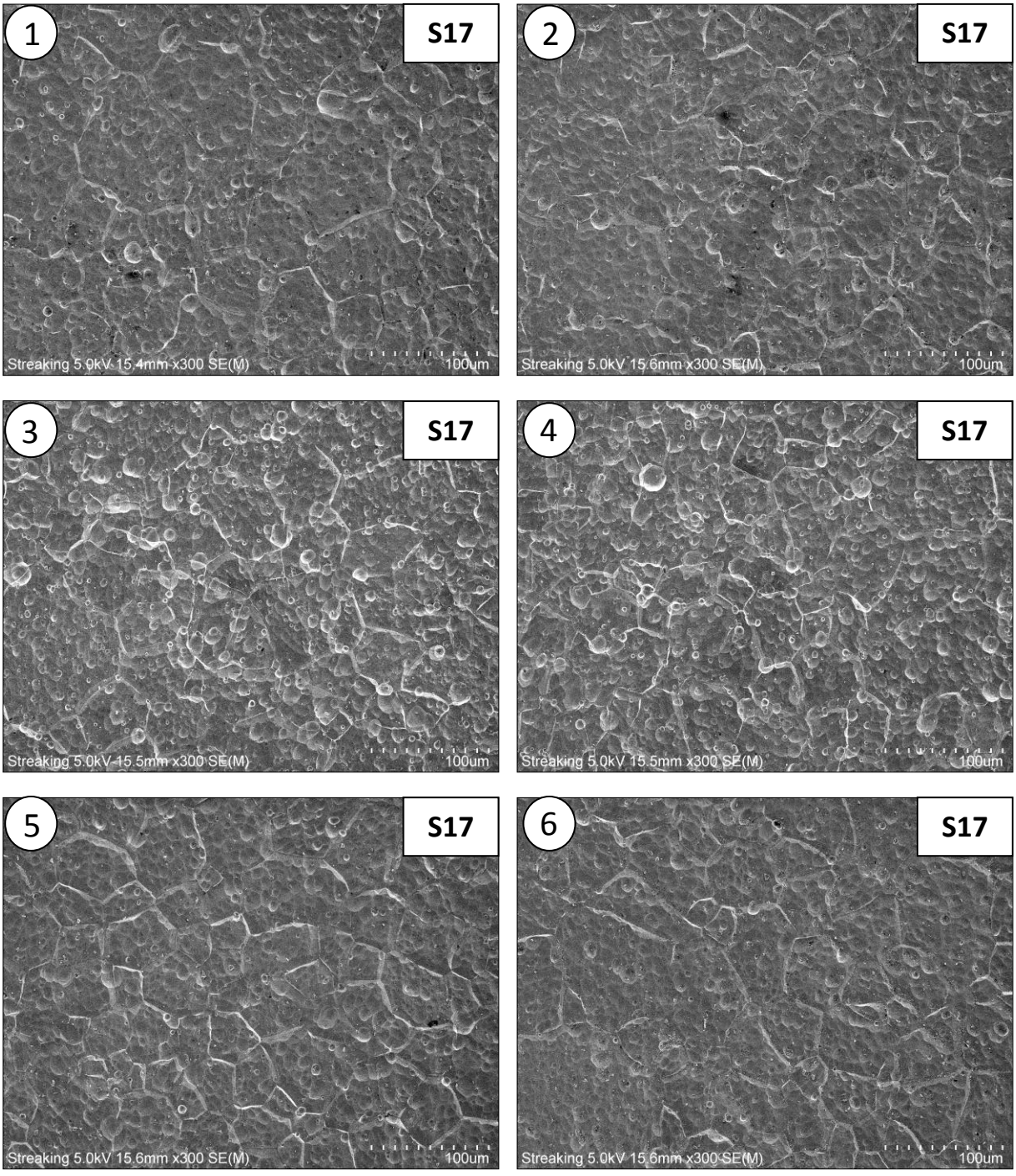

3-80 SEM images taken from six fields of view on the surface of sample S17 at 300X magnification, fields of view 3 and 4 are from inside the dull gloss streak band region and the remaining fields of view are from outside the extrudate surrounding the streak region

At a closer magnification of 1000X for sample S17 it can again be seen that the surface is more heavily pitted as shown in Figure 3-81 where fields of view 3 and 4 are from inside the dull gloss streak band.

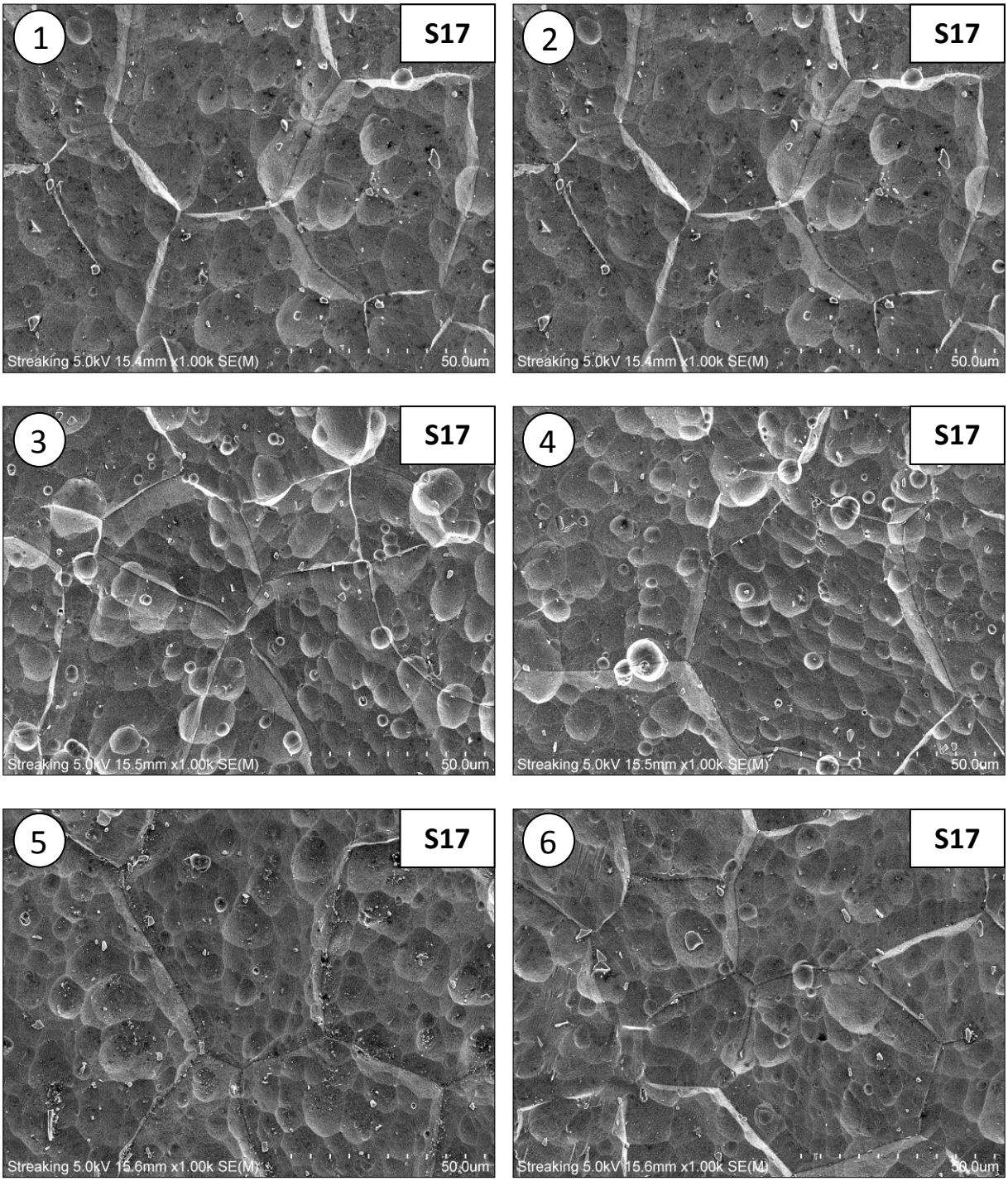

3-81 SEM images taken from six fields of view on the surface of sample S17 at 1000X magnification, fields of view 3 and 4 are from inside gloss streak band region and the remaining fields of view are from the extrudate surrounding the streak region

Magnification was further increased to 4000X for the six fields of view in and out of the streak zone as shown in Figure 3-82.

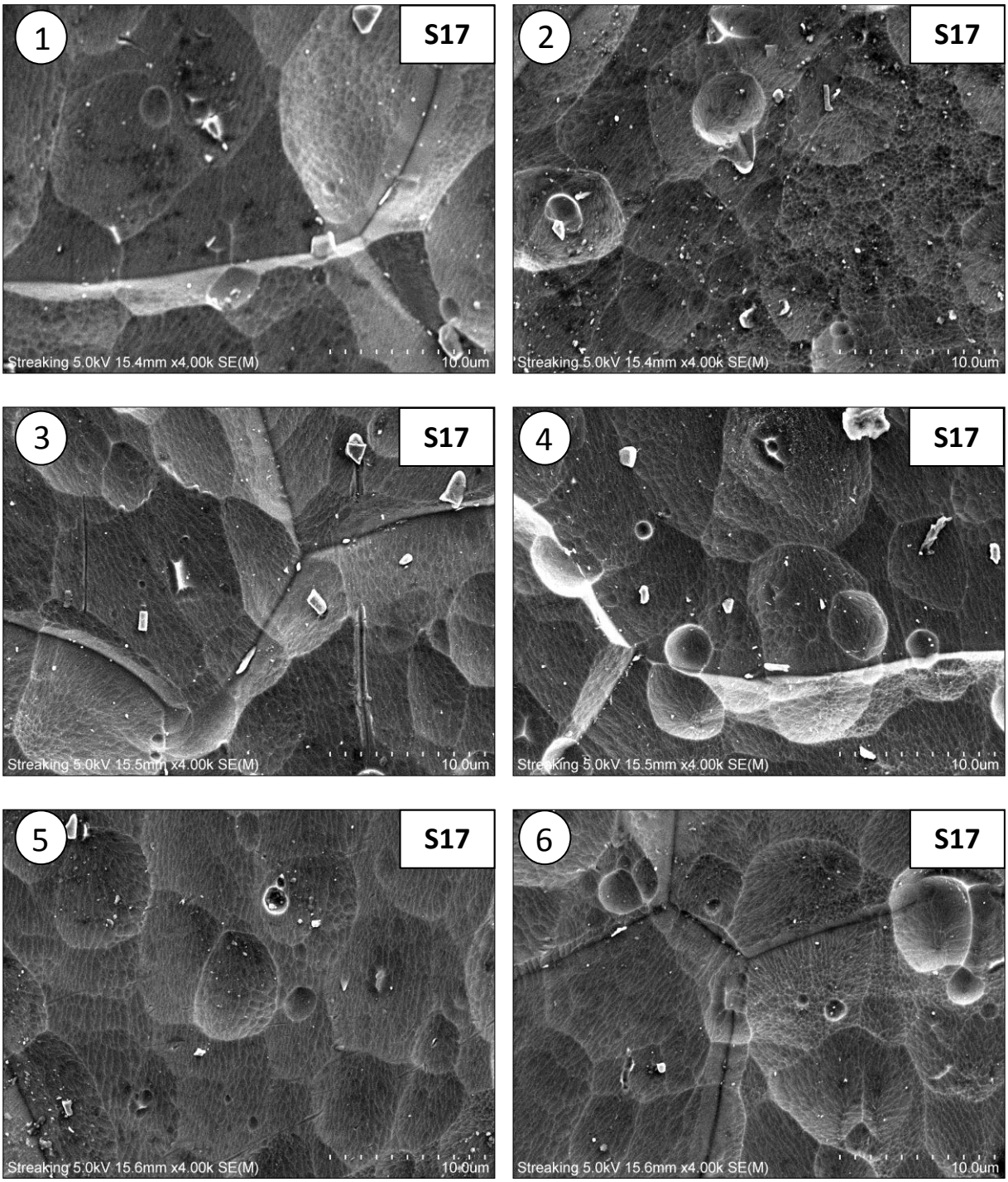

3-82 SEM images taken from six fields of view on the surface of sample S17 at 4000X magnification, fields of view 3 and 4 are from inside gloss streak band region and the remaining fields of view are from the extrudate surrounding the streak region

Thus it is more clearly identified that a dull gloss streak region has a rougher surface due to a higher concentration of pitting. A glossy streak region surface on the other hand has a lower concentration of pitting and thus a smoother surface.

Overall from SEM analysis it is confirmed that there is increased pitting on a dull streak surface and less pitting on a glossy streak surface.

3.3.9. The Correlation between Roughness and the Types of Streaking Observed

It has been identified in previous sections that three modes of streaking occur at low, medium and high etching durations. The three types of streaking are characterised as outlined in table 3-5 below.

Table 3-5 - Types of streaking observed for product type 605344

Streak type No.	Characterisation of streak	Etching Duration classification
1	Glossy Single band streaking	Low
2	Parallel band dull streaks	Medium
3	Dull single band streaking	High

It was found through optical and scanning electron microscopy that the surface topography varied in and out of the streak region. The topography varied in terms of pitting in and out of the streak region. The glossier surface was found to have a lower degree of topographical features or smoother surface and the duller surface a higher degree of topographical features mainly caused by increased pitting. To confirm that surface topography differences as explained above are correctly identified from the optical and scanning electron microscopy analysis and observation, roughness tests were conducted on the surface of samples S12, S15 and S17 which each showed modes 1, 2 and 3 streaking respectively as outlined in Table 3-5. Sample S12 showed a glossy streak and a duller surrounding extrudate surface. Roughness testing should find that the glossy streak region should have a smoother surface than the surrounding extrudate as was identified using optical and scanning electron microscopy. Figure 3-83 shows the data acquired for five roughness test in and out of the glossy streak region. The stylus was run parallel to the die lines (die lines are formed during extruding due to interaction between the extrusion and die interfaces). It can be seen that for all tests the roughness (Ra) values were less in the streak region due to the lower incidence of pitting and subsequently less overall matting of the surface. Looking at Figure 1-8 when the roughness increases between 0-0.2 Ra the glossiness rapidly decreases. Therefore only this small difference in roughness could have a large difference in surface gloss in and out of the streak region.

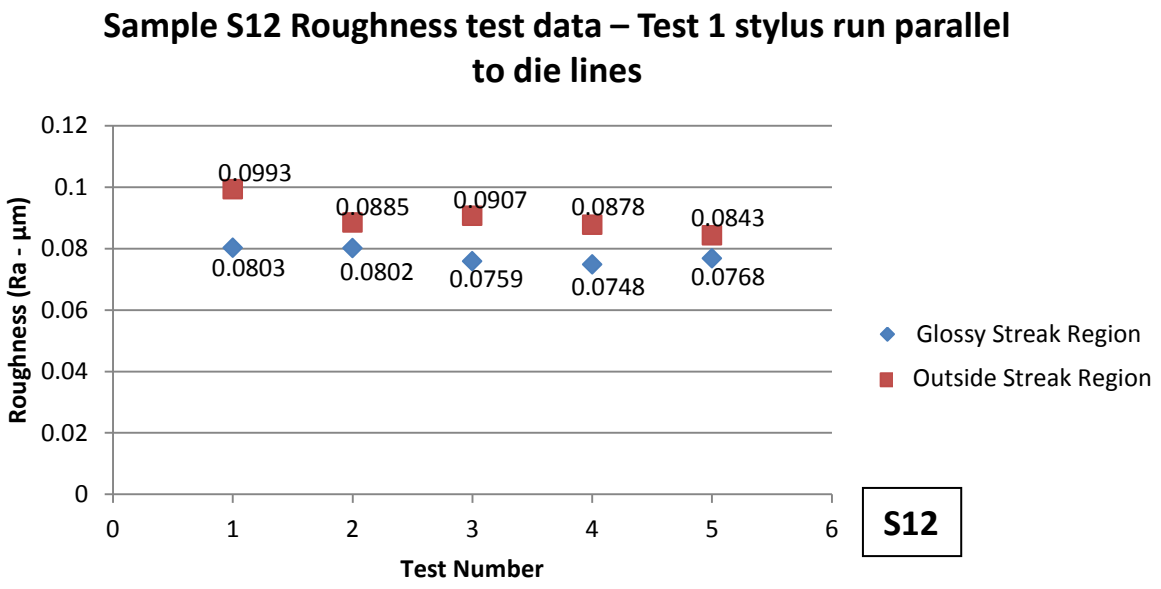

3-83 The above graph shows the results of five roughness tests on the surface of sample S12 in and out of the streak region. The stylus which measures the deflections caused by surface topography change was run parallel to the direction of die lines formed during extruding

For further confirmation that the surface is smoother in the glossy streak region a further five tests were conducted in and out of the streak zone with the stylus run normal to the die lines. It is again proved that the surface is smoother in the glossy streak region as shown from the roughness data in figure 3-84.

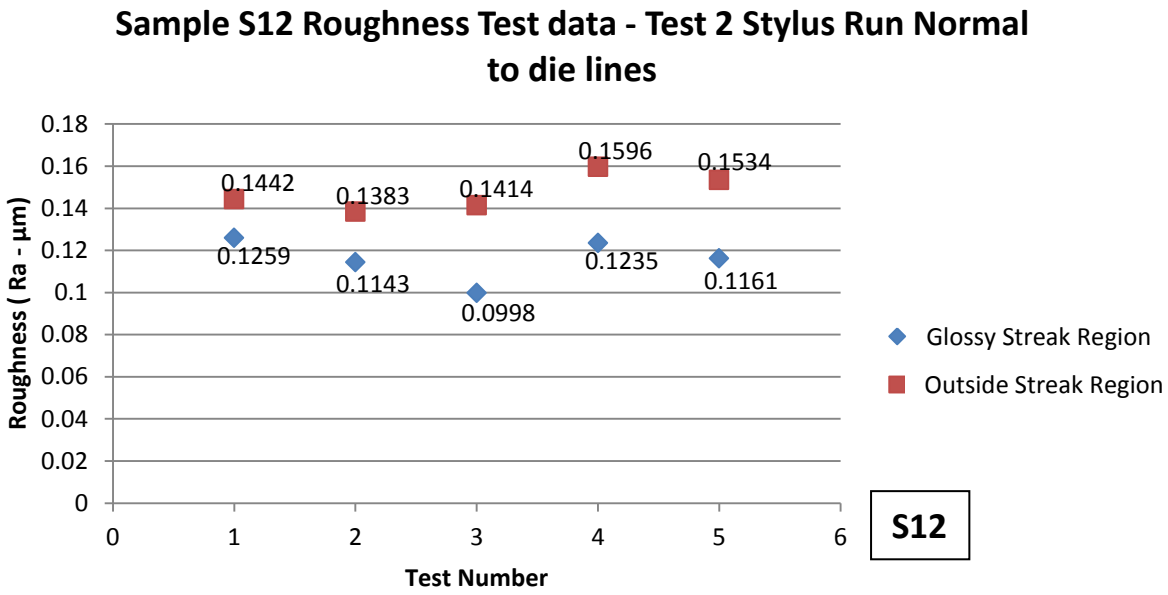

3-84 The above graph shows the results of five roughness tests on the surface of sample S12 in and out of the streak region. The stylus which measures the deflections caused by surface topography change was run normal to the direction of die lines formed during extruding

This roughness data for sample S12 agrees with what was observed using optical and scanning electron microscopy observation and analysis in which the glossy streak region was less pitted and matte than the surrounding extrudate. The next sample S15 exhibited mode 2 streaking as specified in Table 10. Figure 3-85 below shows that overall the roughness was higher in the region of the parallel streak bands with roughness tests taken alternately in each band and the stylus run parallel to the die lines. The faintness and low visibility of these streaks means that the difference in roughness in and out of the streak region is not significant.

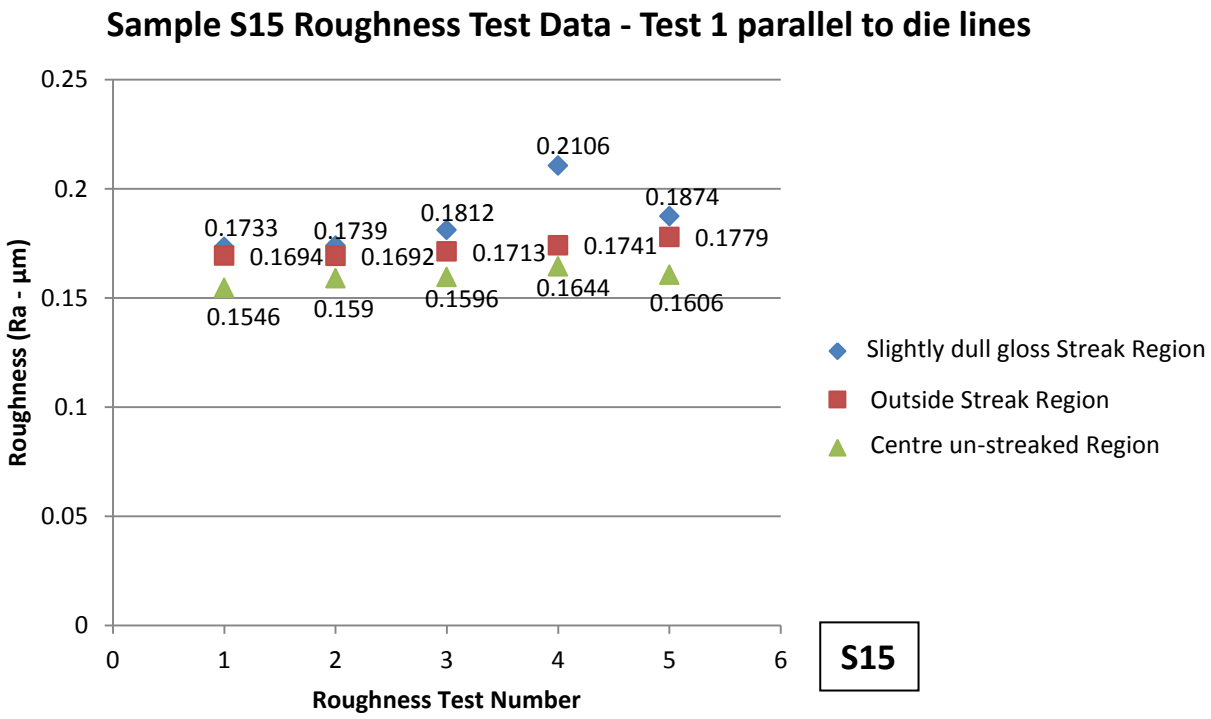

3-85 The above graph shows the results of five roughness tests on the surface of sample S15 in and out of the streak region. The stylus which measures the deflections caused by surface topography change was run parallel to the direction of die lines formed during extruding

Running the stylus normal to the die lines on sample S15 it is found that roughness differences in and out of the streak zone cannot be ascertained clearly although the roughness is noticeably rougher for the centre un-streaked region as shown in Figure 3-86. The fact that no clear difference in roughness is present in the streak region and the surrounding extrudate may suggest the roughness tester has reached its limitation in terms of the size of measurement of topographical features as mentioned in section 2.11 and illustrated in figure 2-16.

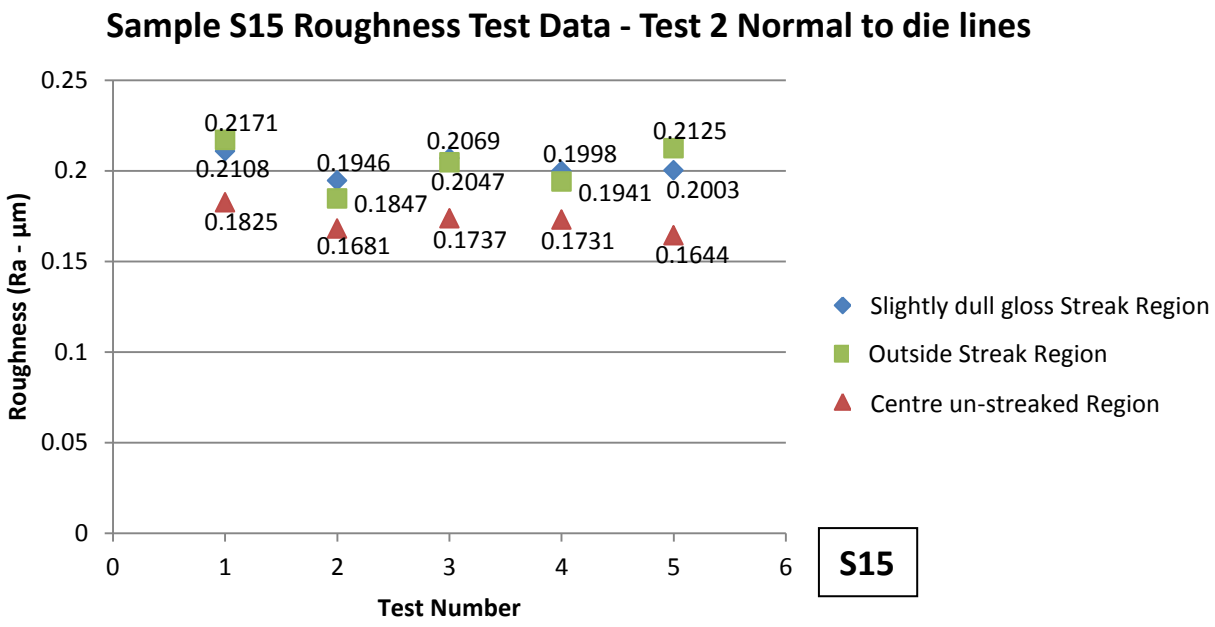

3-86 The above graph shows the results of five roughness tests on the surface of sample S15 in and out of the streak region. The stylus which measures the deflections caused by surface topography change was run normal to the direction of die lines formed during extruding

The last sample S17 exhibited mode 3 streaking as outlined in Table 9. This sample displayed a single band dull gloss streak which was highly visible. Roughness tests running the stylus parallel to the die lines shows roughness is slightly increased in the streak region as shown in figure 3-87.

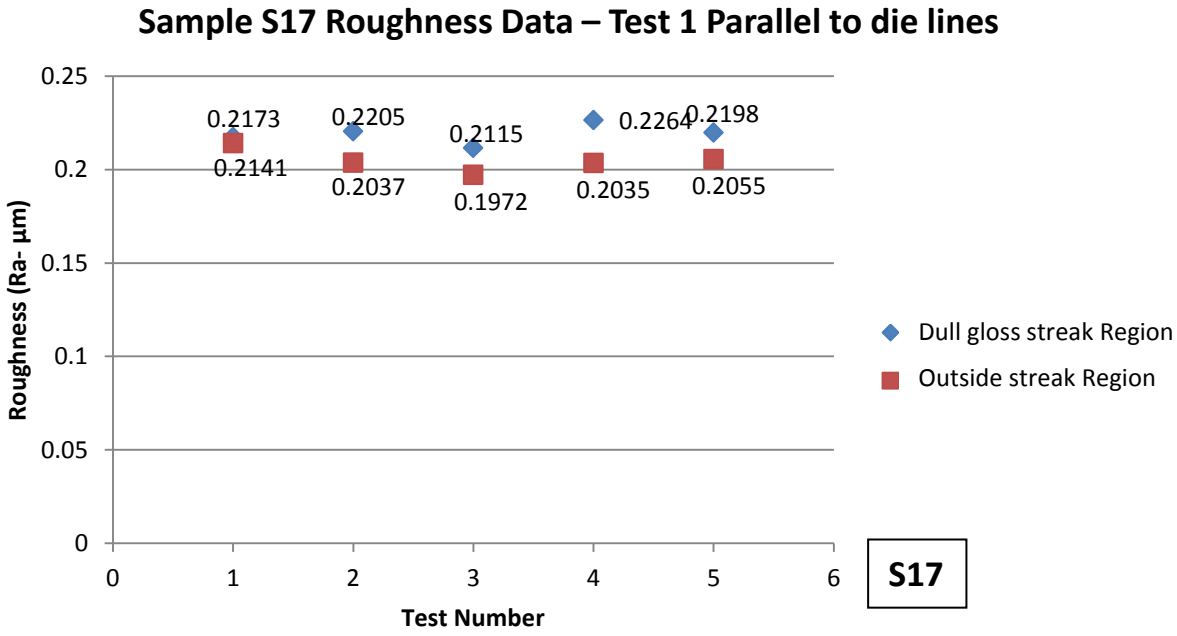

3-87 The above graph shows the results of five roughness tests on the surface of sample S17 in and out of the streak region. The stylus which measures the deflections caused by surface topography change was run parallel to the direction of die lines formed during extruding

Running the stylus normal to the die lines again shows an increased roughness in the streaked region as shown from the roughness test data in figure 3-88.

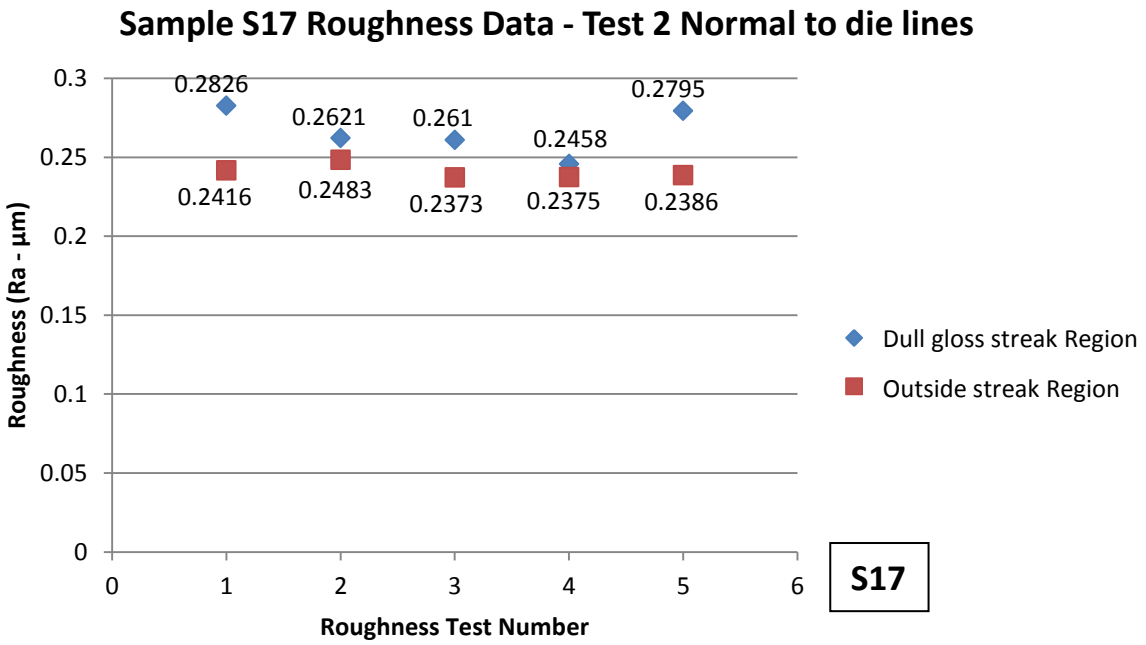

3-88 The above graph shows the results of five roughness tests on the surface of sample S17 in and out of the streak region. The stylus which measures the deflections caused by surface topography change was run normal to the direction of die lines formed during extruding

Therefore from roughness analysis it is further proved that the gloss of the surface differing is due to differences in surface roughness. This change in surface roughness as identified using SEM and optical microscopy is due to differences in pitting and the general matting of the surface due to differing etching response in the streak region.

3.5. Summary of Findings and Probable Reasons for Thermomechanical Streaking

The process at which streaking occurred was found to be during etching. At the initial stages of etching a glossy streak will form. This is due to the rougher surface outside the streak region on the mill finish as-extruded product which etches faster. The reasons and proof of this is outlined in section 3.3.5. The faster etching causes a more heavily pitted surface outside the streak region and the streak region is therefore smoother and thus glossier. As etch duration progresses low prominence parallel band dull gloss streaks appear and then after a longer etch a single band highly prominent streak appears. The duller gloss was found to directly relate to a rougher more heavily pitted streak surface. The model of this streaking evolution according to etch duration is outlined in section 3.3.2. This model indicates differing thermomechanical conditions in the streak region. The following outlines the probable reasons for thermomechanical streaking. The primary cause of thermo mechanical streaking is most probably due to die design. When a billet is forced through the orifices of a die friction is generated between the metal and the die. Depending on section thickness the metal flow will differ causing differing strain and strain rates in different areas of the extrusion as it is being extruded. The non-uniformity of metal flow may result in a variation in surface microstructure in the transition area between the fast and slow moving regions [9]. Also due to friction and plastic deformation heat generation occurs changing the temperature profile in localized regions. The difference in heat generation and temperature in different locations influence further metal flow and deformation and can result in an inhomogeneous surface microstructure such as grain size, grain orientation and intermetallics [9]. The following is a visual examination of the main extrusion product being investigated, product type 605344. Two versions of this extrusion were manufactured at Falum. The first extrusion version had highly visible streak lines as can be seen in figure 3-89 and the second was designed differently so that these streaks did not appear.

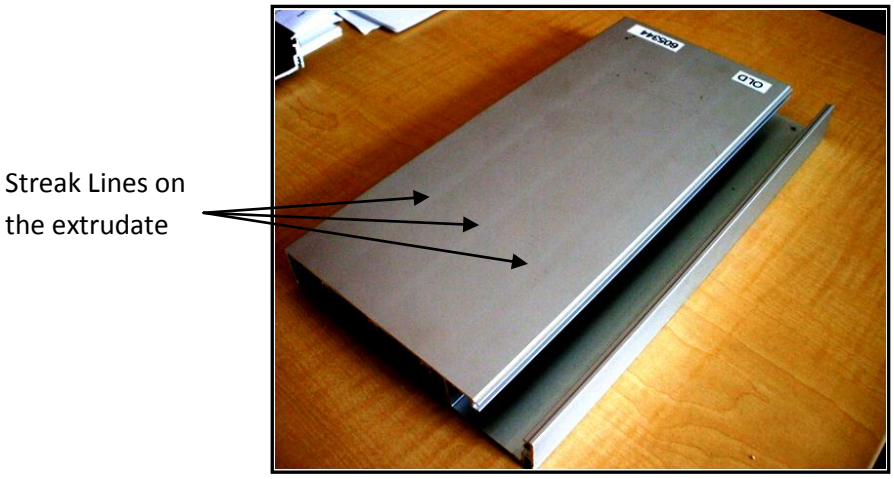

3-89 Product type 605344 showing streak lines running the length of the extrusion

The second extrusion version was designed to mitigate the streaking seen in figure 3-89 through modification of the extrusion design. The differences between the two extrusion versions can be seen from cross sectional images shown in figures 3-90 (a) and (b). The changes for the modified extrusion which was designed to eliminate streaking consisted of increasing the thicknesses t, decreasing the thickness of fin sections t_f and reducing the angle of re-entrant corners θ (corners where the interior angle is greater than 180 degrees) of the screw tabs. All streaks occurred above the regions of the screw tabs as highlighted by vertical arrows.

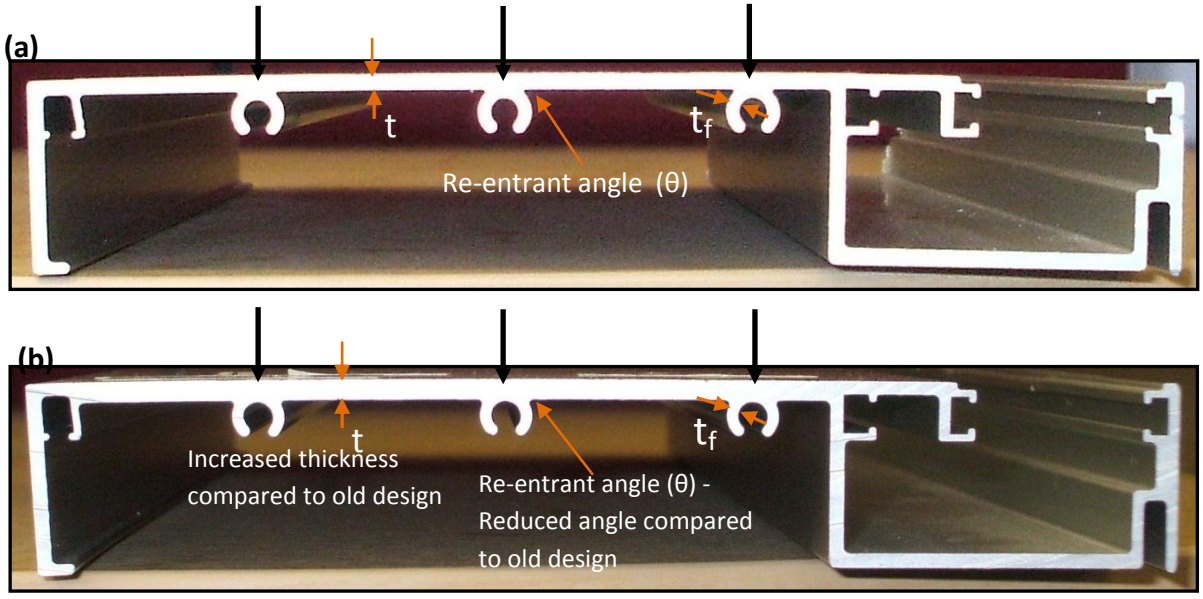

Figure 3-90 (a) Cross sectional view of extrusion version 1 - Old Design (b) Cross Sectional view of extrusion version 2 modified design

During extrusion mechanical properties of grain size, grain orientations and intermetallics can start to differ in and out of the streak zone due to varying strain rates and/or thermal conditions in and out of the streak zone. In the case of this product the varying strain rates and/or thermal conditions would be due to the greater deformation required at the location of the screw joints. Using the parameters outlined in figure 3-91 and the above knowledge the following relationship can be established:

$$\frac{\dot{\varepsilon}_{1a}}{\dot{\varepsilon}_{1b}} \gg \frac{\dot{\varepsilon}_{2a}}{\dot{\varepsilon}_{2b}} and/or \frac{T_{1a}}{T_{1b}} \gg \frac{T_{2a}}{T_{2b}}$$

Where $\dot{\varepsilon}$ is the strain rate and T the temperature.Therefore the strain rate/temperature in and out of the streak region for extrusion version 1 – old design figure 3-91 (a) must differ to a larger degree than the strain rate/temperature in and out of the streak region for extrusion version 2 –modified version figure 3-91 (b).

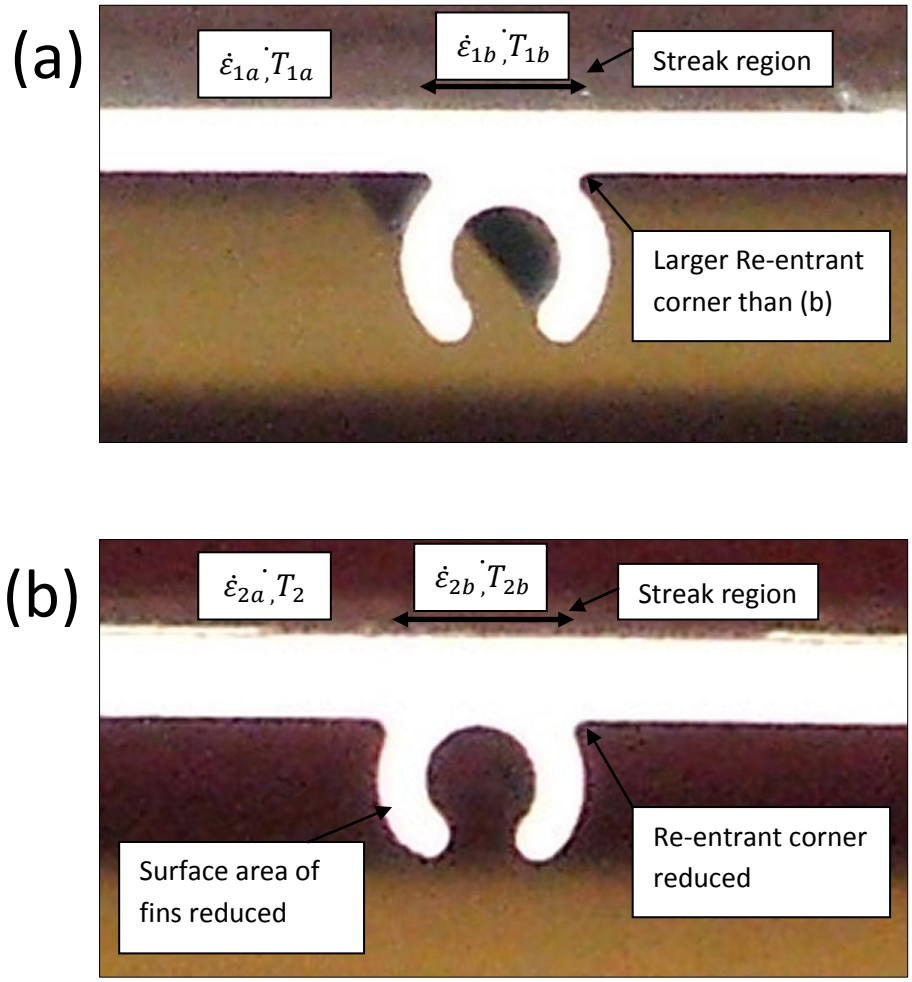

Figure 3-91– Diagram outlining thermo-mechanical extrusion parameters (a) Extrusion version 1 –old design (b) Extrusion version 2 – modified design

In relation to differing strain rates and temperature in and out of the streak region it is noted by Sheppard [4] that force and hence extrusion pressure is a strong function of strain rate and temperature. The pressure required to extrude can be related into four parts:

1. The pressure required to deform the metal homogeneously
2. The pressure required to overcome the friction mainly at the container/Billet interface.
3. The pressure required to compensate for losses due to redundant work.
4. The pressure required to ensure breakout.

Analysing figure 3-91(a) and (b) which was the old extrusion design and the modified design respectively it is apparent that (a) has a greater contact/surface area due to larger fins. This would hence cause increased frictional resistance increasing the pressure load as stated in point 2 above. In relation to point 3 above a major source of redundant work is re-entrant corners (corners where the interior angle is greater than 180 degrees) which are significantly larger for the old design as can be seen from figure 3-91(a) thus increasing pressure. Sheppard [4]states that increased complexity of shape where there are re-entrant corners or thin fin sections causes increases in extrusion load and hence altered strain rates and temperature. This will in turn result in differing grain size, aspect ratios and boundaries or differing distributions of intermetallics thereby causing etching pits to occur. As such deformation $(\varepsilon, \dot{\varepsilon})$ and Temperature must most likely be equal or differ to a lesser degree in and out of the streak zone to achieve uniformity across the extrusion surface and hence reduce the likely hood of streaking appearing. In essence variations in thermomechanical conditions in and out of the streak zone are the most probable root causes of streaking the sub factors which stem from this have been previously explained in section 1.5.

3.6. Conclusion

The following points summarise the findings made for this study of streaking and the mechanisms which cause this phenomenon.

- It was found that initial dark streak regions on the extrusion before surface treatment were caused by a greater density of die lines outside the streak region.
- The following sub points outline the findings made for the effects of grain size and pitting which could cause streaking.
    - By electro-polishing to reveal grain boundary grooves but not etch out other features it was found that grain size differed in and out of the streak zone by around 18%. Although grain size differed and hence grain boundary density would also differ which could alter the roughness and surface gloss, streaking did not appear. Through analysis it was found however that a grain size difference of 15-21% difference only corresponds to 1-3% difference in grain boundary groove density in and out of the streak region.
    - By etching it was found streaks were induced on the surface of the streak prone extrusion samples through the mechanism of different degrees of pitting in and out of the streak region.
- By polishing samples to different degrees and then etching and comparing distributions of surface pits it was found that etching response is affected by the surface roughness. In essence a rougher surface will etch faster than a smoother surface. Knowing that the as extruded product of the steak prone product being investigated has a smoother surface in the streak region and a rougher surface outside the streak region, the appearance of streaking was actually mitigated. This roughness difference in and out of the streak region is possibly due to differences at the die-extrusion interface in and out of the streak region (i.e. Temperature differences in and out of the streak region which may cause differing wear characteristics of the die in and out of the streak region).
- By etching for different durations it was established three different types or modes of streaking occurred:
    - Low etch duration – Glossy single band streak
    - Medium etch duration – Dull gloss parallel band streaks
    - High etch duration – Dull gloss single band streak

The glossy single band streak which occurs at low etch durations is caused by the differences in surface roughness on the as extruded product in and out of the streak region and subsequent faster etch and hence more heavily pitted and dull surface outside the streak region. The dull streaking at medium and high etch durations is due to a more heavily pitted surface in the streak region.

- Overall the dull streaking commonly observed in extrusion manufacturing occurred in the subsurface region at the location of the extrusion profile in which the cross sectional thickness varied.
- It was found through analysis that the streak could be removed after 60 microns of surface material removal. For the standard 15 minute etching time streaking would be induced as a single band prominent streak on the surface. Another surface finishing technique known as abrasive blasting would remove 100 micron of surface material hence meaning even if etching was used in addition to clean the surface of the blasted product streaking would not occur. Therefore it would be beneficial to first abrasive blast and etch for a short duration to achieve a matte surface finish desired by the customer. This would eliminate any chance of etch induced streaking assuming that material removal is still within tolerances.

3.7. Further Research

The following points outline suggested further research on the streaking phenomenon from the findings made in this study.

- Identify on another streak prone extrusion that the findings made in this study are the same and applicable for all cases of thermomechanical streaking.
- Ascertain whether intermetallics or grain orientations, both which could cause an altered etching response differ in and out of the streak region. It was observed on visual inspection that iron rich intermetallic particles may differ in and out of the streak region. This observation must be quantified to provide further evidence and ultimately proof.
- Measure if temperature differs in and out of the streak region at the extrusion-die interface. This temperature difference could the following:
    a) A smoother less densely die lined surface in the streak region
    b) Differing distributions of intermetallics in and out of the streak region
    c) A preferred grain orientation in the streak region which differs from outside the streak region.

Appendix A – Heyn Grain Size Method

A1 – Grain Size Relationships

Table A1– Grain Size Relationships

Grain Size No. G	N_A Grains/Unit Area		$\bar{A}$ Average Grain Area		$\bar{d}$ Average Diameter		$\bar{\ell}$ Mean Intercept		N_L
	No./in.^{2} at 100X	No./mm^2 at 1X	mm^2	μm^2	mm	μm	mm	μm	No./mm
00	0.25	3.88	0.2581	258064	0.5080	508.0	0.4525	452.5	2.21
0	0.50	7.75	0.1290	129032	0.3592	359.2	0.3200	320.0	3.12
0.5	0.71	10.96	0.0912	91239	0.3021	302.1	0.2691	269.1	3.72
1.0	1.00	15.50	0.0645	64516	0.2540	254.0	0.2263	226.3	4.42
1.5	1.41	21.92	0.0456	45620	0.2136	213.6	0.1903	190.3	5.26
2.0	2.00	31.00	0.0323	32258	0.1796	179.6	0.1600	160.0	6.25
2.5	2.83	43.84	0.0228	22810	0.1510	151.0	0.1345	134.5	7.43
3.0	4.00	62.00	0.0161	16129	0.1270	127.0	0.1131	113.1	8.84
3.5	5.66	87.68	0.0114	11405	0.1068	106.8	0.0951	95.1	10.51
4.0	8.00	124.00	0.00806	8065	0.0898	89.8	0.0800	80.0	12.50
4.5	11.31	175.36	0.00570	5703	0.0755	75.5	0.0673	67.3	14.87
5.0	16.00	248.00	0.00403	4032	0.0635	63.5	0.0566	56.6	17.68
5.5	22.63	350.73	0.00285	2851	0.0534	53.4	0.0476	47.6	21.02
6.0	32.00	496.00	0.00202	2016	0.0449	44.9	0.0400	40.0	25.00
6.5	45.25	701.45	0.00143	1426	0.0378	37.8	0.0336	33.6	29.73
7.0	64.00	992.00	0.00101	1008	0.0318	31.8	0.0283	28.3	35.36
7.5	90.51	1402.9	0.00071	713	0.0267	26.7	0.0238	23.8	42.04
8.0	128.00	1984.0	0.00050	504	0.0225	22.5	0.0200	20.0	50.00
8.5	181.02	2805.8	0.00036	356	0.0189	18.9	0.0168	16.8	59.46
9.0	256.00	3968.0	0.00025	252	0.0159	15.9	0.0141	14.1	70.71
9.5	362.04	5611.6	0.00018	178	0.0133	13.3	0.0119	11.9	84.09
10.0	512.00	7936.0	0.00013	126	0.0112	11.2	0.0100	10.0	100.0
10.5	724.08	11223.2	0.000089	89.1	0.0094	9.4	0.0084	8.4	118.9
11.0	1024.00	15872.0	0.000063	63.0	0.0079	7.9	0.0071	7.1	141.4
11.5	1448.15	22446.4	0.000045	44.6	0.0067	6.7	0.0060	5.9	168.2
12.0	2048.00	31744.1	0.000032	31.5	0.0056	5.6	0.0050	5.0	200.0
12.5	2896.31	44892.9	0.000022	22.3	0.0047	4.7	0.0042	4.2	237.8
13.0	4096.00	63488.1	0.000016	15.8	0.0040	4.0	0.0035	3.5	282.8
13.5	5792.62	89785.8	0.000011	11.1	0.0033	3.3	0.0030	3.0	336.4
14.0	8192.00	126976.3	0.000008	7.9	0.0028	2.8	0.0025	2.5	400.0

A2 - 95% Confidence Internal Multipliers

Table A2 - 95% Confidence Internal Multipliers, t

No. of Fields, *n*	*t*	No. of Fields, *n*	*t*
5	2.776	13	2.179
6	2.571	14	2.160
7	2.447	15	2.145
8	2.365	16	2.131
9	2.306	17	2.120
10	2.262	18	2.110
11	2.228	19	2.101
12	2.201	20	2.093

A3 – Heyn Grain Size Method Calculations

The following outlines the calculations for the Heyn linear intercept procedure as outlined in ASTM Designation E 112 – 96 and described in the methodology section 2.6. The following data results shown in Table A3-1 were accumulated from the six fields of view shown in Figure 3-9 from outside the streak zone. See section 2.6 for information on the Heyn procedure and the data acquisition method used to obtain this table of data.

Table A3 -1 - Results from conducting the Heyn procedure on the six view fields from outside the streak region as shown in figure 60

Field of View	L**(length of test line - mm)**	N_i**(Number of intercepts with a test line)**	N_L**(number of intercepts per unit length of test line)**	l **(mean lineal intercept length)**
1	3.85 mm	170.5	44.29	0.0226
2	3.85 mm	189	49.09	0.0204
3	3.85 mm	169	43.90	0.0228
4	3.85 mm	174	45.19	0.0221
5	3.85 mm	162.5	42.21	0.0237
6	3.85 mm	166.5	43.25	0.0231

Before calculating grain size information the relative accuracy of this analysis will be calculated. The aim is for the relative accuracy to be well below the recommended 10% maximum. If it is above 10% more view fields and an increased test line length would be necessary. To do this it is first necessary to calculate the average mean lineal length $\bar{l}_L$.

$$\bar{X} = \bar{l}_L = \frac{0.1347}{6} = 0.02245 \qquad (a3)$$

From this the standard deviation is calculated using the individual mean lineal lengths from table A3-1 and the average mean lineal length (a3). The value n is the number of view fields measured which is 6.

$$standard\ deviation = s = \left[\frac{\sum(X_i - \bar{X})^2}{n-1}\right]^{1/2} = \left[\frac{\sum(l_i - \bar{l})^2}{n-1}\right]^{1/2} = 1.264 \times 10^{-3} (b3)$$

Using the standard deviation the 95% confidence interval is calculated where n is again the number of view fields which is six, *s* the standard deviation and *t* the 95% confidence internal multipliers found in appendix A, table A2.

$$95\% CI = \frac{t \cdot s}{\sqrt{n}} = \frac{2.571 \cdot 1.264 \times 10^{-3}}{\sqrt{6}} = 1.327 \times 10^{-3} (c3)$$

By dividing the 95% confidence interval by the by the average mean lineal length and multiplying by 100 the percentage of relative accuracy is obtained.

$$\%RA = \frac{95\%\ CI}{\bar{X}} \cdot 100 = \frac{1.327 \times 10^{-3}}{0.02245} \cdot 100 = 5.91\%\ (d3)$$

Since the relative accuracy of this analysis is well within 10% the next step is to calculate the grain size number and the properties of average grain area, diameter and distribution per mm^2. First the average number of intercepts per unit length of test line ($\bar{N}_L$) is calculated from all six fields of view.

$$\bar{N}_L = \frac{267.93}{6} = 44.655 \qquad (e3)$$

Using the mean number of intercepts per unit length of test line $\bar{N}_L$ found in (b) the Grain Size number is calculated as:

$$G = (6.643856\ log_{10}\bar{N}_L) - 3.288 = (6.643856 \cdot log_{10} \cdot 44.655) - 3.288 = 7.673 \quad (f3)$$

Before calculating the grain properties the series of steps carried out to find the grain size number (G) for the six fields outside the streak region must be carried out again to find the grain size number for inside the streak region. This is necessary so the grain properties of either region can be compared.

The following data shown in table A3-2 was accumulated from the six fields of view shown in Figure 3-10 from inside the streak region. As mentioned previously for the data shown in table A3-2, see section 2.6 for information on the Heyn procedure and the method used to acquire the tabulated data.

Table A3-2 - Results from conducting the Heyn procedure on the six view fields from outside the streak region as shown in figure 61

Field of View	L(length of test line - mm)	N_i(Number of intercepts with a test line)	N_L(number of intercepts per unit length of test line)	l (mean lineal intercept length)
1	3.85 mm	203.5	52.86	0.01892
2	3.85 mm	196	50.91	0.01964
3	3.85 mm	185	48.05	0.02081
4	3.85 mm	195	50.65	0.01974
5	3.85 mm	190	49.35	0.02026
6	3.85 mm	201	52.21	0.01915

Like the Grain size analysis for the six fields of view from outside the streak region the relative accuracy is first calculated to ensure that the relative accuracy is within 10%. If higher than 10% additional fields of view must be added and or test line length increased. The first step is to calculate the average mean lineal length$\bar{l}_L$.

$$\bar{X} = \bar{l}_L = \frac{0.11852}{6} = 0.01975 \quad (a4)$$

The standard deviation is then calculated as follows with the number of fields of view (n) again being six.

$$standard\ deviation = \ s = \left[\frac{\sum(X_{i-}\ \bar{X})^2}{n-1}\right]^{1/2} = \left[\frac{\sum(l_{i-}\ \bar{l})^2}{n-1}\right]^{1/2} = 6.993 \times 10^{-4} (b4)$$

Finally the 95% confidence interval is calculated where *t* is found from table A2 in appendix A and then the percentage of relative accuracy calculated from the 95% confidence interval and the average mean lineal length.

$$95\%CI = \frac{t \cdot s}{\sqrt{n}} = \frac{2.571 \cdot 6.993 \times 10^{-4}}{\sqrt{6}} = 7.339 \times 10^{-4} (c4)$$

$$\%RA = \frac{95\%\ CI}{\bar{X}} \cdot 100 = \frac{7.339 \times 10^{-4}}{0.01975} \cdot 100 = 3.72\%(d4)$$

Therefore the relative accuracy at 3.72% is well within the recommended 10% maximum. The grain size number for the six fields inside the streak region can now be calculated.

$$\bar{N}_L = \frac{304.03}{6} = 50.67 \qquad (e4)$$

$$G = (6.643856\ log_{10}\bar{N}_L) - 3.288 = (6.643856 \cdot log_{10} \cdot 50.67) - 3.288 = 8.038 \quad (f4)$$

From calculations (f3) and (f4) the following grain size numbers were calculated as shown in Table A3-3. Furthermore calculations (d3) and (d4) calculated the relative accuracies of these grain size numbers.

Table A3-3 - Grain Size number data including upper and lower limits of relative accuracy

	Grain Size Number, G	% Relative accuracy	Grain size number G, upper limit	Grain size number G, lower limit
For the six fields of view outside the streak region	7.673	5.91%	8.13	7.22
For the six fields of view inside the streak region	8.038	3.72%	8.34	7.74

Using the grain size numbers (G) shown in Table A3-3 and interpolation of data shown in table A1 appendix A the Average Grain area, diameter and number of grains per mm^2 could be calculated as shown in Table 5 along with the upper and lower limits of relative accuracy. See appendix A4 for interpolation calculations to find the average grain area.

A4 – Interpolation Calculations of the Grain Size Numbers

The following is the interpolation calculations from table A1 to find the average grain area from the grain size numbers shown in table A3-3.

A4-1. Outside the Streak Region

$$Average\ Grain\ Area = 713 + (504 - 713) \cdot \left(\frac{7.673 - 7.5}{8 - 7.5}\right) = 641\mu m^2$$

$$Average\ Grain\ Area\ (upper\ limit) = 1008 + (713 - 1008) \cdot \left(\frac{7.22 - 7}{7.5 - 7}\right) = 878.2\mu m^2$$

$$Average\ Grain\ Area\ (lower\ limit) = 504 + (356 - 504) \cdot \left(\frac{8.13 - 8}{8.5 - 8}\right) = 465.52\mu m^2$$

A4-2. Inside the Streak Region

$$Average\ Grain\ Area = 504 + (356 - 504) \cdot \left(\frac{8.038 - 8}{8.5 - 8}\right) = 493\mu m^2$$

$$Average\ Grain\ Area\ (upper\ limit) = 713 + (504 - 713) \cdot \left(\frac{7.74 - 7.5}{8 - 7.5}\right) = 612.68\mu m^2$$

$$Average\ Grain\ Area\ (lower\ limit) = 504 + (356 - 504) \cdot \left(\frac{8.34 - 8}{8.5 - 8}\right) = 403.36\mu m^2$$

Appendix B – Calculation for Grain Boundary Groove Fraction

The following is the method used to find the difference in grain boundary densities in and out of the streak region analytically using the average grain size in and out of the streak region found using image J. The average grain size values in and out of the streak region obtained using Image J is shown in Table B-1. The values for average grain size were used from the image J analysis and not the Heyn grain size analysis because of the wide differences in grain size seen in the microstructure in and out of the streak zone which makes the Heyn grain size procedure less accurate.

Table B-1 Average Grain size in and out of the streak region acquired using Image J analysis

	Average grain size across six fields of view
Inside the Streak Region	329.50μm^2
Outside the streak region	389.83μm^2

B1 – Analysis of a 3x3 Honeycomb Grain Matrix

The first analysis using the method devised will be carried out using a 3 X 3 honeycomb grain matrix as shown in Figure B1-1 below.

1. Find the number of side (S) so a total grain boundary length formula can be devised.
As can be seen adjacent to the honeycomb structure shown in Figure B1-1 each of the six equal sides of a hexagon is equal to S. The number of sides (S) which each represents a grain boundary groove length comes to thirty five. Therefore the total grain boundary length is equal to:

$$Total\ Grain\ Bondary\ length = 35S \quad (a1)$$

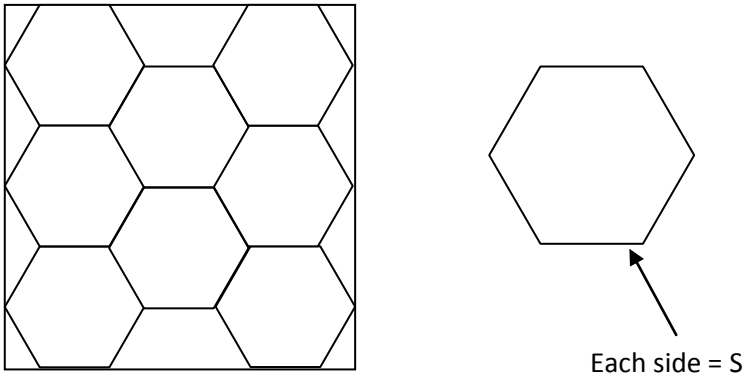

Figure B1-1–3x3 honeycomb grain structure

2. Find the length of each side of the hexagon (S) for the grain sizes specified in table B1.

The area of each grain (1 hexagon) is equal to:

$$Area\ of\ Grain\ (Hexagon) = \frac{S^2 n}{4\tan\left(\frac{\pi}{n}\right)} \quad (b1)$$

The variable n equals the number of sides which is six. Therefore using this formula S can be determined as follows for the average grain size in and out of the streak region.

$$Inside\ the\ streak\ region \rightarrow 329.50m^2 = \frac{S^2 6}{4\tan\left(\frac{\pi}{6}\right)}$$

$$Outside\ the\ streak\ region \rightarrow 389.83\mu m^2 = \frac{S^2 6}{4\tan\left(\frac{\pi}{6}\right)}$$

$$Inside\ the\ streak\ region \rightarrow S = \sqrt{2.3094 * 329.50/6} = 11.26\ \mu m$$

$$Outside\ the\ streak\ region \rightarrow S = \sqrt{2.3094 * 389.83/6} = 12.25\ \mu m$$

Table B1-2 - Length of each side (S) of a six sided hexagon grain in and out of the streak region

	Inside streak Region	Outside streak region
S (Length of one side of a six sided hexagon grain)	11.26 μm	12.25 μm

3. Find the total grain boundary length in and out of the streak region for a 3x3 honeycomb grain matrix

Using formula (a1) the total grain boundary length can then be found. The values for the total grain boundary length in and out of the streak region are shown in Table B1-3.

$$Total\ Grain\ Boundary\ length\ (In\ streak\ region) = 35\mathrm{S} = 35(11.26)$$
$$= 394.1\mu\mathrm{m}\ \ (b5)$$

$$Total\ Grain\ Boundary\ length\ (Outside\ streak\ region) = 35\mathrm{S} = 35(12.25)$$
$$= 428.75\mu\mathrm{m}\ \ (\mathrm{b6})$$

Table B1-3 - Total grain boundary length in an out of the streak region for a 3x3 honeycomb grain matrix

	Inside streak Region	Outside streak region
Total grain boundary length	394.1μm	428.75μm

4. Find the total grain boundary area in and out of the streak region for a 3x3 honeycomb grain matrix

From the total grain boundary length for a 3X3 honeycomb grain matrix in and out of the streak region the total area of the grain boundary grooves can be found multiplying the length by an estimated width of 3μm for the grain boundary grooves. This estimation was made by analysing SEM images of the specimen surface as shown in Figure B1-2.

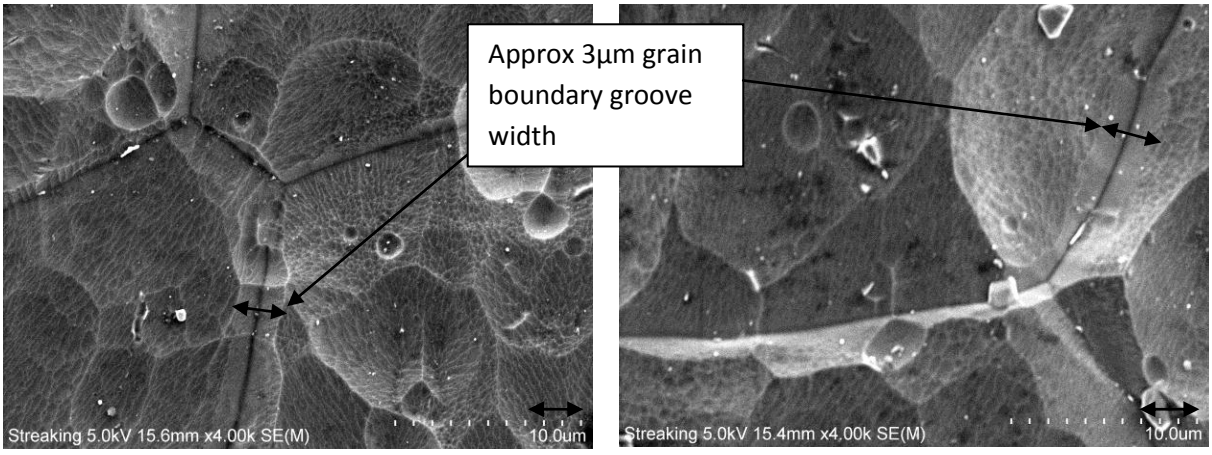

Figure B1-2 – Grain boundary groove width estimation using high resolution SEM images

Using the total grain boundary lengths multiplied by the approximate grain boundary groove width the total grain boundary groove area in and out of the streak region was calculated and is shown in Table B1-4.

Table B1-4 - Total area of grain boundary grooves for a 3 x 3 honeycomb grain matrix in and out of the streak region

	Area of Grain boundary grooves (for a 3 X 3 honeycomb grain matrix)
Inside the Streak Region	1182.3μm^2
Outside the streak region	1286.25μm^2

5. Find the total area for a 3x3 honeycomb grain matrix in and out of the streak region.

The 3 x 3 honeycomb grain matrices for in and out of the streak region will be different sizes due to the different grain sizes in and out of the streak region. To compare the distribution of grain boundary grooves in and out of the streak region the total area of each honeycomb grain matrix must be calculated for in and out of the streak region. Figure B1-3 shows the components to find the height and width of the honeycomb grain matrix where S is the length of one side, $H = (S)\cos(30°)$, GBW = Grain Boundary Width = 3μm and $W = (S)\cos(60°)$.

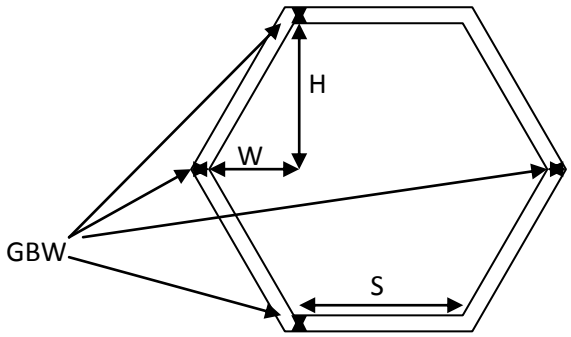

Figure B1-3 – Length components required to find the entire area of the honeycomb grain matrix

Therefore using the length components shown in Figure B1-3 the total area of the 3x3 honeycomb grain matrices for in and out of the streak zone is calculated as:

$$Area\ of\ 3x3\ honeycomb\ grain\ matrix = width\ \times height$$
$$= \{[(S \cdot \cos(60)) \cdot 4] + [GBW \cdot 4\ ] + [3 \cdot S]\}$$
$$* \ \{(S \cdot \cos(30)) \cdot 6 + [GBW \cdot 4]\}\ (i1)$$

The total matrix areas for in and out of the streak zone are shown in Table B1-5 below.

Table B1-5 - Total area of a 3x3 honeycomb grain matrix in and out of the streak region

	Area of 3x3 honeycomb grain matrix
Inside the streak region	$4817\mu m^2$
Outside the streak region	$5542\mu m^2$

6. Find the area of the combined grain interiors in and out of the streak region.

Using the grain boundary groove area values from Table B1-4 and the total area of the honeycomb matrices shown in Table B1-5 the difference in grain boundary groove distribution in and out of the streak zone can be calculated. First the values for the total area of the grain interiors in and out of the streak region calculated from the total matrix area minus the grain boundary groove area is shown in Table B1-6.

Table B1-6 - Total area of the grain interiors in and out of the streak region

	Total combined area of grain interiors
Inside the streak region	$3635\ \mu m^2$
Outside the streak region	$4255.75\ \mu m^2$

7. Find the fraction of grain boundary grooves vs. the grain interiors in and out of the streak region

The percentage of grain boundary groove area was then found as shown in Table B1-7 with the remaining percentage being the percentage area of the grain interiors.

Table B1-7 - Fraction of grain boundary grooves Vs. Grain Interiors

	% of grain boundary grooves
Inside the streak region	$\% = \frac{1182.3}{3635} * 100 = \mathbf{32.53}\%$
Outside the streak region	$\% = \frac{1286.25}{4255.75} * 100 = \mathbf{30.22}\%$

From Table B1-7 it can be seen that there is a slightly increased fraction of grain boundary grooves inside the streak region. The difference in grain boundary groove distribution in and out of the streak region is 7.1%.

$$\%\ Difference\ in\ grain\ boundary\ groove\ fraction\ in\ and\ out\ of\ the\ streak\ region$$
$$= 1 - \frac{30.22}{32.53} * 100 = 7.1\%\ (j1)$$

B2 – Analysis of a 5x5 Honeycomb Grain Matrix

To further confirm the method and the difference in grain boundary densities of 7.1% a larger 5 x 5 honeycomb matrix was analysed as shown in Figure B2-4 below.

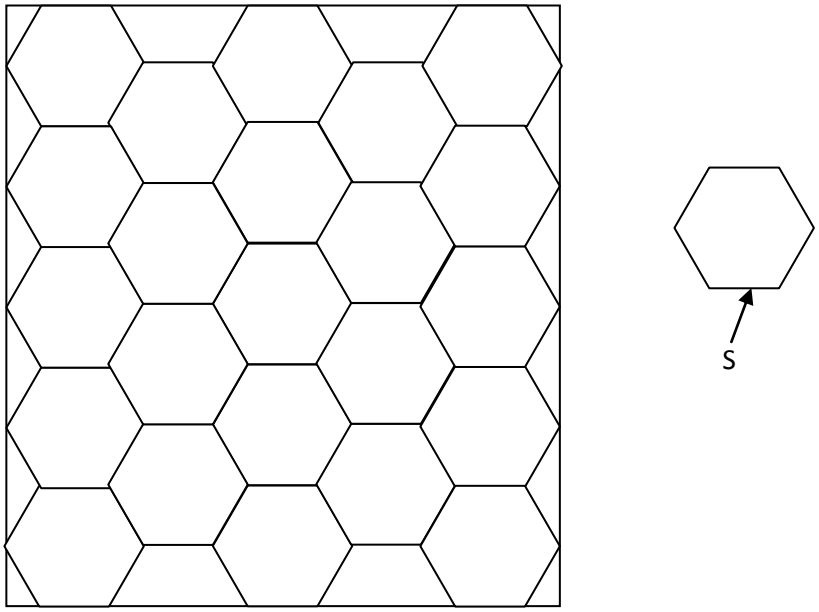

Figure B2-4 – 5 x 5 honeycomb grain matrix (Total number of sides (S) = 88)

1. Find the number of side (S) and use to find the total length of the grain boundaries for a 5x5 honeycomb grain matrix in and out of the streak region.

Previously the length of each side (S) of a six sided hexagon for the average grain size in and out of the streak region was found to be 11.26μm and 12.25μm respectively. Knowing that the number of sides (S) for a 5 x 5 honeycomb grain matrix is 88 the total grain boundary length for a 5 x 5 honeycomb grain matrix in and out of the streak region is 88*S. The total length values for the grain boundaries in and out of the streak region are shown in Table B2-8 below.

Table B2-8 - Total grain boundary length in an out of the streak region for a 5x5 honeycomb grain matrix

	Inside streak Region	Outside streak region
Total grain boundary length	990.88μm	1078μm

2. Find the total grain boundary area in and out of the streak region for a 3x3 honeycomb grain matrix

The total grain boundary groove area in and out of the streak zone is found by multiplying the grain boundary lengths from Table B2-8 by the estimated grain boundary groove width of 3μm which was outlined in figure B1-2. Therefore the total area of the grain boundary grooves for in and out of the streak zone is shown in Table B2-9.

Table B2-9 - Total area of grain boundary grooves for a 5 x 5 honeycomb grain matrix in and out of the streak region

	Area of Grain boundary grooves (5 x 5 honeycomb grain matrix)
Inside the Streak Region	2972.64μm^2
Outside the streak region	3234μm^2

3. Find the area of a 3x3 honeycomb grain matrix in and out of the streak region

Using the components outlined in Figure B1-3 the total area of the 5x5 honeycomb grain matrices in and out of the streak region is:

$$Area\ of\ 5x5\ honeycomb\ grain\ matrix = width\ \times height$$
$$= \{[(S \cdot \cos(60)) \cdot 6] + [GBW \cdot 6\ ] + [5 \cdot S]\}$$
$$* \ \{(S \cdot \cos(30)) \cdot 10 + [GBW \cdot 6]\}(c2)$$

From formula c2 above the values for the area of a 5x5 honeycomb grain for in and out of the streak region is shown in table B2-10 below.

Table B2-10 - Total area of the 5x5 honeycomb grain matrix for in and out of the streak region

	Area of 5x5 honeycomb grain matrix
Inside the streak region	12488μm^2
Outside the streak region	14394μm^2

4. Find the total area of the grain interiors for a 5x5 honeycomb grain matrix in and out of the streak region.

By subtracting the area of the grain boundary grooves from the entire area of the grain matrix the total area of the grain interiors can be found as shown in Table B2-11.

Table B2-11 -Total area of the grain interiors in and out of the streak region for a 5x5 honeycomb grain matrix

	Total area of grain interiors
Inside the streak region	9515.36 μm^2
Outside the streak region	11160 μm^2

5. Find the fraction of grain boundary grooves vs. grain interiors in and out of the streak region

Therefore the percentage of grain boundary groove areas in and out of the streak zone for a 5x5 honeycomb grain matrix is shown in Table B2-12.

Table B2-12 - Fraction of grain boundary grooves Vs. Grain Interiors for a 5 x 5 grain matrix

	% of grain boundary grooves
Inside the streak region	$\% = \frac{2972.64}{9515.36} * 100 = \mathbf{31.24}\%$
Outside the streak region	$\% = \frac{3234}{11160} * 100 = \mathbf{29}\%$

Again the difference in grain boundary groove distribution in and out of the streak region is found to be 7.1%.

$$\%\ Difference\ in\ grain\ boundary\ groove\ fraction\ in\ and\ out\ of\ the\ streak\ region = 1 - \frac{29}{31.22} * 100 = 7.1\%\ (d2)$$

Therefore for the fraction of grain boundary grooves in and out of the streak region only a small difference was present as shown from the data in tables B1-7 and B2-12. This small percentage difference means image J analysis would not accurate enough to detect these differences in grain boundary densities in and out of the streak region.

Overall it was found that a difference in the fraction of grain boundary grooves in and out of the streak region was approximately 7.1% which was the same as found for a 3x3 honeycomb grain matrix.

Appendix C – Roughness Testing Data

The following is the roughness data collected for section 3.1 in which the surface roughness of the as-extruded mill finish specimen was analysed in and out of the streak region for differences in roughness. Table C-1 shows the data obtained and figure 3-5 shows the data graphed in each of the six regions for the five roughness tests.

Table C-13 - Roughness Data collected in and out of the streak regions on the surface of the as-extruded mill finish extrusion

		Test 1	Test 2	Test 3	Test 4	Test 5	Average Surface Roughness
Region	1	0.107	0.1054	0.1271	0.1162	0.0859	0.10832
	2	0.077	0.062	0.0714	0.0661	0.0639	0.06808
	3	0.1115	0.123	0.1208	0.1181	0.1296	0.1206
	4	0.0914	0.0859	0.0662	0.0749	0.0925	0.08218
	5	0.1134	0.1146	0.1563	0.1358	0.1216	0.12834
	6	0.0895	0.099	0.088	0.0895	0.0861	0.09042

Bibliography

1. Meng, C., *Effect of Preheating Condition on Strength of AA6060 Aluminium Alloy for Extrusion*, in *School of Engineering*. 2010, AUT University: Auckland.
2. Qamar, S.Z., A.F.M. Arif, and A.K. Sheikh, *Analysis of Product Defects in a typical Aluminium Extrusion Facility.* Materials and manufacturing processes, 2004. **19**(3): p. 391-405.
3. Peris, G.R., *Effects of extrusion conditions on "Die Pick-Up" formed during extrusion of aluminium alloy AA6060*, in *School of Engineering*. 2007, AUT University: Auckland.
4. Sheppard, T., *Extrusion of Aluminium Alloys*. 1999, Dordrecht: Kluwer Academic Publishers.
5. Cambridge, U.o. *Extrusion*. 2000 [cited 2011 24th March 2011]; Available from: http://www.matter.org.uk/glossary/detail.asp?dbid=648.
6. Khorasanizadeh, S., *The effects of shot and grit blasting process parameters on steel pipes coating adhesion.* World academy of science, engineering and technology, 2010. **66**.
7. O'Neil. *Anodizing*. 2005 [cited 29th June 2011].
8. Shih, T.S., P.S. Wei, and Y.S. Huang, *Optical properties of anodic aluminium oxide films on Al1050 alloys.* Surface & Coatings Technology, 2007. **202**.
9. Zhu, H., et al., *The formation of streak defects on anodized Aluminium Extrusions.* JOM, 2010. **62**(5): p. 46-51.
10. O'Neil, K. *Finishing*. 2005 [cited 7th Octo 2011].
11. International, A., *Standard Test Methods for Determi9ning Average Grain Size: Designation E112 - 96*, A. International, Editor. 2004, ASTM International.
12. Technologies, P., *Electrolytic Polishing*. 2010.
13. Zhu, H., et al., *Effect of initial microstructure on surface appearance of anodized aluminium extrusions.* The Minerals, Metals & Materials Society, 2009. **40A**.
14. O. Lundera, b., B. Olsenb, and K. Nisancioglub, *Pre-treatment of AA6060 aluminium alloyfor adhesive bonding.* International Journal of Adhesion & Adhesives, 2001. **22**: p. 143-150.
15. Zhang, W., *Report on flow line project for fletcher aluminium*. 2008, The University of Auckland: Auckland.
16. Zhu, H., et al. *Investigation of Die Streaks on Anodised Aluminium Extrusions*. in *4th Australian Pacific Extrusion Conference* 2009. Melbourne Australia: Institute of Materials Engineering Australasia.